The Novel Modes of Action of Ribosomal Antibiotics

BY
KRISHNA KANNAN
B. Tech., Anna University, 2006

DISSERTATION
Submitted as partial fulfillment of the requirements for the degree of Doctor of Philosophy in Pharmacognosy in the Graduate College of the University of Illinois at Chicago, 2013

Chicago, Illinois

Committee Members
Alexander S. Mankin, Advisor and Chair
William E. Walden, Microbiology and Immunology
Scott G. Franzblau
Michael J. Federle
Miljan Simonović, Biochemistry and Molecular Genetics

I dedicate this dissertation to my wonderful parents,

Kannan and Vijayalakshmi,

whose support and affection knew no bounds and helped me achieve this goal.

ACKNOWLEDGEMENTS

I am very grateful to my advisor Shura Mankin, an outstanding mentor, for his guidance, patience and support. He kept me motivated throughout my graduate study to achieve nothing short of excellence. His ability to think critically about any given research problem has inspired and influenced me over the years and still continues to do so. It was a real privilege to work under his directions for the past five years; I have learnt much more than a graduate student could hope for.

I want to thank several members of the Mankin lab, past and present, for all their insightful discussions and suggestions. Special thanks to Dr. Nora Vázquez-Laslop, who originally conceived the project involving macrolide antibiotics, for being constantly available for both scientific and personal discussions. I am grateful to two former graduate students of the lab, Dr. Jacqueline M. LaMarre and Dr. Haripriya Ramu, who served as excellent role models for me. I am highly indebted to Dorota Klepacki for teaching me most of the techniques I know today and also for being an absolutely fantastic co-worker. I want to thank Anusha Rethi Paul Raj and Joseph Dang who did excellent work in the lab and helped me to advance my research projects significantly. Last but not least, I am very grateful to the current lab members Pulkit Gupta, Teresa Szal, Dr. Cédric Orelle, Mashal AlMutairi and Shanmugapriya Sothiselvam and the past members Dr. Bindiya Kaushal, Anna Ochabowicz and Dr. Blanca Martinez-Garriga for their support and friendship and for making the Mankin lab a great place to work.

ACKNOWLEDGEMENTS (continued)

I thank my committee members Dr. William Walden, Dr. Michael Federle, Dr. Scott Franzblau and Dr. Miljan Simonović, for their support and suggestions over the years.

KK

TABLE OF CONTENTS

TABLE OF CONTENTS (continued)

LIST OF FIGURES

LIST OF FIGURES (continued)

LIST OF FIGURES (continued)

LIST OF TABLES

LIST OF ABBREVIATIONS

PTC	Peptidyl transferase center
rRNA	Ribosomal RNA
NPET	Nascent peptide exit tunnel
IF	Initiation factor
EF	Elongation factor
RF	Release factor
RRF	Ribosome recycling factor
CHL	Chloramphenicol
LZD	Linezolid
ERY	Erythromycin
TEL	Telithromycin
AZM	Azithromycin
QUI	Quinupristin
CLI	Clindamycin
TAO	Troleandomycin
TET	Tetracycline
A_{600}	Absorbance measured at 600 nano meter wavelength
MIC	Minimum inhibitory concentration
MH-CA	Muller-Hinton Cation-Adjusted
LB	Luria-Bertani medium
TCA	Trichloro acetic acid
ATP	Adenosine triphosphate

LIST OF ABBREVIATIONS (continued)

SDS-PAGE	Sodium dodecyl sulfate-polyacrylamide gel electrophoresis
Ni-NTA	Nickel-nitriloacetic acid
ORF	Open reading frame
Ψ	Pseudouridine
PDB	Protein data bank
EDTA	Ethylenediaminetetraacetic acid
NaCl	Sodium Chloride
HCl	Hydrochloric acid
NaOH	Sodium hydroxide
e.g.	Example
IC_{50}	Concentration of the drug producing 50% inhibition
IC_{90}	Concentration of the drug producing 90% inhibition

SUMMARY

Bacterial infections are treated using natural and synthetic small molecules called antibiotics. The emergence of resistant strains and the increased incidence of bacterial infections have had a major impact on the healthcare field. The need for novel antibiotics is urgent due to the remarkable ability of bacteria to evolve resistance mechanisms.

The ribosome is an important target for antibiotics owing to its indispensability for the sustenance of life. A large proportion of clinically used antibiotics target this protein synthesis machinery. Ribosomal antibiotics have been and continue to be viewed as excellent drugs against pathogenic bacteria. Although the mode of action of drugs targeting the ribosome have been studied for decades, some experimental results do not fit into the widely accepted models for several of these antibiotics, implying a lack of thorough understanding of the how these drugs inhibit translation. In this study, we reassess the mechanism of action of several clinically relevant drugs that target the ribosome.

Macrolide antibiotics and their derivatives, ketolides, bind to the ribosomal exit tunnel through which all the newly synthesized proteins leave the ribosome. In the presence of a macrolide/ketolide molecule, the egress of the nascent chain is obstructed and further protein synthesis is inhibited. Conventionally, ribosomal antibiotics including macrolides and ketolides have been viewed as indiscriminate inhibitors of protein synthesis. However, we observed that these drugs, even at high concentrations, allow selective residual translation of specific proteins. Furthermore, a completely different class of antibiotic (streptogramin-B), which also binds to the exit tunnel, likewise allowed escape of specific proteins from inhibition. We also observed that treatment of cells with

ketolides results in the accumulation of incomplete proteins. One of the interesting outcomes of this study was the finding that more potent antibiotics (ketolides) also allow more protein synthesis compared to the conventional macrolides. Collectively, our results help rationalize the reasons behind the improved efficacy of ketolides over macrolides which might pave the way for developing better ribosome tunnel binding antibiotics that selectively inhibit the synthesis of specific polypeptides.

The peptidyl transferase center (PTC) is arguably the most important functional center of the ribosome and hence, understandably, is targeted by several classes of antibiotics. Most of these drugs inhibit the proper placement of the tRNA ligands during protein synthesis. Specifically, chloramphenicol (CHL) and linezolid (LZD) inhibit the accommodation of any acceptor aminoacyl-tRNA in the ribosome. A notable deviation from this widely accepted model emerged from our studies. We show that CHL and LZD inhibit the association of certain aminoacyl-tRNAs to the ribosomes selectively at specific mRNA codons. Our results show that the nascent peptide amino acid sequence and the nature of the tRNA substrates can impact the drug's ability to inhibit elongation. We hypothesize that specific functional states of the translating ribosome that are generated during elongation could be necessary for the binding and action of LZD and/or CHL. Our results bring into question the common understanding of the mode of action of these drugs and provide a more comprehensive view that accommodates several previous biochemical observations that remained unexplained. Until recently, CHL was a widely clinically used antibiotic and LZD is one of the newest antibiotics currently used against

drug-resistant bacteria. Hence, a better understanding of these antibiotics is critical for the development of future antibiotics targeting the PTC.

In addition to investigating the mode of antibiotic action in this work, we also addressed an important aspect of gene regulation that operates through the interaction between the nascent chain, the small molecule effector and the ribosome tunnel. We show through multiple examples that the chemical structure of the small molecule bound in the exit tunnel, the structure of the tunnel, and the amino acid sequence of the nascent chain together determine the translational fate of a protein.

I. BACKGROUND AND SIGNIFICANCE

1.1 Overview of the ribosome structure and protein synthesis

Ribosomes perform one of the most fundamental processes in the cell, protein synthesis. This large and well-conserved macromolecular machine is composed of RNA and proteins with the ribosomal RNA (rRNA) contributing to nearly two-thirds of the weight of the ribosome in bacteria. The ribosome is composed of two subunits, large and small (50S and 30S respectively, in bacteria). The large subunit contains the functionally critical peptidyl transferase center (PTC) that catalyzes the peptide bond formation. The small subunit carries the decoding center where the interactions of the tRNA anticodon with the mRNA codon are monitored (Ban et al., 2000; reviewed in Schmeing et al., 2009). The newly synthesized polypeptides leave the ribosome through a channel called the nascent peptide exit tunnel (NPET) that extends from the catalytic center to the exterior solvent side of the 50S subunit (Figure 1A) (Yonath, 1987). There are three functional sites for tRNAs in the ribosome: the A-site which serves as the entry site for the aminoacyl-tRNA, the P-site where the peptidyl-tRNA is placed and the E-site through which the tRNAs depart the ribosome (Figure 1A) (reviewed in Demeshkina et al., 2010).

The process of protein synthesis involves the translation of codon information in the mRNA into a sequence of amino acids of the protein. The amino acids are delivered to the ribosome as aminoacyl-tRNAs and the ribosome catalyzes the formation of the peptide bond between the C-terminal amino acid of the peptide esterified to the P-site bound tRNA and the aminoacyl moiety of the A-site bound aminoacyl-tRNA. Protein synthesis involves three major steps: initiation, elongation and termination (Figure 1B). In bacteria, the small ribosomal subunit associates with mRNA and the initiator fMet-

tRNA with the help of initiation factors IF1, IF2 and IF3. After the association of the large ribosomal subunit, the 70S initiation complex, containing the ribosome, mRNA and fMet-tRNA in the P-site, is formed, which then enters elongation cycle. In each round of elongation, the incoming amino acid is brought to the A-site by the aminoacyl-tRNA in a ternary complex with the elongation factor EF-Tu and GTP. The aminoacyl-tRNA is accommodated into the A-site in a multi-step process making it competent to serve as a peptide bond acceptor. As a result of a new peptide bond formation, the growing peptide is transferred from the P-site bound peptidyl-tRNA to the A-site tRNA and is elongated by one amino acid. Upon binding of translocation elongation factor EF-G, the A-site and P-site tRNAs are shifted (through several intermediates) to the P-site and the E-site, respectively and the mRNA is moved by one codon. The elongation cycle continues until the A-site mRNA codon is a stop codon. Release factors (RFs) 1 or 2 recognize the stop codon and hydrolyze the peptide from the tRNA in the P-site. The ribosome recycling factor (RRF) along with EF-G dissociate the ribosome into 50S and 30S subunits and recycle them for another round of translation.

1.2 The Ribosome as an antibiotic target

Because protein synthesis is indispensable for cell survival, it is a not surprising that the ribosome constitutes one of the major antibiotic targets in bacteria (reviewed in Vazquez, 1979; Yonath, 2005; Wilson, 2009). The functions of the ribosome can be inhibited by several classes of natural, synthetic and semisynthetic antibiotics affecting different steps of translation. Most of the drugs inhibiting translation bind directly to the ribosome. However, some of the drugs may inhibit protein production by inhibiting

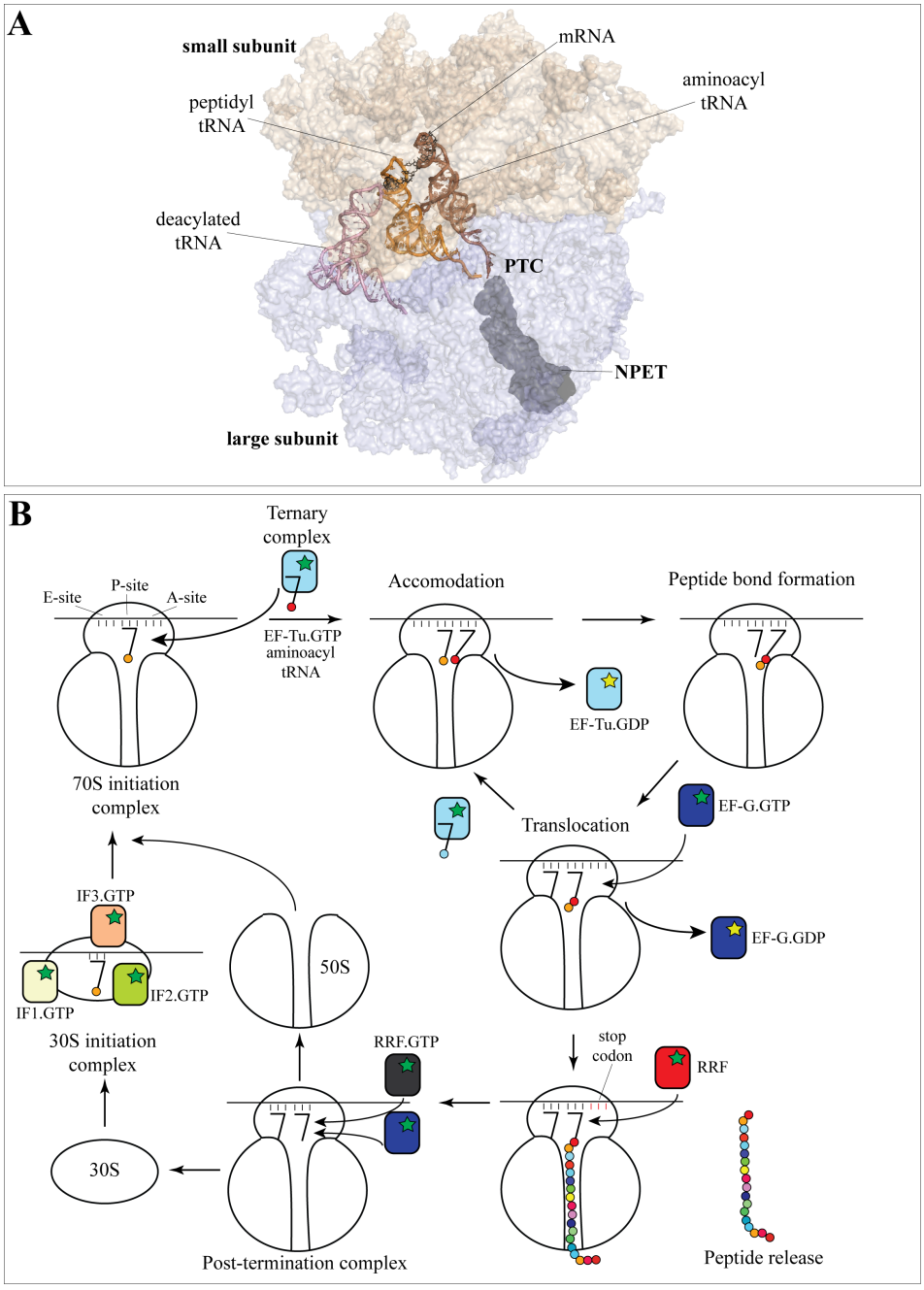

Figure 1. Ribosome structure and protein synthesis. (A) Structure of ribosome bound by mRNA, aminoacyl-tRNA (A-site), peptidyl-tRNA (P-site) and deacylated-tRNA (E-site). (B) Overview of protein synthesis. See text for details.

the activity of elongation factors and other extra ribosomal factors such as aminoacyl-tRNA synthetases (Hughes et al., 1978). Several decades of extensive studies have shown that antibiotics target the functional centers of the ribosome such as the decoding center in the 30S subunit, the PTC in the 50S subunit, or the NPET. Contrary to antibiotics interfering with cell wall synthesis or DNA-replication, almost all ribosomal antibiotics are bacteriostatic. The exceptions to this general rule are drugs from the aminoglycoside class, which exhibit considerable bactericidal activity. These drugs render the ribosome error-prone by promoting misreading of the mRNA codons and production of faulty proteins that can trigger oxidative stress and cell-death (Kohanski et al., 2007).

1.3 Macrolide antibiotics

Macrolides are an important class of antibiotics effective against pathogenic Gram-positive bacteria. These mostly bacteriostatic drugs are commonly used to treat infections of the respiratory tract, skin, soft tissue, urogenital tract and orodental space. Macrolides were introduced into medical practice almost 60 years ago and continue to be viewed as excellent antibiotics with high potency and low toxicity. Erythromycin A, a natural product of *Saccharopolyspora erythraea*, was the first macrolide to be advanced into medical use in the early 1950s for the treatment of bacterial infections (McGuire et al., 1952) (Figure 2A). Erythromycin (ERY) is effective against many Gram-positive pathogenic bacteria including *Staphylococcus aureus*, *Streptococcus pneumoniae*, *S. pyogenes* and *Enterococcus sp.* and some Gram-negative bacteria such as *Neisseria gonorrhoeae*, *Bordetella pertussis*, *Haemophilus influenzae* and intracellular pathogens such as *Mycoplasma sp.*, *Legionella sp.*, and *Chlamydia sp.* Semisynthetic derivatives of ERY, including drugs such as clarithromycin, roxithromycin and azithromycin (AZM)

(Figure 2B) which belong to the second generation of macrolides, exhibit increased acid stability, better oral bioavailability, improved pharmacodynamics and broader antimicrobial spectrum. The second-generation macrolides showed particularly improved activity against *Haemophilus influenzae* and intracellular pathogens such as *Mycobacterium avium-intracellulare* (reviewed in Oleinick, 1975). The emergence and the broad spread of resistance to macrolide antibiotics prompted the development of the new, third-generation macrolides. Ketolides, representing this newest class (Figure 2B), show improved potency against many sensitive bacteria and some strains resistant to previous generation of macrolides and are often associated with bactericidal activity (Ackermann et al., 2003). Macrolide antibiotics with an extended macrolactone ring such as 16-membered macrolides, now find extensive use in veterinary medicine, and are sometimes also used in humans (Figure 4A).

1.3.1 Structure of macrolide antibiotics

Clinically useful macrolides are characterized by the presence of a 14-, 15-, or 16-member macrolactone ring, to which several neutral or amino sugars and other side chains are attached (Figures 2 and 4). The prototypical natural macrolide antibiotic, ERY, is composed of a 14-member lactone ring that carries two sugars, cladinose and desosamine, attached at positions C3 and C5, respectively (Figure 2A). In the semisynthetic AZM, the macrolactone ring of ERY is extended by an additional nitrogen atom (Figure 2B). The 16-membered macrolides like tylosin or carbomycin contain an extended disaccharide at the C5 position and often possess several additional side chains attached to other atoms of the macrolactone (Figure 4A). In ketolides, a keto group replaces the C3 cladinose of ERY. In addition, ketolides carry a 11,12 cyclic carbamate

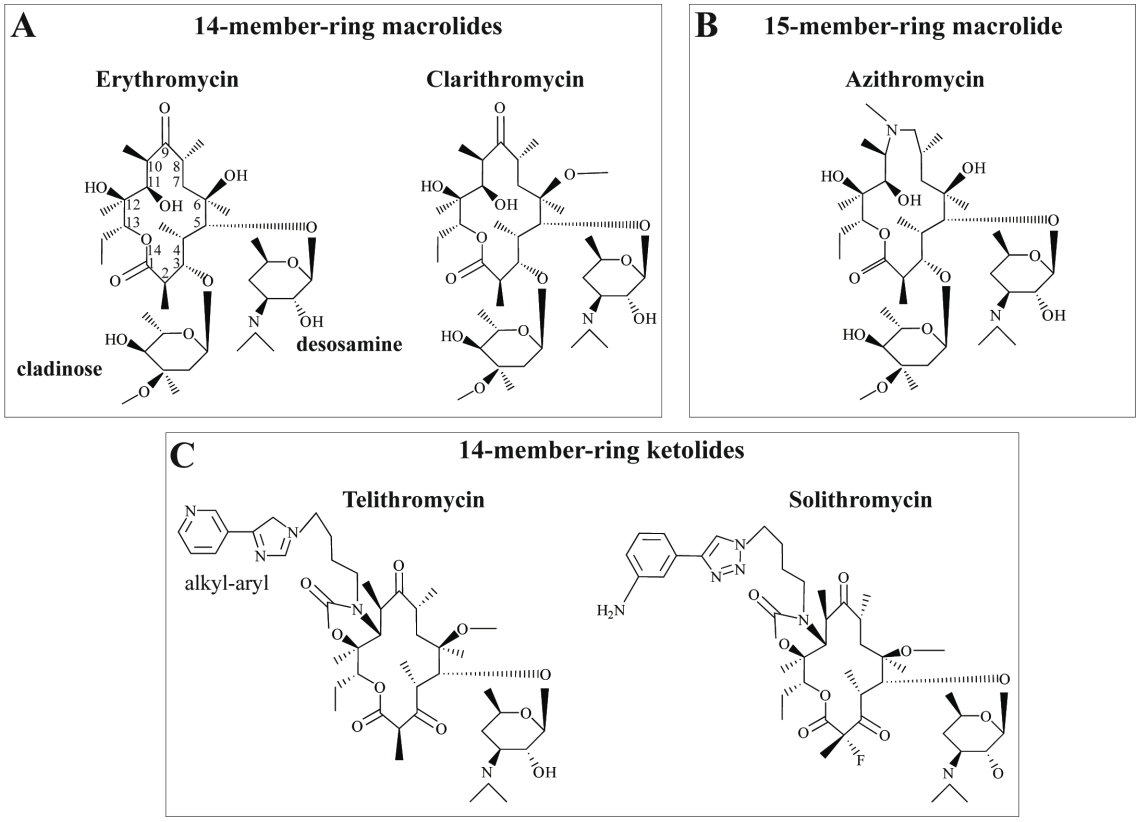

Figure 2. Chemical structures of different macrolide antibiotics. (A) 14-member macrolactone ring containing macrolides ERY and clarithromycin, (B) 15-member macrolactone ring containing AZM and (C) ketolides, TEL and solithromycin, are shown. Atoms of the macrolactone ring are marked on the ERY structure. Side chains discussed in this study are labeled.

and an extended alkyl-aryl side chain that can be linked at different sites to the macrolactone moiety (Figure 2C). Some clinically promising ketolides (e.g. solithromycin) are additionally fluorinated at C2 (Figure 2C) (Putnam et al., 2010). Both the macrolactone ring and the side chains of macrolide antibiotics contribute to the binding affinity of the drug to the ribosomal target. While variation in the structure of the central macrolactone ring has little influence on the mode of drug-binding or inhibition of translation, the structure of the side chains directly affects the interaction of the drug with specific rRNA residues, the mechanism of macrolide action, and the drug's propensity to activate resistance mechanisms (Hansen et al., 2002; Dunkle et al., 2010).

1.3.2 Macrolide binding site

Macrolides bind in the upper chamber of the NPET, between the PTC and the constriction formed by proteins L4 and L22 (Figures 3A and B). The binding site is composed predominantly of rRNA nucleotides belonging to domains II and V of the 23S rRNA. The central macrolactone ring of the drug establishes hydrophobic interactions with the rRNA residues 2057, 2611 and 2058 that form the tunnel wall on the side of the PTC A-site (*Escherichia coli* numbering of rRNA nucleotides is used throughout this study) (Figure 3C) (Schlunzen et al., 2001). In most of the available high-resolution crystallographic structures, the macrolactone is positioned flat against the wall with the side chains protruding either up the tunnel, towards the PTC active site, or down, towards the tunnel constriction (Hansen et al., 2002; Dunkle et al., 2010). The C5 amino sugar (desosamine in the 14- and 15- member ring macrolides or mycaminose of the mycarose-mycaminose disaccharide in the 16-member ring macrolides) extends in the direction of the PTC and is drawn close to the crevice between the bases of the adenine residues

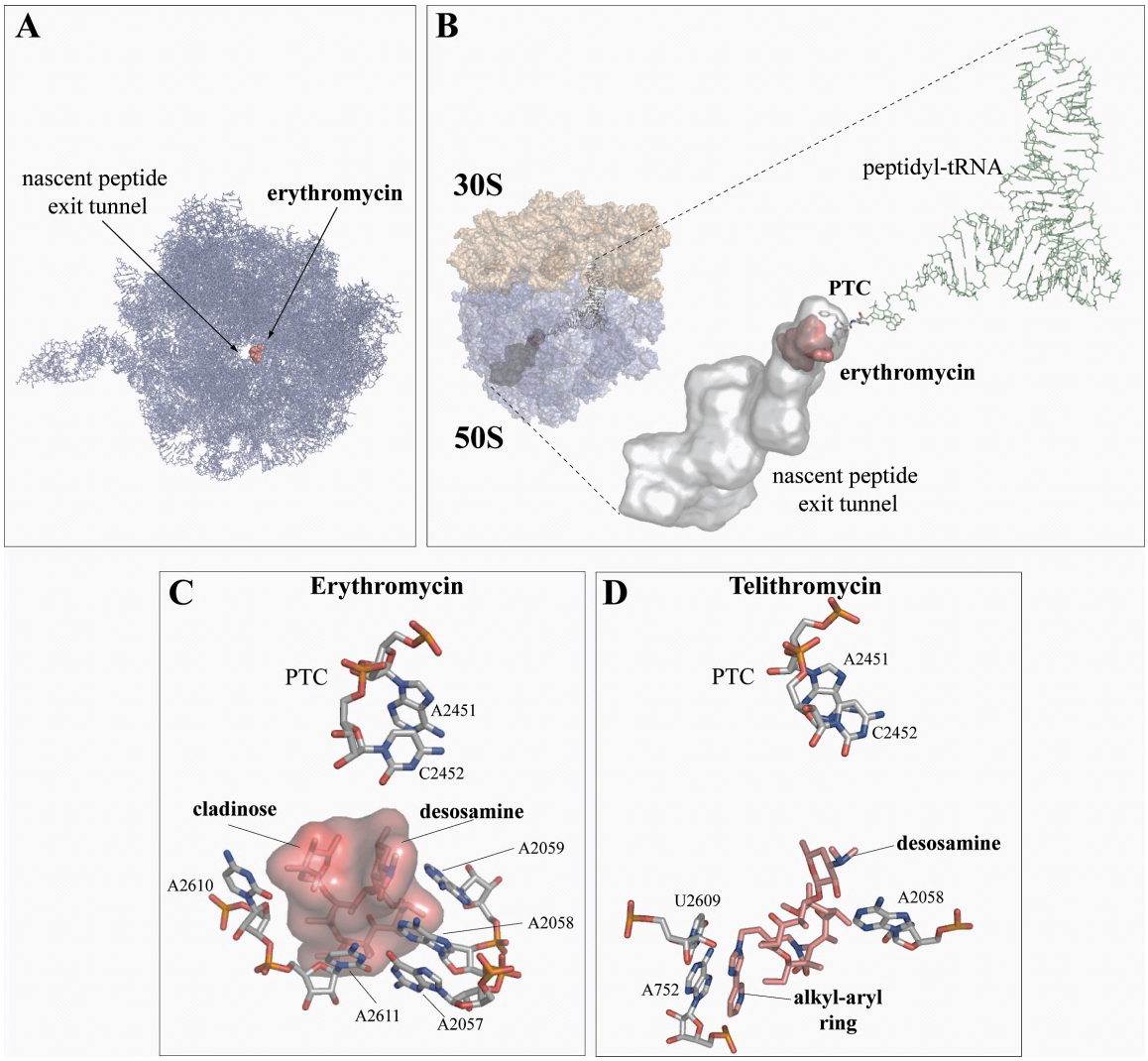

Figure 3. Binding site of macrolide antibiotics in the ribosome. (A) Macrolide antibiotics (like ERY) obstruct the exit tunnel. View down NPET from the interface side of the large ribosomal subunit. ERY molecule is shown in salmon. (B) ERY binds in the exit tunnel close to the PTC. Small (30S) and large (50S) ribosomal subunits are colored yellow and blue, respectively. Surface of the exit tunnel is shown in grey and peptidyl-tRNA with a short nascent peptide in green. Atoms of the ERY molecule are shown as salmon-colored spheres. (C) rRNA residues in the ERY binding site in the *E. coli* ribosome (PDB accession number 3OFR) (Dunkle et al., 2011). ERY molecule is shown as sticks-and-surface representation. (D) Conformation of TEL in the *E. coli* ribosome (PDB accession number 3OAT) (Dunkle et al., 2011). Alkyl-aryl side chain of TEL that stacks upon the A752-U2609 base pair is marked. In (C) and (D), the 23S rRNA residues A2451 and C2452 located in the PTC A-site are shown for orientation. Figure adapted from Kannan et al., 2011.

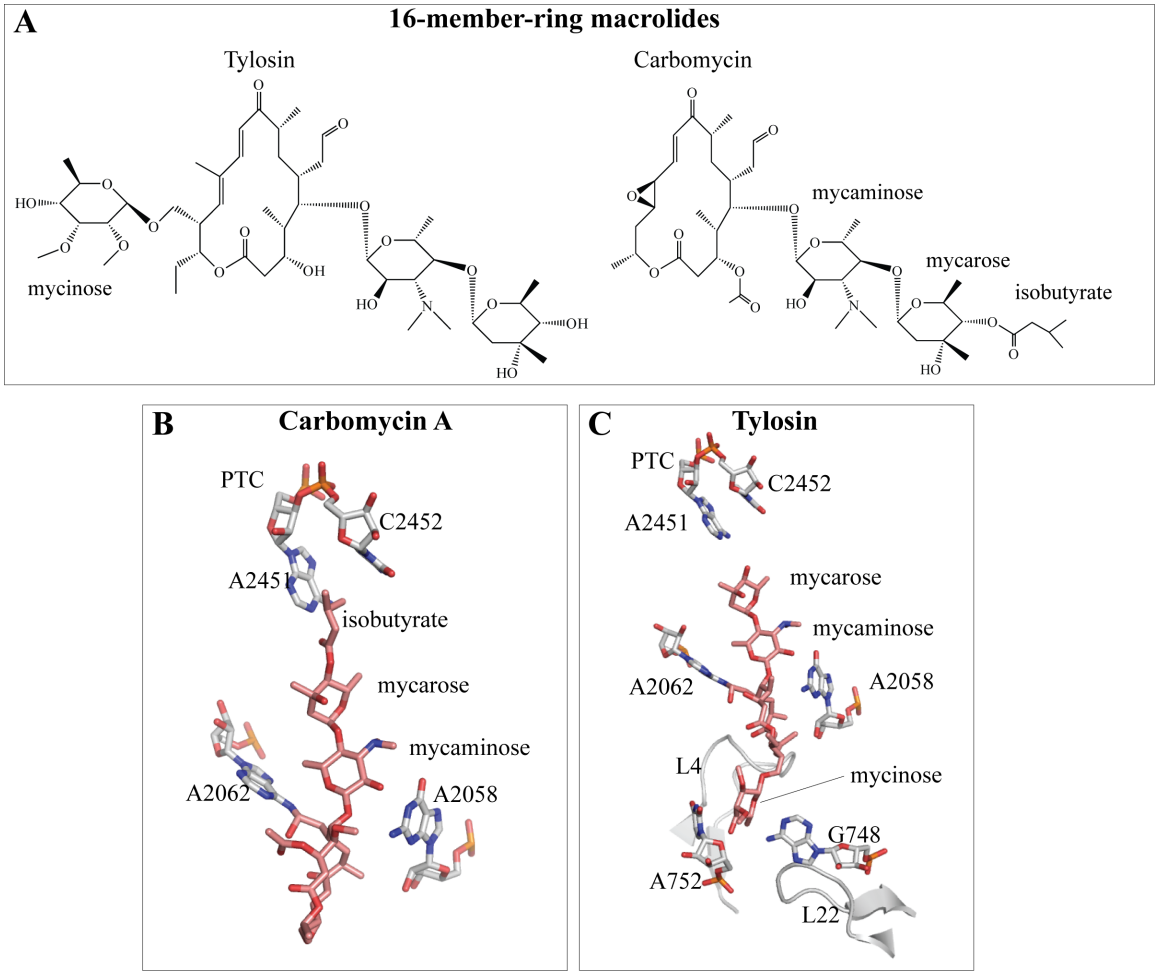

Figure 4. 16-membered macrolide antibiotics: structure and binding. (A) Chemical structures of 16-member ring macrolide antibiotics, tylosin and carbomycin. (B) Mycaminose-mycarose-isobutyrate side chain of carbomycin A can reach into the PTC (*Haloarcula marismortui* 50S subunit, PDB accession number 1K8A (Hansen et al., 2002)). Mycinose side-chain of tylosin stretches towards the loop of helix 35 and comes into close contact with the rRNA residues A752 and G748 and ribosomal proteins L4 and L22 (*H. marismortui* 50S subunit, PDB accession number 1K9M (Hansen et al., 2002)). Figure adapted from Kannan et al., 2011.

A2058 and A2059 (Figures 3C, 4B and C). A hydrogen bond donated by the 2'-OH of the desosamine to the N1 of A2058 additionally contributes to drug binding. The interactions of the C5 side chain with A2058 and A2059 are very important for drug binding; dimethylation of the exocyclic amine of A2058 by erythromycin resistance methyltransferases (Erms) or mutations of A2058 or A2059 dramatically reduce the affinity of all macrolides for the ribosome (Vester et al., 1987; Weisblum, 1995a). While the C5 desosamine of the 14- and 15-member ring macrolides does not reach the PTC, the longer disaccharide C5 side chains of the 16-member ring macrolides approaches the PTC active site more closely and can affect the catalysis of peptide bond formation directly (Figure 4). The C5 disaccharide in carbomycin and josamycin is further extended by an isobutyrate moiety that reaches directly into the PTC A-site, where it is positioned in the hydrophobic crevice formed by residues A2451 and C2452 in the heart of the catalytic center (Figure 4B) (Poulsen et al., 2000). The 16-member macrolides establish a covalent interaction with the ribosome. A continuous electron density between the ethyl-aldehyde group at the C6 position of the macrolide molecule and the exocyclic amine of A2062 is observed in the crystal structure (Hansen et al., 2002). Although, 14-membered macrolides do not form a covalent bond with A2062, the binding of macrolides like ERY induces a significant conformational change in this nucleotide (Tu et al., 2005).

The C3 cladinose is absent in ketolides and 16-member ring macrolides. However, the presence of an extended alkyl-aryl side-chain in ketolides or additional side chains in 16-member ring macrolides compensate for the absence of cladinose because they increase the drug's affinity for the ribosome by establishing other interactions with the nucleotides of domain II of 23S rRNA. Recent crystallographic structures of

telithromycin (TEL), the first clinically approved ketolide, complexed to the *E. coli* or *Thermus thermophilus* ribosomes confirmed the previously proposed close contacts of the side chain with the loop of helix 35 (Figure 3D) (Schlunzen et al., 2003; Bulkley et al., 2010; Dunkle et al., 2010). Similarly, the C14-linked mycinose of the 16-member macrolide tylosin interacts with bases at positions 748, 751 and 752 in the helix 35 loop (Figure 4C) (Hansen et al., 2002).

1.3.3 The commonly accepted mechanism of action of macrolides

According to the commonly accepted model, macrolide antibiotics inhibit protein synthesis by obstructing the growth of the nascent peptide chain. The 14- and 15-atom lactone ring macrolides have little effect during the early rounds of translation. Only after the first few amino acids are polymerized and the growing polypeptide reaches the site of drug binding, does the subsequent progression of the peptide through the NPET become inhibited followed by the dissociation of the peptidyl-tRNA from the ribosome (Figure 5) (Otaka et al., 1975; Menninger et al., 1982). With the cladinose-containing 14- and 15-membered macrolides bound in the tunnel, the dissociated peptidyl-tRNAs carry up to 4 to 9 amino acid-long peptide (Tenson et al., 2003). Ketolides, which lack the C3 cladinose, allow polymerization of 9-10 amino acids (Tenson et al., 2003). In addition to the direct effect of the drug on ribosomal protein synthesis, accumulation of peptidyl-tRNA, leading to the exhaustion of the pool of free tRNAs in the cell, could be an important factor contributing to cessation of translation in macrolide-treated cells Menninger et al., 1982). Corroborating this idea is the fact that cells deficient in peptidyl-tRNA hydrolase exhibit hypersusceptibility to macrolide antibiotics (Menninger, 1979).

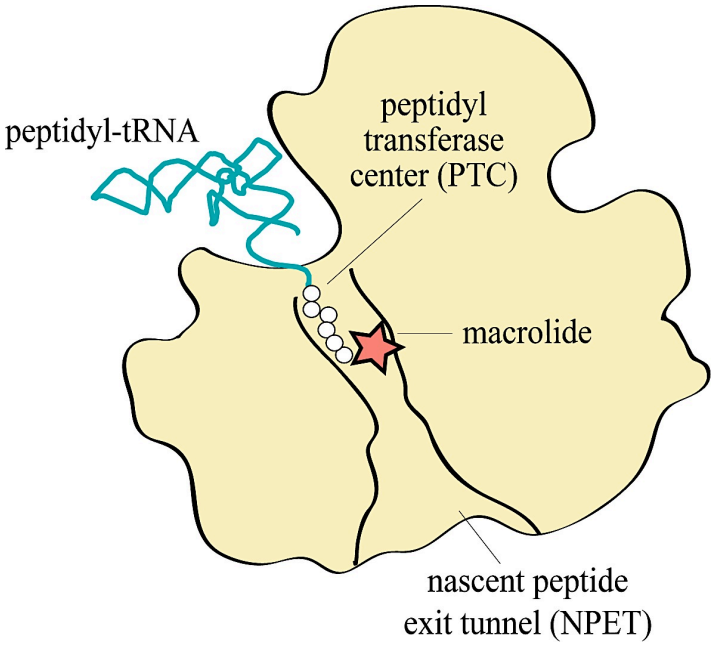

Figure 5. Mode of action of macrolide antibiotics. Binding of macrolide antibiotics in the NPET obstruct the progression of the nascent peptide.

In contrast to the 14- and 15-member ring macrolides that do not inhibit polymerization of the first few amino acids, the 16-membered macrolides that carry a disaccharide (mycaminose-mycarose) side chain at the C5 position can block translation at earlier stages (Figure 4). The mycaminose-mycarose chain that reaches into the PTC can directly interfere with the formation of the second or even first peptide bond (Poulsen et al., 2000). In carbomycin A and josamycin, the disaccharide molecule is further extended by an isobutyrate group, which reaches into the amino acid binding pocket of the PTC A-site and inhibits the placement of the incoming aminoacyl-tRNA, thus halting the formation of the first peptide bond.

Besides the interference with peptide elongation and inhibition of peptide bond formation (in the case of 16-member-ring macrolides), macrolides are also shown to promote read-through of stop codons located close to the translation initiation site, suggesting a negative effect on the accuracy of translation (Thompson et al., 2004). Although this observation is intriguing, it remains unclear how the interplay of the drug, the nascent peptide and the ribosome contributes to this effect and whether this mode of macrolide action is manifested only at the early stages of translation.

Treatment of bacteria with low concentrations of macrolides leads to differential inhibition of production of many cellular polypeptides, including ribosomal proteins. Unbalanced synthesis of ribosomal components results in aberrant ribosome assembly (Champney et al., 2002a-c; Siibak et al., 2009). This effect may exacerbate the inhibitory action of the drugs on translation and cell growth.

1.4 Other antibiotics binding to the NPET

Another major class of drugs that bind to the NPET is the streptogramin B antibiotics (for example, quinupristin (QUI)) (Figure 6). Crystallographic structures have revealed that streptogramin B antibiotics bind at the same location in the NPET where macrolides and ketolides bind (Tu et al., 2005) (Figures 6 and 7C). Similar to 14-member ring macrolides, streptogramin B antibiotics inhibit the progression of the nascent chain after the formation of first few peptide bonds, which indicates that their mode of action is similar to that of 14- or 15-member macrolactone ring containing macrolides or ketolides (reviewed in Vazquez, 1975; Tenson et al., 2003). Naturally occurring streptogramin B antibiotics produced by *Streptomyces sp.* are usually generated in conjunction with the chemically unrelated streptogramin A compounds, and together these drugs exhibit significant synergy in binding to the ribosome and inhibition of protein synthesis (Contreras et al., 1977a; Ennis 1974). The streptogramin A molecule binds to the PTC and has been shown to increase the affinity of streptogramin B to the NPET (Contreras et al., 1977a).

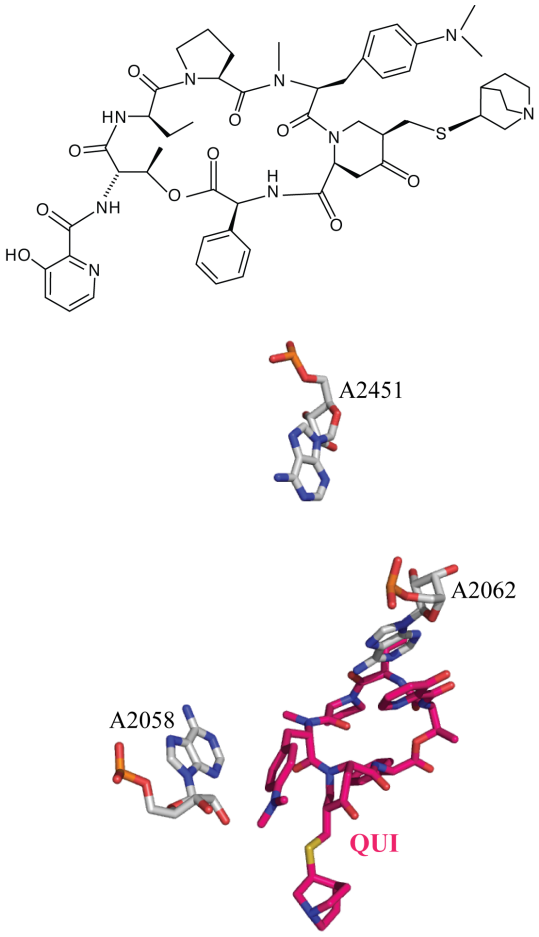

Figure 6. Structure of QUI and its binding mode. Chemical structure of QUI and its binding conformation in the NPET of the *H. marismortui* ribosome is shown (Tu et al., 2005; PDB accession number 1YJW). A2062 and A2058 that directly interact with the drug, protected in foot printing assays in the presence of QUI, and whose mutation confers resistance to QUI are shown. A2451, a PTC nucleotide is also shown for orientation.

1.5 Current model for the mode of action of drugs binding to the A-site of the ribosome

1.5.1 Antibiotics targeting the peptidyl transferase center

The catalytic center of the ribosome is the site of action of a variety of clinically useful antibiotics. These small molecules can be broadly categorized into three groups based on the functional site to which they bind and act: a) A-site binding drugs such as phenicols, oxazolidinones, licosamides, sparsomycins, and anisomycins, b) P-site binding drugs such as blasticidin S, and c) drugs that bind to both A- and P-sites such as streptogramin A and pleuromutilins (reviewed in Wilson, 2009). The binding site and the mode of action of three classes of antibiotics, which bind exclusively to the A-site of the PTC, will be discussed in the following sections (Figure 7C).

1.5.1.1 Phenicols

Chloramphenicol (CHL), an example of the phenicol class of antibiotics, is one of the oldest ribosomal antibiotics used to treat bacterial infections (Figure 8A). CHL is a broad spectrum antibiotic with high permeability in cells and tissues (reviewed in Vazquez, 1979). The use of CHL has been curtailed in recent years due to its toxic effects related to inhibition of mitochondrial protein synthesis. However, CHL is still utilized for treating specific infections along with the use of its derivatives such as thiamphenicol and florfenicol in veterinary medicine in the US and in humans in some countries.

CHL inhibits translation in bacteria as well as in the mitochondria and chloroplasts of eukaryotic cells (reviewed in Vazquez, 1979). Footprinting results show that CHL alters the modification of nucleotides surrounding the PTC A-site such as A2451, G2505 and U2506 (Moazed et al., 1987a) (Figure 8A). Crystallographic

structures of ribosomes complexed with CHL have shown that the drug binds to the A-site of the PTC and interacts with the nucleotides G2061 and G2505 (Schlunzen et al., 2001; Bulkley et al., 2010) (Figures 8A). Mutations of nucleotide residues positioned directly at or close to the binding site, for example, 2451, 2503, 2504, 2447 and 2452, render cells resistant to the drug (Ettayebi et al., 1985; Vester et al., 1988). CHL binds at a position overlapping the amino acid moiety of the incoming acceptor tRNA and hence, preventing its association with the ribosome (Figure 7C). CHL is considered a classic inhibitor of the peptidyl transfer reaction (Celma et al., 1971) and thus, is viewed as a typical elongation inhibitor, which 'freezes' polysomes on the mRNA *in vivo* (Ennis, 1972).

1.5.1.2 Lincosamides

Lincomycin and its semi-synthetic derivative, clindamycin (CLI) (Figure 8B) are the two clinically used lincosamides that exhibit high potency against Gram-positive bacteria and weak activity against Gram-negative bacteria. CLI also exhibits antiplasmodial activity (reviewed in Spizek et al., 2004).

Lincosamides bind to the ribosome at the A-site of PTC although their placement is somewhat shifted towards the NPET compared to CHL binding (Figure 7C). The prolyl-moiety of CLI occupies the same site as the amino acid group of the A-site tRNA and the sugar-moiety of CLI interacts with residues A2058 and A2062 (Schlunzen et al., 2001;Bulkley et al., 2010) (Figures 7C and 8B). Therefore, dimethylation of A2058 by the resistance Erm methyltransferases or mutation of this nucleotide renders cells resistant to CLI (Poehlsgaard et al., 2005). Like CHL, lincosamides effectively inhibit the model peptidyl transferase reaction (involving puromycin as an acceptor substrate),

however, unlike CHL, these drugs cannot bind to the polysomes carrying nascent peptides (Contreras et al., 1977b). Hence, CLI inhibits specifically the first peptide bond formation rather than translation elongation.

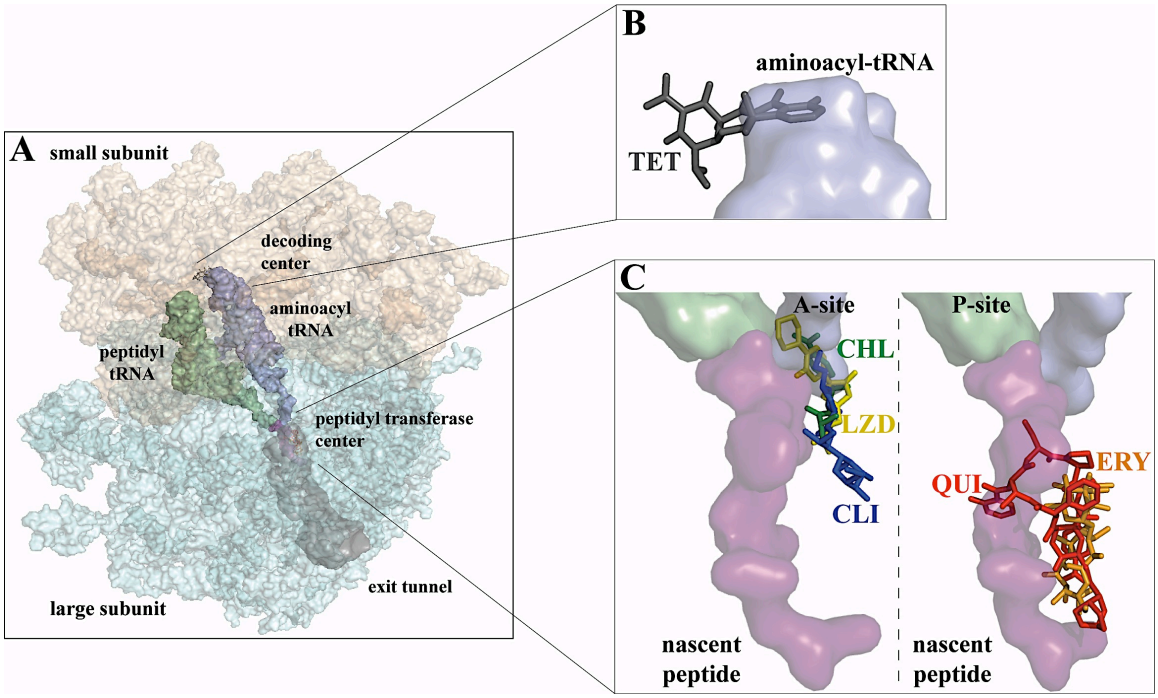

Figure 7. Binding site and action of different ribosomal antibiotics. (A) A general overview of different sites of drug action in the ribosome. The decoding center of the small subunit and the PTC and NPET of the large subunit are marked where the drugs bind. (B) TET binds to the 30S subunit and interferes with the placement of aminoacyl tRNA. TET is shown in grey and the anticodon loop of the aminoacyl tRNA is represented in pale blue (Brodersen et al., 2000; PDB accession number 1HNW). (C) PTC- and NPET-binding drugs. CHL (green), LZD (yellow) and CLI (blue) bind to the A-site of the PTC and inhibit the accommodation of the aminoacyl tRNA. PDB accession numbers are 3OFZ (CLI), 3OFC (CHL) and 3DLL (LZD) (Wilson et al., 2008; Dunkle et al., 2010). QUI (red) and ERY (orange) bind to the NPET and inhibit the progression of the nascent chain in the tunnel (PDB accession number 1YJW) (Tu et al., 2005). A nascent chain modeled into the NPET is shown in pale pink, peptidyl tRNA in pale green and aminoacyl tRNA in pale blue. In (A) and (B), antibiotics are shown as sticks while the ribosome, tRNAs and the nascent peptide are represented by surfaces.

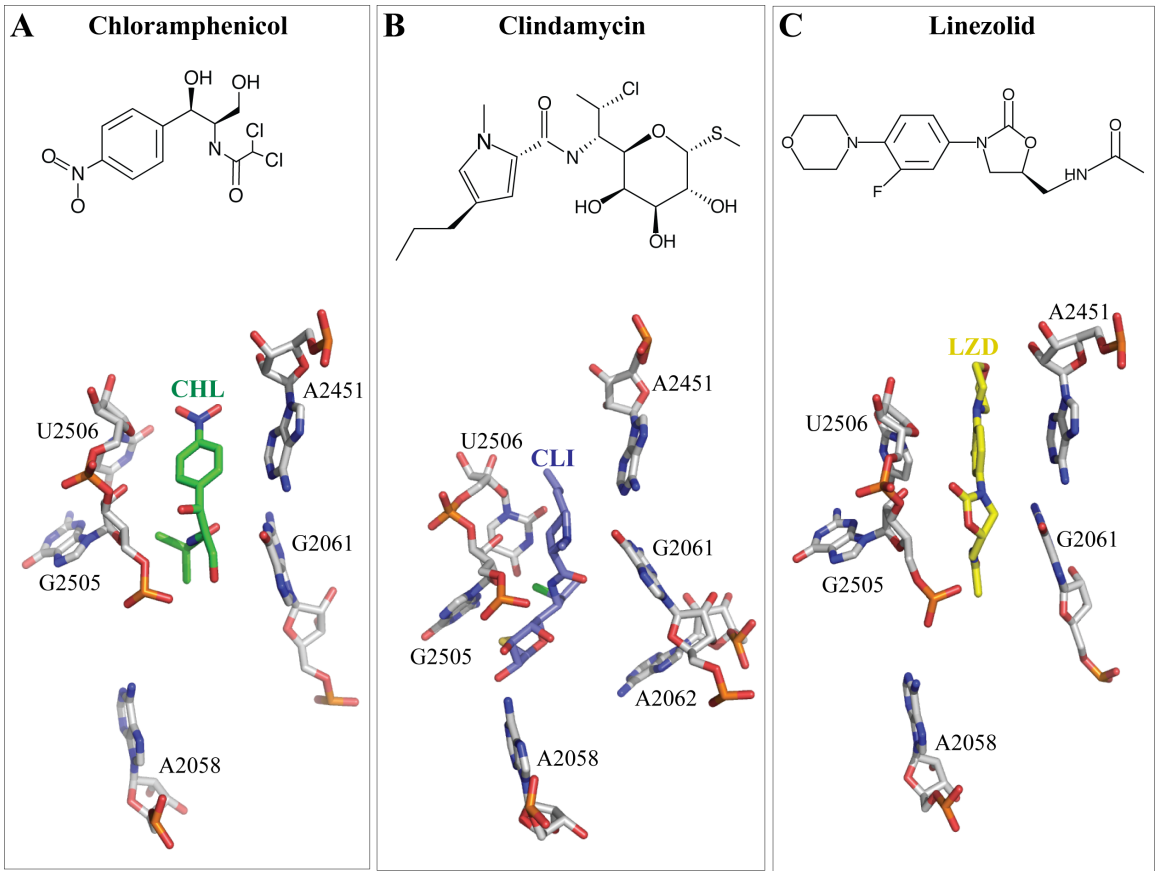

Figure 8. Structure and binding interactions of the PTC antibiotics. Chemical structures of (A) CHL, (B) CLI and (C) LZD targeting the A-site of the PTC are shown. Nucleotides discussed in this study that directly interact with antibiotics, whose mutations confer resistance to or undergo a conformational change during the binding of these antibiotics are indicated (Dunkle et al., 2010; PDB accession numbers 3OFZ (CLI), 3OFC (CHL); Wilson et al., 2008; PDB accession number 3DLL (LZD)).

1.5.1.3 Oxazolidinones

Linezolid (LZD) (Figure 8C) is the first clinical antibiotic from this class and when approved by FDA in 2000, had the distinction of being the first compound with a principally novel structure to be introduced into the medical practice in several decades. LZD is effective against many Gram-positive pathogens including strains that are often resistant to other antibacterial compounds. The importance of LZD in the clinic could not be stressed more than by merely stating that it is usually used as the last line of treatment against multi-drug resistant pathogens. The crystal structure of LZD bound to the large ribosomal subunit showed that it occupies the same site as CHL (Figure 7C) (Wilson et al., 2008; Ippolito et al., 2008). LZD cross-links to the PTC nucleotides A2602, A2451 and U2506, and mutations at positions 2451, 2452, 2504 and 2505 and at other distal locations confer LZD resistance (Figure 8C) (Colca et al., 2003; reviewed in Wilson, 2009). In spite of the detailed structural and biochemical characterization of the binding site, the mechanistic understanding of this antibiotic has been less than straightforward. Unlike CHL or CLI, LZD does not inhibit the reaction between fMet-tRNA and puromycin (Kloss et al., 1999; Fernandez-Munos et al., 1973; Kouvela et al., 2006). Further, LZD can only outcompete CHL or CLI from their binding sites at concentrations much higher than that needed to inhibit translation; LZD inhibits *in vitro* translation with an IC_{50} = 1.8 μM, however, ~1mM LZD is needed to displace 50% of CHL from the ribosome (Shinabarger et al. 1997; Skripkin et al. 2008). These observations have led to the hypothesis that LZD might bind better to the actively translating ribosomes rather than vacant ribosomal particles. However, this hypothesis is yet to be verified experimentally and thus the mechanism of action of LZD remains unclear.

1.5.2 Antibiotics targeting the decoding center

1.5.2.1 Tetracyclines

This group of antibiotics includes the prototype, tetracycline (TET), and its analogs oxytetracycline, chlortetracycline, minoacycline and doxycycline. TET (Figure 9) inhibits both bacterial and eukaryotic translation in cell-free systems but is preferentially accumulated inside bacterial cells.

Crystal structures of TET complexed to the *Deinococcus radiodurans* and *Thermus thermophilus* small ribosomal subunit revealed six and two sites for TET, respectively (Pioletti et al., 2001; Brodersen et al., 2000). Site 1 is located in the A-site of the small ribosomal subunit. With the highest occupancy in crystal structures and with the highest affinity for TET in binding assays, this site is considered to be the biologically relevant site for inhibition (Figure 7B) (Tritton, 1977; Goldman et al., 1983). This has been further confirmed by the occurrence of exclusive protection of nucleotides U1052 and A1054 present near this primary binding site in footprinting experiments (Figure 9) (Moazed et al., 1987b). Moreover, a mutation at the primary site (1058) can provide high resistance to TET (Figure 9) (Ross et al., 1998; Gerrits et al., 2002).

Binding of TET at the primary site interferes with the proper accommodation of the aminoacyl-tRNA. The drug does not affect the initial interaction between the mRNA codon and the tRNA anticodon but inhibits the subsequent accommodation of the aminoacyl-tRNA since the drug sterically clashes with the anticodon loop in the post-accommodated state of the tRNA (Pioletti et al., 2001; Brodersen et al., 2000) (Figure 7B). As a result of TET binding, the ribosomes remain stalled with an empty A-site, unable to bind the aminoacyl-tRNA.

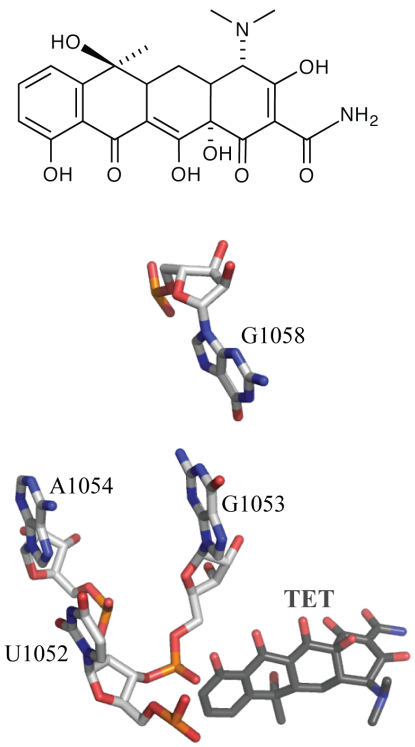

Figure 9. Structure and binding site of the small subunit inhibitor TET. Chemical structure of TET and its binding conformation at the primary site in the decoding center of the *T. thermophilus* shown (Brodersen et al., 2000; PDB accession number 1HNW). Nucleotides U1052 and A1054 that are protected in the foot printing assays, G1053, which directly interacts with TET and G1058, whose mutation confers TET resistance are indicated.

In the sections above, we described the commonly accepted mode of action of several ribosomal antibiotics belonging to the macrolide, streptogramin B, phenicol and oxazolidinone classes. However, there are several biochemical results that are not readily reconciled into these accepted models (described in the 'Introduction and rationale' section of Chapters 3-5). For example, although drugs targeting the ribosome are considered to be unbiased inhibitors of translation, by virtue of the use of several model substrates, it is known that these antibiotics can differentially inhibit translation depending on the mRNA template used in the assay. In order to rectify such discrepancies (and more) between the experimental facts and the commonly accepted models, through this study, we reexamine the mode of action of these antibiotics. The results of our studies allow us to propose new models of action for these antibiotics. We believe that the novel view of the modes of antibiotic action described here could lead to the discovery of novel and superior antibacterials.

II. MATERIALS AND METHODS

2.1 Reagents

ERY, CLI, clarithromycin and ampicillin were purchased from Sigma-Aldrich. CHL, TET and kanamycin were purchased from ThermoFisher Scientific. LZD was obtained from Pharmacia-Pfizer (New York City, NY) and TEL was obtained from Hoechst Marion Roussel-Sanofi (Bridgewater, NJ). Clarithromycin was purchased from United States Pharmacopeia. Solithromycin was obtained from CEMPRA Pharmaceuticals (Chapel Hill, NC). The pBAD22 vector was a gift from Dr. Hyunwoo Lee at UIC. The enzymes and chemicals used in the protocols described below are accompanied by the manufacturer's information.

2.2 Bacterial strains, plasmids and primers

The bacterial strains, primers and plasmids used in this study are listed in Tables I, II and III respectively.

2.2.1 Construction of *E. coli* strain BWDK

A macrolide-sensitive mutant strain was created in order to facilitate the use of drug concentrations much higher than the minimal inhibitory concentration (MIC). We obtained the *E. coli* strain JW3003 from the Keio collection (Baba et al., 2006) in which the gene encoding the efflux pump *tol*C was replaced with a kanamycin-resistance marker. The marker was cured from this strain by Dorota Klepacki in the lab by using the procedure published by Datsenko et al. (2000) and the resulting strain lacking the *tol*C and kanamycin-resistance genes was used.

2.2.2 Preparation of *E. coli* strains expressing mutant ribosomes

The mutations A2062G, U2609C and Ψ746G were introduced in the 23S rRNA gene in the pLK35 plasmid (Douthwaite et al., 1989) as described in the section 2.3.2. The mutant plasmids were transformed into *E. coli* strain SQtolC cells (Table I). Transformants were selected on LB agar plates containing 100 μg/mL ampicillin. Elimination of the prrnC-*sac*B plasmid containing the wild type rRNA operon was carried out following Zaporojets et al. (2003) with some modifications. Specifically, two ampicillin-resistant clones of each mutant were grown in LB/ampicillin (100 μg/mL) medium to the stationary phase, diluted 1:1000 in the same medium and grown to the stationary phase again. The cycle was repeated one more time followed by a final dilution in the same medium lacking sodium chloride but containing 5% sucrose. Cells were grown up to an optical density of 0.5, serially diluted, and 100 μL of 10^{-5}, 10^{-6} and 10^{-7} dilutions were plated on LB agar plates containing 5% sucrose but lacking sodium chloride. The loss of the wild-type rRNA encoding plasmid was verified by replica plating 100 colonies on LB/ampicillin (100 μg/mL) and LB/ kanamycin (50 μg/mL) and selecting for kanamycin-sensitive and ampicillin-resistant colonies. The cells carrying the pLK35 plasmid were further verified to contain the NPET mutation by sequencing the PCR fragment encompassing the mutated nucleotide amplified from the total DNA.

2.3 Plasmids

All the plasmids used in the study are listed in Table III.

2.3.1 Construction of plasmids expressing OsmC-His_6 and H-NS_{12} OsmC-His_6

The *osmC* gene and its variants were PCR-amplified from the *E. coli* strain K12 using different combinations of direct and reverse primers. All the direct primers carried

the EcoRI recognition sequence and all the reverse primers carried the HindIII recognition sequence, which were later used for cloning in the respective sites of the pBAD22 vector (Guzman LM, 1995). The wild type OsmC gene was amplified using primers pBAD22-MCS-osmCfwd and osmC-his6-HindIIIrev. For the fusion construct *hns*$_{12}$*osm*C, the twelve codons of the *hns* gene and the EcoRI recognition sequence were appended to *osm*C using the primers pBAD22-MCS-hns fwd and ptac hns$_{12}$osmC during PCR. The reverse primer osmC-his6-HindIII rev, included sequences that added six histidine amino acids to the C-terminus of OsmC or H-NS$_{12}$OsmC proteins in order to facilitate their purification. The PCR products were purified using the Wizard® SV Gel and PCR Clean-Up System (Promega, Madison, WI) and digested with EcoRI and Hind III enzymes (Fermentas-Thermo Scientific, Waltham, MA) using standard procedures. The enzymes were then heat-inactivated at 80°C and the digested DNA was purified using the kit mentioned above. The digested and purified PCR products were cloned into the pBAD22 plasmid (Guzman LM, 1995) and transformed into *E. coli* strain JM109. The plasmids were isolated from 5 mL overnight cultures (LB/ 100 μg/mL ampicillin) using the High Pure Plasmid Kit (Roche Applied Science, Branford, CT) and structures of the resulting constructs were verified by sequencing at the DNA facility, Research Resources Center of the University of Illinois at Chicago.

2.3.2 Construction of rRNA mutant plasmids

Mutations at specific positions of the 23S rRNA gene were engineered in the plasmid pLK35 containing the entire *rrn*B operon under the control of the P_L promoter (Douthwaite et al., 1989). The mutations were introduced using the QuikChange Lightning Multi Site-Directed Mutagenesis Kit (Stratagene-Agilent, Santa Clara, CA)

following the manufacturer's instructions. Specifically, a degenerate primer Ψ746V was used to generate three possible mutations at position 746. The Ψ746G mutant was used in subsequent experiments. U2609C and A2062G mutant plasmids were generated previously by Dr. Nora Vázquez-Laslop and Dorota Klepacki in this lab. Following site directed mutagenesis, the plasmids were transformed into XL-10 Gold Ultracompetent cells (Stratagene) and selected on LB/ ampicillin (100 μg/mL) plates. Plasmids isolated from several clones were subjected to sequencing and the desired mutants were identified and stored.

TABLE I. LIST OF BACTERIAL STRAINS USED IN THIS STUDY

Strain	Organism	Description	Source
JW3003	*E. coli*	Antibiotic hypersensitive strain in which *tol*C gene was replaced with the kanamycin marker. F-, *Δ(ara*D-*ara*B*)567*, *ΔlacZ4787*(::*rrn*B-3), λ^-, *ΔtolC732::kan*, *rph-1*,*Δ(rha*D-*rha*B*)568*, *hsd*R*514*	Baba et al., 2006
BWDK	*E. coli*	Same as JW3003, but the kan gene was removed	This study
Newman	*S. aureus*	Clinical strain. ATCC 25904	Duthie et al., 1952
RN4220	*S. aureus*	Derived from NCTC8325. Laboratory strain-restriction deficient. ATCC 35556	Giachino et al., 2001
JM109	*E. coli*	Laboratory *E. coli* strain. F', *Δ(gpt-lac)0*, *glnV44*(AS), λ^-, *rfb*C1?, *gyr*A96(NalR),*rec*A1, *end*A1, *spo*T1?, *thi*E1, *hsd*R17, F128-x	Promega
SQtolC	*E. coli*	A derivative of the SQ171 strain lacking chromosomal rRNA alleles in which *tol*C gene was removed. SQ171 genotype- F-, *Δ(rrs*H-*asp*U*)794(::FRT)*, λ^-, *Δ(rrf*G-*rrs*G*)791(::FRT)*, *Δ(rrf*F-*rrs*D*)793(::FRT)*, *rph-1*, *Δ(rrs*C-*trp*T*)795(::FRT)*, *Δ(rrs*A-*rrf*A*)792(::FRT)*, *Δ(rrs*B-*rrf*B*)790(::FRT)*, *Δ(rrs*E-*rrf*E*)789(::FRT)*, ptRNA67, pKK3535	Unpublished from a previous study

TABLE II. DNA PRIMERS USED IN THIS STUDY

Name	Sequence 5'→3'
Primers used for cloning *osmC* and *hns$_{12}$osmC* into pBAD22 vector	
pBAD22-MCS-osmC fwd	GGGCTAGCAGGAGGAATTCACCATGACAATCCATAAGAAAGGTCAG
pBAD22-MCS-hns fwd	GGGCTAGCAGGAGGAATTCACCATGAGCGAAGCACTTAAAATTCT
osmC-his$_6$-HindIII rev	GGAAGCTTATTAGTGATGATGATGATGATGCGATTTCAACTGGTAATCCAG
Primers used for toe-printing	
NV1 (*ermCL* stalling site)	GGTTATAATGAATTTTGCTTATTAAC
EF-G$_{390}$ rev(*fusA* stalling site)	ATTAGTCTTTCAGACCGATAGCAGC
hns$_{18}$luc TP-3 (*luc* stalling site)	AGTTCTATGCGGAAGGGCCA
osmC$_{100}$ rev	AAAACGCGTGTTAAATCCAT
hns toeprinting-4	CTAATTTTTCCAGCATTTCT
mipA$_{100}$ rev	TTTATATGGGTGTTCAACGA
cspA$_{110}$ rev	ATAGCAGAGAAGTGTACGAA
Primers used for generating templates for *in vitro* transcription/translation	
Ptac BamHI fwd	ACGGATCCTTGACAATTAATCATCGGCTCGTATAATGTGTGGAATTGTGAGAGGAGGAAAACATATG
ptac hns fwd	TGAGAGGAGGAAAACATATGAGCGAAGCACTTAAAAT
hns rev	TTATTGCTTGATCAGGAAATCG
T7 hns fwd	ATTAATACGACTCACTATAGGGATATAAGGAGGAAAACATATGAGCGAAGCACTTAAAAT
T7-SD(mut)-TAA hns fwd	ATTAATACGACTCACTATAGGGATATATCCTCCAAAACATTAAAGCGAAG CACTTAAAAT
hns ermCL rev1	AATGAACTGTGCTGATTACAAAAATACTAAAAATGCCTTGCTTGATCAGGAAATCGT
hns ermCL rev2	TTTAATTTGGTTATAATGAATTTTGCTTATTAACGATTCATTATAACCACTTATTTTTTGTTTGGTTGATAATGAACTGTGCTGATTACA
ptac osmC fwd	TGAGAGGAGGAAAACATATGACAATCCATAAGAAAGGTCA
osmC rev	TTACGATTTCAACTGGTAATCC
ptac hns$_{18}$osmC	TGAGAGGAGGAAAACATATGAGCGAAGCACTTAAAATTCTGAACAACATCCGTACTCTTCGTGCGCAGGCAACAATCCATAAGAAAGGTC
ptac hns$_{15}$osmC	TGAGAGGAGGAAAACATATGAGCGAAGCACTTAAAATTCTGAACAACATCCGTACTCTTCGTACAATCCATAAGAAAGGTCAGGC
ptac hns$_{12}$osmC	TGAGAGGAGGAAAACATATGAGCGAAGCACTTAAAATTCTGAACAACATCCGTACAATCCATAAGAAAGGTCAGGC
ptac hns$_{11}$osmC	TGAGAGGAGGAAAACATATGAGCGAAGCACTTAAAATTCTGAACAACATCACAATCCATAAGAAAGGTCAGGC
ptac hns$_{10}$osmC	TGAGAGGAGGAAAACATATGAGCGAAGCACTTAAAATTCTGAACAACACAATCCATAAGAAAGGTCAGGC

TABLE II. DNA PRIMERS USED IN THIS STUDY (continued)

ptac hns_{9}osmC	TGAGAGGAGGAAAACATATGAGCGAAGCACTTAAAATTCTGAA CACAATCCATAAGAAAGGTCAGGC
ptac hns_{8}osmC	TGAGAGGAGGAAAACATATGAGCGAAGCACTTAAAATTCTGAC AATCCATAAGAAAGGTCAGGC
ptac hns_{7}osmC	TGAGAGGAGGAAAACATATGAGCGAAGCACTTAAAATTACAAT CCATAAGAAAGGTCAGGC
ptac hns_{6}osmC	TGAGAGGAGGAAAACATATGAGCGAAGCACTTAAAACAATCCA TAAGAAAGGTCAGGC
ptac $osmC_{1-6}$ hns_{7-12} osmC	TGAGAGGAGGAAAACATATGACAATCCATAAGAAAATTCTGAA CAACATCCGTGGCGATATCAAACGCGGGAA
ptac hns_{1-6} $lacZ\alpha_{7-12}$ osmC fwd	TGAGAGGAGGAAAACATATGAGCGAAGCACTTAAATCGAGCTC GGTACCCGGGACAATCCATAAGAAAGGTCAG
ptac hns_{1-6} $osmC_{7-12}$ osmC fwd	TGAGAGGAGGAAAACATATGAGCGAAGCACTTAAAGGTCAGG CACACTGGGAAACAATCCATAAGAAAGGTCAG
ptac hns_{12} CR osmC fwd	TGAGAGGAGGAAAACATATG TCA GAG GCT CTG AAG ATC CTT AAT AAT ATT CGA ACAATCC ATAAGAAAGG TCAG
ptac $hspQ_{18}$osmC fwd	TGAGAGGAGGAAAACATATGATTGCCAGCAAATTCGGTATCGG CCAGCAGGTCCGCCATTCCCTGTTAGGTACAATCCATAAGAAA GGTCAG
Ptac fusA fwd	ACGGATCCTTGACAATTAATCATCGGCTCGTATAATGTGTGGAA TTGTGAGAGGAGGAAAACATATGGCTCGTACAACACCC
fusA rev	TTATTTACCACGGGCTTCAAT
EF-G_{360}-rev	ATTAGAAACGCTCACGTGCAGCTT
EF-G_{420}-rev	ATTAAACTGCGATGGAGATTACCG
T7 EF-G fwd	ATTAATACGACTCACTATAGGGATATAAGGAGGAAAACAT ATGGCTCGTA CAACACCC
T7-SDmut-TAA EF-G fwd	ATTAATACGACTCACTATAGGGATATATCCTCCAAAACAT TAAGCTCGTA CAACACCCAT
EF-$G_{348-357}$ FS fwd	GTTAACTCTGGTGATTACCGTACTGAACTCCGTGAAAGCTGCAC GGAGCGTTTCGGTCGT
tac luc fwd	TTGACAATTAATCATCGGCTCGTATAATGTGTGGAATTGTGAGA GGAGGAAAACAT ATGGAAGACGCCAAAAACAT
luc rev	TTACAATTTGGACTTTCCGC
ptac hns_{18}luc fwd	TGAGAGGAGGAAAACATATGAGCGAAGCACTTAAAATTCTGAA CAACATCCGTACTCTTCGTGCGCAGGCAGAAGACGCCAAAAAC ATAA
$luc_{180-189}$ FS(+1) fwd-1	CAGGGATTTCAGTCGGATGTACACGTTCGTCACATCTCATCTCC TCCCGGTTTTAATGA
luc_{160}ermCL rev	ATGAACTGTGCTGATTACAAAAATACTAAAAATGCCTAATTTTT TTTGCACGTTCAAAAT
ompX$_{18}$luc fwd	TGAGAGGAGGAAAACATATGAAAAAAATTGCATGTCTTTCAGC ACTGGCCGCAGTTCTGGCTTTCACCGCAGAAGACGCCAAAAAC ATAA

TABLE II. DNA PRIMERS USED IN THIS STUDY (continued)

T7 yibA fwd	ATTAATACGACTCACTATAGGGATATAAGGAGGAAAACATATG TCAAATACATACCAGAAAAGAAAG
yibA rev	CTATGAACGCTTCAGCTTATCAA
T7 cspA fwd	ATTAATACGACTCACTATAGGGATATAAGGAGGAAAACATATG TCCGGTAAAATGACTGG
cspA rev	TCTGTGCTTTTAAGCAGAGA
T7 mipA fwd	ATTAATACGACTCACTATAGGGATATAAGGAGGAAAACATGTG ACCAAACTCAAACTTCT
mipA rev	TCAGAATTTGTAGGTGATCC
T7 osmC fwd	ATTAATACGACTCACTATAGGGATATAAGGAGGAAAACATATG ACAATCCATAAGAAAGG
Degenerate primer for generating mutations at 746	
Ψ746V	ACCGAACCGACTAATGVTGAAAAATTAGCG

TABLE III. PLASMIDS USED IN THIS STUDY

Name	Selection	Description	Source
pOsmCH	Ampicillin	*osmC-his*$_6$ gene cloned into pBAD22 .	This study
pH-NS$_{12}$OsmCH	Ampicillin	*hns*$_{12}$*osmC-his*$_6$ cloned into pBAD22.	This study
pLK35/A2062G	Ampicillin	Plasmid expressing *rrn*B operon carrying the A2062G mutation in the 23S rRNA gene	Unpublished from a previous study
pLK35/U2609C	Ampicillin	Plasmid expressing *rrn*B operon carrying the U2609C mutation in the 23S rRNA gene	Vázquez-Laslop et al., 2011b
pLK35/U746G	Ampicillin	Plasmid expressing *rrn*B operon carrying the U746G mutation in the 23S rRNA gene	This study

2.4 Determination of MIC of antibiotics on bacterial strains

E. coli was grown in the M9 minimal medium (Miller JH, 1992) supplemented with all 20 amino acids (Sigma-Aldrich, St. Louis, MO) except methionine (M9AA-M) to a final concentration of 40 μg/mL. Composition of the M9 medium (in mM): Na_2HPO_4, 42.25; KH_2PO_4, 22.1; NaCl, 8.5; NH_4Cl, 4.7; $MgSO_4$, 1; $CaCl_2$, 0.1; Thiamine, 0.003. This medium was supplemented with all the amino acids (Sigma-Aldrich, St. Louis, MO) except methionine (M9AA-M) that were added to a final concentration of 40 μg/mL. *S. aureus* cells were grown in a chemically defined medium (Hilliard et al., 1999) containing all 20 amino acids (Sigma-Aldrich, St. Louis, MO) except methionine (CDM-M). Composition of the CDM medium (in mM): Na_2HPO_4, 42.25; KH_2PO_4, 22.1; NaCl, 8.5; NH_4Cl, 4.7; $MgSO_4$, 1; $CaCl_2$, 0.1; Thiamine, 0.003; Nicotinic acid, 0.16. CDM was supplemented with L-amino acids Ala, Asn, Asp, Glu, Gly, Pro and Ser at 0.1 mM final concentration and Arg, Cys, Gln, His, Ile, Lys, Phe, Thr, Trp, Tyr and Val at 0.2 mM final concentration. All the chemicals used to make the M9 and CDM media were purchased from Sigma-Aldrich.

E. coli strain BWDK cells were grown overnight at 37°C in M9AA-M medium. Overnight cultures were then diluted 1:200 in the same medium and grown to exponential phase (A_{600} = 0.2). The cells were subsequently diluted to A_{600} = 0.002 and 150 μL aliquots were added to the wells of 96-well plates supplemented with varying concentrations of antibiotics (2-fold serial dilutions). Plates were incubated at 37°C without shaking. Readings of cell density were taken after 18 hours of incubation at 37°C and the concentration of the drug at which no cell growth occurred was recorded as the MIC (Table IV).

For the determination of the antibiotic MIC for *S. aureus* strains, the cells were initially grown overnight in Muller-Hinton cation-adjusted medium (MH-CA, TekNova, Hollister, CA). The following day cells were diluted 1:200 in the same medium and grown until they reached exponential phase (A_{600} = 0.4). The cultures were then diluted 1:200 into the CDM-M medium to a final density A_{600} = 0.002 and the MIC was determined as described above for *E. coli* (Table IV).

TABLE IV. MINIMUM INHIBITORY CONCENTRATIONS OF RIBOSOMAL ANTIBIOTICS

Strain	Antibiotic	MIC (μg/mL)
E. coli strain BWDK	ERY	1
E. coli strain BWDK	AZM	1
E. coli strain BWDK	TEL	0.5
E. coli strain BWDK	Solithromycin	0.5
E. coli strain BWDK	CHL	1
E. coli strain SQ171	TEL	32
E. coli strain SQ171/A2062U	TEL	32
E. coli strain SQtolC	ERY	1
E. coli strain SQtolC/A2062G	ERY	1
E. coli strain SQtolC/U2609C	ERY	1
E. coli strain SQtolC/Ψ746G	ERY	1
S. aureus strain Newman	ERY	0.25
S. aureus strain Newman	TEL	0.125
S. aureus strain RN4220	CLI	0.016
S. aureus strain RN4220	CHL	2
S. aureus strain RN4220	LZD	0.5
S. aureus strain RN4220	ERY	0.0625
S. aureus strain RN4220	QUI	1
S. aureus strain RN4220	TET	0.0625

2.5 Cell viability assay

Exponentially growing cultures of BWDK cells were exposed to 100-fold MIC of ERY (100 μg/mL) or TEL (50 μg/mL) for four hours. The cultures were serially diluted in triplicates for each experiment and 100 μL of 10^{-2}, 10^{-4} and 10^{-6} serial dilutions were plated on LB agar without antibiotics. The colonies were counted after 16 hours of incubation at 37°C. The number of cells at the time of addition of antibiotics was taken as the no-drug control.

2.6 Metabolic labeling of proteins

The antibiotic hypersensitive *E. coli* strain BWDK (Table I) was grown overnight in M9AA-M medium and diluted 1:200 the next morning in the same medium. 100 μl of exponentially growing cells (A_{600} = 0.2) were exposed to different antibiotics at concentrations ranging from 1- to 100-fold MIC for 15 minutes, after which cells were incubated with 1 μCi [^{35}S]-methionine (specific activity 1175 Ci/mmol, MP Biomedicals) for an additional minute. The proteins were precipitated by adding an equal volume of ice-cold 25% trichloroacetic acid (TCA, ThermoFisher Scientific) containing 2% casamino acids (ThermoFisher Scientific). After incubating for 30 minutes on ice and then 30 minutes at 100°C, samples were passed through G4 glass fiber filters (ThermoFisher Scientific). The filters were washed three times with 3 mL of ice cold 5% TCA, and once with 3 mL of acetone (ThermoFisher Scientific), air dried, and the amount of retained radioactivity was determined by scintillation counting using a TopCount NXT instrument (Perkin Elmer, Shelton, CT). The data were normalized relative to the 'no drug' control. For the time course experiments, 100-fold MIC of each antibiotic was added to 100 μL of exponentially growing cells and incubated for 1, 2.5, 5,

10, 15 or 30 minutes. Following incubation, 1 μCi of [^{35}S]-methionine was added and the cells were incubated for one more minute. The following steps were repeated as described above.

For *S. aureus* strain RN4220, an overnight culture grown in MH-CA medium was diluted 1:200 in CDM-M medium and the remainder of the procedure for metabolic labeling was the same as performed with *E. coli*.

2.7 2D-gel electrophoresis analysis of the radiolabeled proteins

Exponentially growing cultures (50 mL) of *E. coli* (strain BWDK, M9AA-M medium) or *S. aureus* (strain Newman, CDM-M medium) were incubated with 100-fold MIC of ERY (100 μg/mL for *E. coli*; 25 μg/mL for *S. aureus*), TEL (50 μg/mL for *E. coli*; 12.5 μg/mL for *S. aureus*), AZM (100 μg/mL for *E. coli*), or solithromycin (50 μg/mL for *E. coli*) for 15 minutes at 37°C. [^{35}S]-methionine (250 μCi, specific activity 1175 Ci/mmol) was then added, and the cells were incubated for 3 minutes, followed by the addition of unlabeled L-methionine (Sigma-Aldrich) to final concentration of 80 μg/mL and further incubation for 7 minutes. The cells were pelleted by centrifugation at 4000 *g* for 15 minutes at 4°C. The *E. coli* cells were resuspended in 200 μl of buffer containing 60 mM Tris, pH 6.8, 5% SDS, 10% glycerol and lysed by boiling for 5 minutes. *S. aureus* cells were lysed by resuspending in 200 μl mL of the lysis buffer (Tris-HCl, pH 7.5, 30 mM $MgCl_2$, 30 mM NH_4Cl, 0.1 mg/mL lysostaphin, 100 U of Omnicleave endonuclease (Epicentre, Madison, WI)) and incubation at 37°C for 30 minutes. Cell lysates were centrifuged and the supernatant was passed through a 0.22 μm filter. The extracted proteins (600 μg, *E. coli,* or 200 μg, *S. aureus*) were shipped to the Kendrick Labs, Inc. (Madison, WI) where they were fractionated by two-dimensional gel

electrophoresis (isoelectric focusing in the pH gradient 4-7 during the first dimension followed by size separation on a 10% SDS-PAGE gel in the second dimension) (O'Farrell, 1975). The gels were stained with Coomassie Brilliant Blue, dried, and exposed to the phosphorimager screen overnight. The image was scanned using the Typhoon 9410 Scanner (GE Healthcare Bio-Sciences AB, Uppsala, Sweden).

For each 2D-gel experiment a no-drug, non-radioactive control sample was included from cells grown to exponential phase and harvested before the addition of antibiotic or [^{35}S]-methionine, in order to enable mass spectrometry-assisted identification of protein spots (section 2.8).

Separately for *S. aureus* strain RN4220, 25 mL of actively growing cells (A_{600} = 0.4) was incubated with 100-fold MIC of each antibiotic (Table IV) for 15 minutes. [^{35}S]-methionine (250 μCi, specific activity 1175 Ci/mmol, MP Biomedicals) was added, and cells were incubated for 3 minutes, followed by the addition of unlabeled L-methionine (Sigma-Aldrich) to a final concentration of 80 μg/mL and incubation was continued for seven more minutes. The cells were pelleted and resuspended with 200 μl of osmotic lysis buffer (10 mM Tris, pH 7.4, and 0.3% SDS) containing protease inhibitors, 10 μg of RNase A (Sigma-Aldrich), 20 μg of DNase I (Sigma-Aldrich) and 100 mg of washed glass beads (425-6000 μm, Sigma-Aldrich). The samples were vortexed, sonicated and frozen. The thawed samples were vortexed again to extract proteins. The extracted proteins (~200 μg) were fractionated by two-dimensional gel electrophoresis (O'Farrell, 1975) at Kendrick Labs, Inc. (Madison, WI) within a pH gradient of 4-6 during the first dimension of separation. The pH-resolved proteins were further separated on a 10% gel

using SDS-PAGE. The gels were stained with Coomassie Brilliant Blue, dried, and exposed to the phosphorimager screen for 48 hours and scanned as described above.

2.8 Protein identification

The radiolabeled spots in the 2D gels containing ERY- or TEL-treated samples were computationally correlated with the Coomassie-stained, non-radiolabeled 2D gels (Progenesis SameSpots, Nonlinear Dynamics, Durham, NC). The stained protein spots were cut out and subjected to LC/MS/MS analysis at the Proteomics facility, Research Resources Center of the University of Illinois at Chicago. The resulting raw files were searched against the database of *in silico* trypsin-digested *E. coli* strain BW25113 proteome using Mass Matrix software (Xu et al., 2007)

2.9 Generation of PCR products for *in vitro* translation

DNA templates for *in vitro* transcription/translation were generated using PCR. The appropriate promoter sequences were introduced depending on the type of *in vitro* transcription-translation system. The T7 promoter sequence was directly introduced into the forward PCR primer. However, the P_{tac} promoter was introduced using two successive PCR reactions. During the first PCR, a portion of the tac promoter was added to the template. The end product of this reaction was used as a template in the second PCR. In the second PCR, using the forward primer Ptac-BamHI (Table II) and the gene-specific reverse primer, the complete template was generated with the full sequence of the tac promoter. For all the PCR reactions high fidelity polymerases Phusion HF (New England Biolabs, Ipswich, MA) or Accuprime HF (Life Technologies, Grand Island, NY) were used. The PCR products were purified using the Wizard® SV Gel and PCR Clean-Up System (Promega) and concentrated using the Vacufuge vacuum concentrator

(Eppendorf AG, Hamburg, Germany) to a final concentration of 100-150 ng/μL before use. All *E. coli* genes were amplified from the genomic DNA isolated from *E. coli* strain BW25113 and *luc* from the pBEST-luc vector (Promega).

In order to fuse the *ermCL* coding region to the end of the *hns* gene, two PCR reactions were carried out. In the first reaction, hns ermCL rev1 and T7 hns fwd (Table II) primers were used to amplify the *hns* gene from *E. coli* strain BW25113 genomic DNA. The resultant product was amplified further using the hns ermCL rev2 and T7 hns fwd primers. The NV1 primer-annealing site (Table II) was introduced using the hns ermCL rev2 primer for the *hns-erm*CL fusion template.

2.10 Cell-free protein synthesis and analysis of translation products

In vitro translation was carried out either in the *E. coli* S30 cell-free transcription-translation system for linear templates (Promega) or in the PURE system (New England Biolabs). For translation in the S30 system, the PCR-generated DNA template (0.1-0.5 pmol) carrying the desired gene under the control of the P_{tac} promoter was added to a 5 μL reaction containing 2 μCi of [^{35}S]-methionine (specific activity 1175 Ci/mmol, MP Biomedicals), 1.5 μL of cell-extract, 2 μL of S30-premix solution and 0.5 μL of the amino acid mix (lacking methionine). If included, 0.5 μL of antibiotic was added from a 10X stock of the desired final concentration. After 30-45 min incubation at 37°C, the reactions were treated with 0.5 μg RNase A (Sigma-Aldrich) for 5 min at 37°C and proteins were precipitated with four volumes of ice-cold acetone (ThermoFisher Scientific). Protein pellets were dissolved in 10 μL of the loading dye (BioRad Laboratories, Hercules, CA) and fractionated in a 16.5 % polyacrylamide gel (0.5 mm thick; 6 cm long) using the Tricine-SDS buffer system (Schagger et al., 1987). Gels were

stained with Coomassie Brilliant Blue (Sigma- Aldrich), washed with increasing concentrations of ethanol, dried, exposed overnight to a phosphorimager screen and scanned as described in section 2.7. The protein bands in the image were quantified using the ImageJ software (http://rsbweb.nih.gov/ij/). The background intensity was subtracted and the integrated density values were normalized relative to the no-drug control. The normalized band intensity values were fitted to a sigmoidal dose response curve (95% confidence interval) using the Prism software (GraphPad Software, Inc., La Jolla, CA).

The activity of *in vitro* translated firefly luciferase was determined using the Luciferase Assay Reagent (Promega) as recommended by the manufacturer. Specifically, 1 µL of the S30-translation reaction was diluted 1:50 using the GloLysis buffer (Promega) and 30 µL of this mixture was combined with an equal volume of the Bright-Glo™ Luciferase Assay Buffer (Promega). Luminescence counts were measured for 10 seconds on a 96-well Optiwell plate (Perkin Elmer, Shelton, CT) using a TopCount NXT instrument (Perkin Elmer).

2.11 Toe-printing assay

For the toe-printing assay, the DNA templates were transcribed and translated using the PURE system (New England Biolabs). The toe-printing assay for drug-dependent ribosome stalling was carried out as described (Vazquez-Laslop et al., 2008), with minor modifications. The templates coding for the protein sequences under the control of T7 promoter were generated by PCR. Between 0.05-0.1 pmol of the templates were used in a total volume of 5 µl of the PURE *E. coli* cell-free transcription-translation system (Shimizu et al., 2001) containing 2 µl of solution A (New England Biolabs) and 1.5 µl (New England Biolabs) of solution B, and whenever included and unless

mentioned otherwise, 50 μM of the antibiotic. The reactions were incubated for 15 min at 37°C, followed by addition of the ^{32}P-radiolabeled toe-printing primer designed to anneal ~100 nucleotides downstream from the anticipated ribosome stalling site in *fus*A (primer EF-G_{390} rev), *erm*CL (NV1) or *luc* (primer hns_{18}luc TP-3) genes (Table II). In order to probe ribosome stalling near the gene's 5' end, a primer was annealed at ~90-100 nucleotides downstream from the start codon of each template (primers osmC100 rev, hns toeprinting-4, mipA100 rev, cspA110 rev). The primer used for toe-printing was labeled at the 5'-end in a 5 μL reaction containing 20 pmol of the primer, 1.5 μL γ^{32}P ATP (6000 Ci/mmol, MP Biomedicals), 0.5 μL 10X Buffer A (Fermentas) and 1 μL (10 U) T4 polynucleotide kinase (Fermentas). The reaction was incubated at 37°C for 30 minutes and the enzyme was heat inactivated at 90°C for 2 minutes. 0.8 μL of the labeled primer, along with 0.3 μL (12 U) of RiboLock RNase Inhibitor (Fermentas) were added to the translation reaction and further incubated at 37°C for 2 minutes to allow the primer to anneal to the mRNA. The reaction was stopped by incubation on ice for 5 minutes. One μL of a mixture of dNTP (2 mM) and 3 U of reverse transcriptase (Roche Applied Science) was added to the reaction incubated at 37°C for 20 minutes. Following this, 1 μL 10 N NaOH was added and the reaction was incubated at 37°C for 15 minutes. Alkali was then neutralized by adding 0.8 μL of 100% HCl. 200 μL resuspension buffer (0.3 M NaOAc, pH 5.5, 5 mM EDTA and 0.5 % SDS) was added to the reaction and the reverse transcribed DNA was extracted with the same volume of Tris-saturated phenol (Roche Applied Science, pH-7.54-7.74), followed by extraction with the same volume of 100% chloroform (ThermoFisher Scientific). Three volumes (600 μL) of 100% of ethanol were added and incubated -80°C for 30 minutes. The samples were centrifuged for 45 minutes

at 4°C at 21,000 *g*. The pellets were further washed with 500 µL 70 % ethanol and subsequently dried using a Vacufuge vacuum concentrator (Eppendorf AG) for 5 minutes. The pellets were resuspended in 6 µL formamide dye, heated at 100°C for 2 minutes and 1.5 µL was loaded on a 6 % sequencing (0.375 mm) gel. The gel (40 cm) was run at 40 W for ~80 minutes following which it was transferred to a paper (Whatman, GE Healthcare Bio-Sciences AB), dried and exposed to the phosphorimager screen.

2.12 Bioinformatic analysis of the *E. coli* proteome

The *E. coli* proteome was searched for a motif resembling I_7LNNIR_{12} sequence of H-NS using the regular expression [**I**LAVGM]-[I**L**AVGM]-[**N**QST]-[**N**QST]-[**I**LAVGM]-[K**R**H]. The GenomeNet MOTIF tool was utilized for this purpose (http://www.genome.jp/tools/motif/MOTIF2.html). The hits were manually selected for those containing the motif at the N-terminus (1-15 amino acids) of the respective protein.

2.13 Preparation of *E. coli* strains expressing mutant ribosomes

The mutations A2062G, U2609C and Ψ746G were introduced in the 23S rRNA gene in the pLK35 plasmid (Douthwaite et al., 1989) as described in the section 2.3.2. The mutant plasmids were transformed into *E. coli* strain SQtolC cells (Table I). Transformants were selected on LB agar plates containing 100 µg/mL ampicillin. Elimination of the prrnC-*sac*B plasmid containing the wild type rRNA operon was carried out following Zaporojets et al. (2003) with some modifications. Specifically, two ampicillin-resistant clones of each mutant were grown in LB/ampicillin (100 µg/mL) medium to the stationary phase, diluted 1:1000 in the same medium and grown to the stationary phase again. The cycle was repeated one more time followed by a final dilution

in the LB/ampicillin (100 μg/mL) media lacking sodium chloride but containing 5% sucrose. Cells were grown up to an optical density of 0.5, serially diluted, and 100 μL of 10^{-5}, 10^{-6} and 10^{-7} dilutions were plated on LB agar plates containing 5% sucrose but lacking sodium chloride. The loss of the wild-type rRNA encoding plasmid was verified by replica plating of 100 colonies on LB/ampicillin (100 μg/mL) and LB/ kanamycin (50 μg/mL) and selecting for kanamycin-sensitive and ampicillin-resistant colonies. The cells carrying the pLK35 plasmid were further verified to contain the NPET mutation by sequencing the PCR fragment encompassing the mutated nucleotide amplified from the total DNA.

2.14 Protein synthesis by mutant ribosomes

The wild type and A2062U mutant ribosomes were isolated as described by Shimizu et al. (2005) by Dorota Klepacki in this lab.

The *in vitro* translation of the *fus*A or *yib*A genes by wild type and A2062U mutant ribosomes was carried out in 5 μl reactions (Δribosome PURExpress, New England Biolabs) containing 0.5 pmol of DNA templates and 15 pmoles of the ribosomes. After incubation at 37°C in the presence or absence of TEL for 45 minutes (50 μM in the *fus*A-containing reaction or 10 μM during *yib*A expression), the reactions were stopped as described in section 2.10 and analyzed by SDS gel electrophoresis.

2.15 Protein synthesis in the *E. coli* strains expressing mutant ribosomes

E. coli strain SQtolC cells expressing wild type or mutant (A2062G or U2609C) ribosomes were grown in 10 mL of M9AA-M media supplemented with LB/ampicillin (100 μg/mL) at 37°C. Exponentially growing cultures were incubated with 100-fold MIC of ERY (100 μg/mL) for 15 minutes prior to the addition of 100 μCi of [^{35}S]-methionine

(specific activity 1175 Ci/mmol, MP Biomedicals), incubation for 3 minutes and the subsequent addition of an excess of L-methionine (final concentration 80 μg/mL) (Sigma-Aldrich) and further incubation for 7 minutes at 37°C. Cells were harvested by centrifugation, lysed by boiling in SDS gel loading buffer (BioRad Laboratories) and proteins were resolved on a 20 cm long 16.5% SDS gel using on the tricine-buffer system (Schagger et al., 1987) as described in section 2.10.

2.16 Purification of OsmC and H-NS$_{12}$OsmC

BWDK cells containing pBAD22-*osm*C or pBAD22-*hns$_{12}$osm*C plasmids were grown overnight in the M9AA-M medium supplemented with LB/ampicillin (100 μg/mL) at 37°C and then diluted 1:200 in 1.5 mL of the same medium. Expression of *osm*C or *hns$_{12}$osm*C was induced at the exponential phase by the addition of 1 mM L-arabinose. After 30 minutes of induction, no drug or ERY (100 μg/mL) was added and the cells were incubated for 15 minutes. Subsequently, 15 μCi of [^{35}S]-methionine was added to the medium and cells were incubated for 3 more minutes. After chasing for seven minutes with an excess of cold L-methionine (final concentration 80 μg/mL), cells were collected by centrifugation at 4000 *g* at 4°C for 5 minutes.

Cell pellets from 1.5 mL cultures were lysed in 100 μL of B-Per reagent (Thermo Scientific), supplemented with 1X (final concentration) EDTA-free protease inhibitor cocktail (Thermo Scientific) and 3 U of Omnicleave endonuclease (Epicentre). The lysate was incubated with 50 μL of freshly regenerated Ni-NTA agarose resin (QIAGEN, Inc., Valencia, CA) for 30 minutes at 4°C. The resin was pelleted at 1500 *g* for 1 minute at 4°C and washed twice with 200 μL of the binding buffer (20 mM Tris-HCl pH-8, 300 mM NaCl, 10 mM Imidazole). The His-tagged proteins were eluted from the resin using

the elution buffer (20 mM Tris-HCl pH-8, 300 mM NaCl, 250 mM Imidazole). The proteins were then acetone precipitated, resuspended in 10 µL of gel loading buffer and resolved on a 16.5% gel as described in section 2.9.

III. Selective protein synthesis in the presence of macrolide antibiotics

3.1 Introduction and rationale

The proteins assembled in the PTC exit the ribosome through the NPET. The NPET is approximately 100 Å long and 10-20 Å wide, and starts at the PTC, penetrating through the body of the large ribosomal subunit (Yonath et al., 1987; Frank et al., 1995; Nissen et al., 2000; Voss et al., 2006). The tunnel ensures the successful passage of newly made proteins out of the ribosome, and thus is able to accommodate a vast variety of nascent peptide sequences. The ribosomal NPET is the site of action of clinically important macrolide antibiotics (Figures 2 and 5) (Vazquez, 1966a).

Treatment of sensitive bacteria with macrolides curtails protein synthesis and leads to the accumulation of peptidyl-tRNAs (Figure 5) (Brock et al., 1959; Menninger et al., 1994; Taubman et al., 1963). ERY also efficiently inhibits the translation of some synthetic and natural mRNAs *in vitro* (Otaka et al., 1975; Starosta et al., 2010; Tenson et al., 2003). The presence of ERY in a cell-free system abolishes synthesis of long polypeptides leading instead to the production of peptidyl-tRNAs carrying short peptides ranging from 4-8 amino acids (Otaka et al., 1975; Tenson et al., 2003; Vazquez, 1966a).

Mapping the binding site of macrolides in the ribosome has helped rationalize these observations (Ettayebi et al., 1985; Graham et al., 1979; Moazed and Noller, 1987a). Macrolides bind in the NPET near the PTC just above a constriction formed by extended loops of ribosomal proteins L4 and L22 (Bulkley et al., 2010; Dunkle et al., 2010; Schlunzen et al., 2001; Tu et al., 2005). Antibiotic binding dramatically narrows this area of the tunnel, thus hindering the progression of the nascent peptide. Therefore, it is generally thought that translation is aborted when the nascent peptide advancing

through the NPET reaches the site of antibiotic binding. The notion that a macrolide molecule and an extended nascent chain cannot coexist in the NPET is further supported by the inability of ERY to bind to ribosomes carrying long nascent peptides (Andersson et al., 1987; Tai et al., 1974). The 'plug-in-the-bottle' model of macrolide action implies that these drugs, like the majority of protein synthesis inhibitors, indiscriminately stop the production of every protein in the cell during the early stages of their synthesis.

However, some experimental data were hard to reconcile with the conventional 'plug' model (reviewed in Mankin, 2008). The discovery of drug-dependent ribosome stalling during translation of short regulatory peptides controlling expression of macrolide resistance genes raised the possibility of sequence-specific interactions of antibiotics with the nascent peptide (Horinouchi et al., 1980; Mayford et al., 1989). This thought was further reinforced by the identification of short peptides that could co-translationally evict macrolide antibiotics from the ribosome (Lovmar et al., 2006; Tenson et al., 1996; Tenson et al., 2001; Vimberg et al., 2004). Several reports also indicated that the inhibitory effects of macrolides on translation of individual reporters in a cell-free system might vary (Hardesty et al., 1990; Odom et al., 1991; Starosta et al., 2010; Vazquez, 1966). For example, ERY was shown to inhibit the translation of poly(A)-directed-poly(Lys) synthesis but the drug had little effect on poly(U)-directed-poly(Phe) production (Hardesty et al., 1990). Moreover, the tylosin precursor 5-O-mycaminosyl-tylonolid is a potent inhibitor of firefly luciferase synthesis but fails to inhibit green fluorescent protein synthesis (Starosta et al., 2010). Furthermore, the conventional model of macrolide action could not adequately explain why the newer generation of antibiotics (ketolides) exhibits improved bactericidal activity against some

pathogens (Hamilton-Miller et al., 1998; Woosley et al., 2010). Although recent crystallographic studies of the ribosome complexed with macrolide antibiotics confirmed the notion that the drug obstructs the NPET (Bulkley et al., 2010; Dunkle et al., 2010; Schlunzen et al., 2001; Tu et al., 2005), the structures showed that the bound macrolide molecule leaves a considerable amount of room in the NPET. Moore, Steitz and coworkers (Tu et al., 2005) proposed that the residual space could be wide enough to give the nascent peptide an opportunity to slither through. Such a possibility was considered even earlier by Weisblum (1995b). However, it remained unknown whether such an opportunity is ever realized.

In order to clarify the basis for the discrepancies between experimental data and the conventional model of macrolide action, we revisited the mode of action of these antibiotics. Specifically, we asked whether macrolides inhibit translation completely as suggested by the commonly accepted model and tested the validity of the 'plug-in-the-bottle' model. Furthermore, we further investigated whether the macrolide molecule bound to the NPET could allow the simultaneous placement of a nascent peptide as suggested by Tu et al., (2005).

3.2 Experimental results

3.2.1 A selective subset of proteins is synthesized in bacterial cells exposed to high concentrations of macrolide antibiotics

To re-evaluate the mode of translation inhibition by macrolides, we monitored the incorporation of radioactive [^{35}S]-methionine into proteins after the exposure of bacteria to an antibiotic. For these experiments, a macrolide sensitive *E. coli* strain was prepared by inactivating the *tol*C gene. At the minimal inhibitory concentration (MIC) of ERY (1

μg/mL) (Table IV), an expected drop in overall protein synthesis was observed (Figure 10A). Raising the ERY concentration to nearly 20-fold the MIC correlated with a further decrease in protein synthesis down to 5-7% of the untreated control. Unexpectedly, however, further increase in the concentration of the antibiotic had little effect on the residual translation: cells exposed to 100-fold the MIC continued to synthesize proteins at approximately 6% of the level of the control. Even more striking, TEL, a ketolide, known to be a more potent antibiotic than ERY, permitted a much higher level of residual protein synthesis: 20-25% persisted at 100-fold the MIC. The onset of translation inhibition by macrolides was very rapid and the maximal level of inhibition was achieved as early as 5 min after the addition of the drug; however, substantial residual protein synthesis persisted even after 6 hours of incubation with the antibiotic (Figure 10B).

Persistent translation in the presence of macrolides could be accounted for by the accumulation of short peptidyl drop-off products, the low-level expression of all proteins (due to, for example, an occasional dissociation of the drug from the translating ribosomes (Lovmar et al., 2006)) or, alternatively, in a more unconventional scenario, the selective expression of a subset of polypeptides. In order to discriminate between these possibilities, we visualized the proteins synthesized in bacteria exposed to macrolide antibiotics. Exponentially growing cells were incubated with 100-fold the MIC of different macrolides for 15 min. After pulse labeling with [^{35}S]-methionine, the proteins newly synthesized in the presence of the drugs were resolved by 2D gel-electrophoresis (Figure 11). Under these conditions, synthesis of majority of cellular polypeptides is almost completely inhibited by ERY or AZM (Figure 11A).

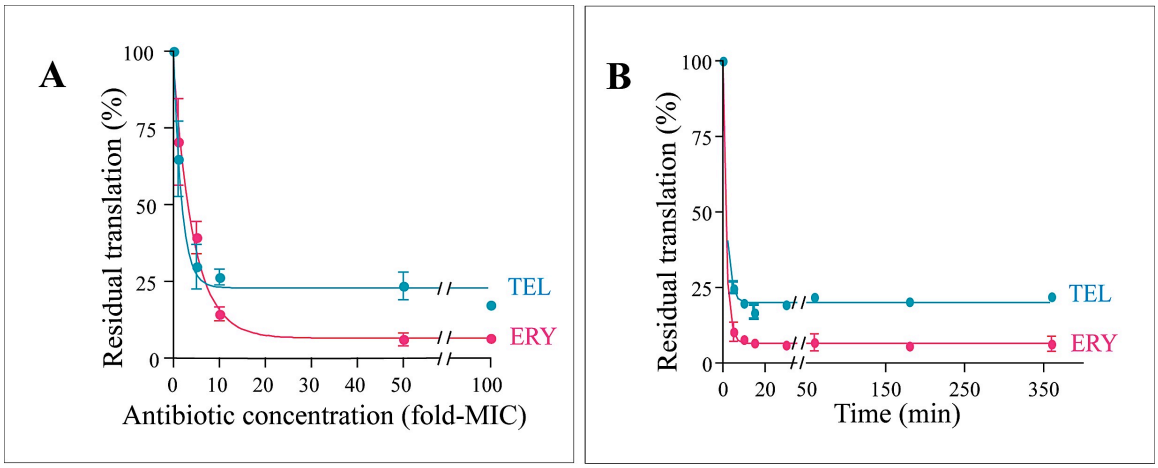

Figure 10. Protein synthesis in cells exposed to macrolide antibiotics. (A) Residual translation in the presence of increasing concentrations of ERY and TEL. Pulse-incorporation of [^{35}S]-methionine in the protein fraction was determined after 15-minute exposure of macrolide-sensitive *E. coli* strain BWDK cells to varying concentrations of the drugs. Minimal drug inhibitory concentrations of *E. coli* strain BWDK is 1 µg/mL for ERY and 0.5 µg/mL for TEL (Table IV). (B) Residual protein synthesis after exposure of *E. coli* cells to 100-fold MIC of ERY or TEL for varying times.

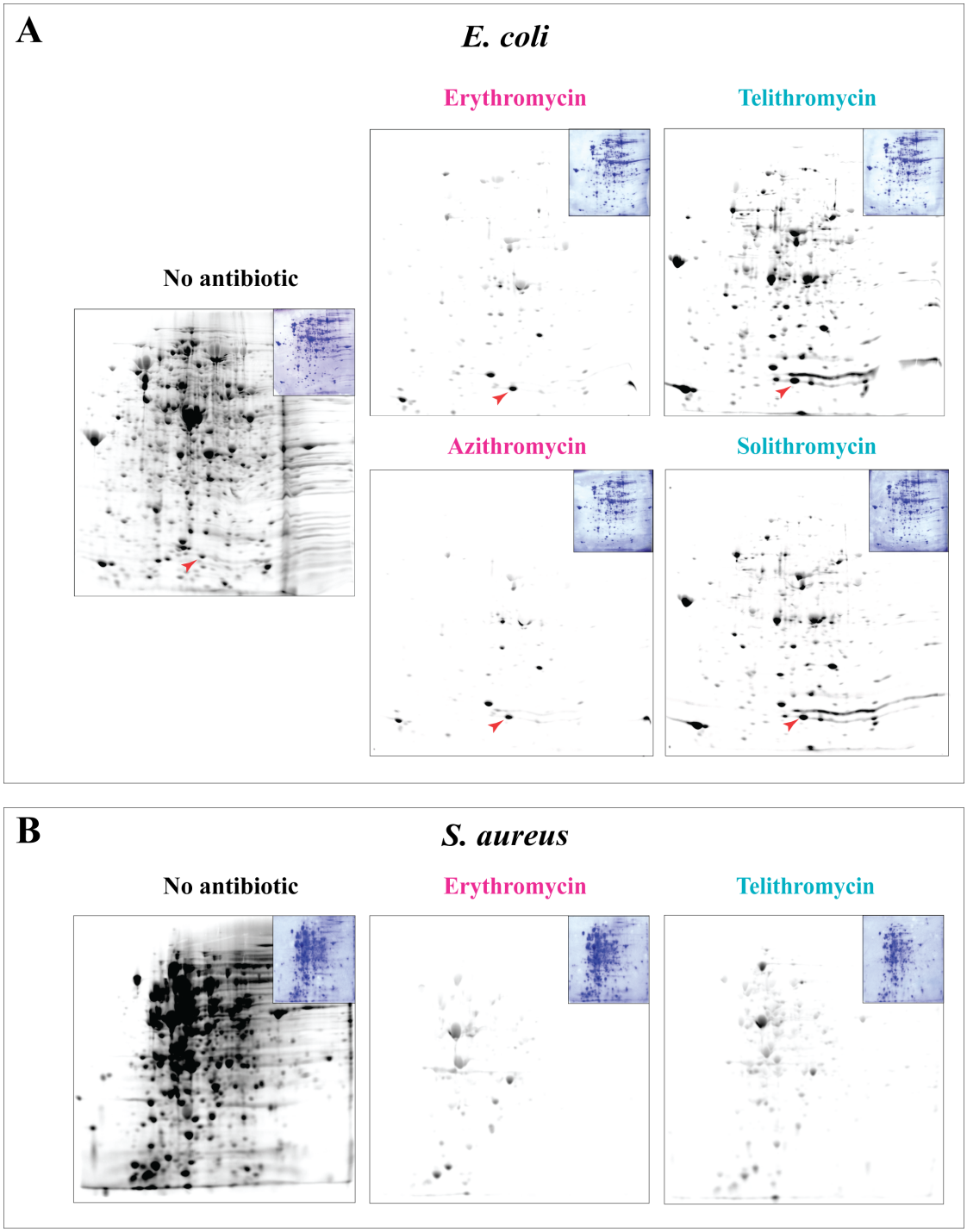

Figure 11. 2D-gel analysis of proteins synthesized *in vivo* in the presence of macrolides. Pulse-labeled proteins, isolated from *E. coli* strain BWDK (A) or *S. aureus* strain Newman (B) Cells exposed for 15 minutes to 100-fold MIC of ERY, TEL, AZM or Solithromycin (for *E. coli*), ERY or TEL (for *S. aureus*) were resolved by 2D gel-electrophoresis. Spots representing the H-NS protein are indicated on the gels by red arrowheads. Coomassie-stained gels are shown in insets.

However, the inhibition of protein synthesis was not uniform, as a small number of labeled protein spots were observed even at high antibiotic concentrations. This indicates that specific polypeptides continue to be actively synthesized in the presence of the antibiotic, albeit at levels somewhat lower compared to the control cells. The spectrum of proteins synthesized in the presence of the drug remained largely unchanged even after prolonged exposure (up to 6 hours) of cells to the antibiotic (Figure 12). In agreement with the bulk radiolabel incorporation experiments (Figure 10), the number of resistant proteins and the level of their translation in cells exposed to ketolides, such as TEL and solithromycin, was higher than in cells treated with ERY or AZM (Figure 11A). Although some proteins were resistant to all macrolides tested (Figure 13, green circles), many polypeptides exhibited drug-specific resistance (Figure 13, blue and magenta circles). It appears that the chemical structure of the drug bound in the NPET defines the spectrum of the resistant polypeptides. The protein-specific inhibitory action of macrolides was not limited to the Gram-negative *E. coli*, but was also observed in the Gram-positive pathogen *S. aureus* strain Newman (Figure 11B), demonstrating the general nature of the phenomenon of selective protein escape from inhibition by macrolide antibiotics.

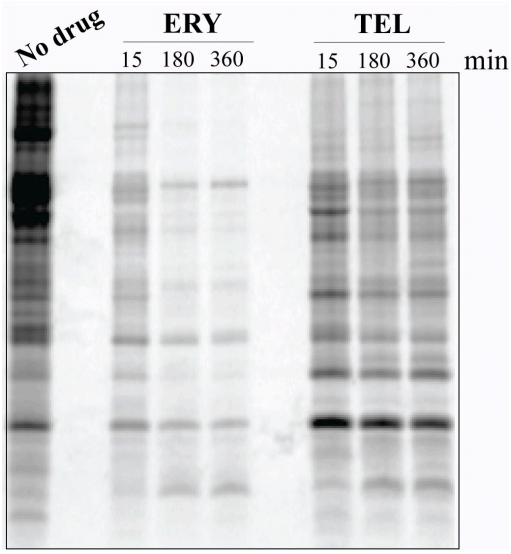

Figure 12. *In vivo* residual translation is barely affected by the length of incubation with macrolides. *E. coli* strain BWDK cells were incubated for 15, 180 and 360 minutes with 100 μg/mL of ERY or 50 μg/mL of TEL. Synthesized proteins were pulse-labeled with [^{35}S]-methionine for 3 minutes and chased for 7 minutes with an excess of unlabeled methionine prior to analysis by SDS-gel electrophoresis.

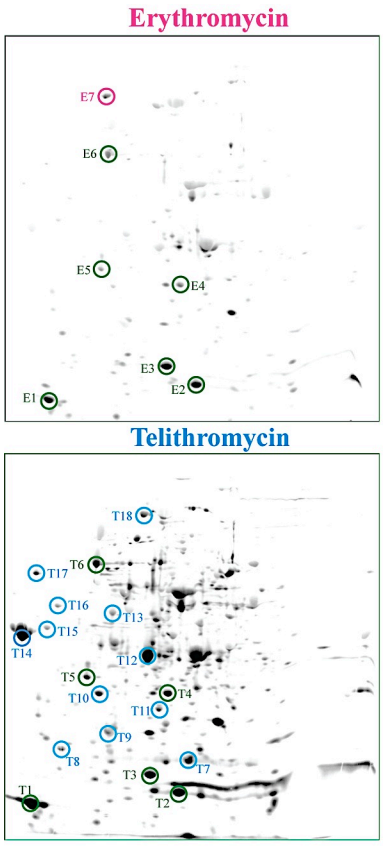

ERY- and TEL-resistant proteins			MM score
E1, T1	L7/L12	MSITKDQIIEAVAAMSVMDV	497
E2, T2	H-NS	MSEALKILNNIRTLRAQARE	463
E3, T3	OmpX	MKKIACLSALAAVLAFTAGT	1002
E4, T4	PspA	MGIFSRFADIVNANINALLE	950
E5, T5	Tsx	MKKTLLAAGAVLALSSSFTV	724
E6, T6	Tig	MQVSVETTQGLGRRVTITIA	2214
ERY-resistant protein			
E7	BamA	MAMKKLLIASLLFSSATVYG	2030
TEL-resistant proteins			
T7	PpiB	MVTFHTNHGDIVIKTFDDKA	441
T8	Crr	MGLFDKLKSLVSDDKKDTGT	367
T9	AhpC	MSLINTKIKPFKNQAFKNGE	957
T10	MipA	MTKLKLLALGVLIATSAGVA	709
T11	Upp	MKIVEVKHPLVKHKLGLMRE	1069
T12	EF-Ts	MAEITASLVKELRERTGAGM	1537
T13	RpoA	MQGSVTEFLKPRLVDIEQVS	1256
T14	OmpC	MKVKVLSLLVPALLVAGAAN	1982
T15	OmpF	MMKRNILAVIVPALLVAGTA	1436
T16	FtsZ	MFEPMELTNDAVIKVIGVGG	1769
T17	FliC	MAQVINTNSLSLITQNNINK	1207
T18	Pnp	MLNPIVRKFQYGQHTVTLET	2041

Figure 13. Macrolide- and ketolide-resistant *E. coli* proteins. Radioactive spots corresponding to proteins identified by mass-spectrometry are circled on the 2D-gels. Proteins expressed in the presence of both ERY and TEL are marked green, TEL-resistant proteins are indicated in blue and the ERY-resistant protein is in magenta. The table lists the 20 amino acid-long N-terminal sequences of the identified proteins. The sequence motif found in several TEL-resistant proteins is underlined. MassMatrix scores (MM) are indicated in the right column.

3.2.2 The N-terminal sequence defines the protein's ability to evade inhibition by macrolide antibiotics

To gain insights into the molecular mechanisms of drug evasion by selected proteins, we examined how ERY affects the translation of individual polypeptides *in vitro*. We first identified some of the proteins synthesized in *E. coli* cells exposed to macrolides. Several spots from the 2D gels (Figure 11A) with the highest relative radioactivity and electrophoretic mobility similar to the untreated control were excised and analyzed by mass-spectrometry. After discarding the proteins with low confidence scores and spots with ambiguous identity assignments, we were able to positively identify 7 proteins that were resistant to ERY and 18 that were resistant to TEL (Figure 13). Four of the ERY resistant polypeptides corresponded to secreted outer membrane (OmpX, Tsx, BamA) or inner membrane (PspA) proteins whose translation is difficult to reproduce faithfully in the cell-free system. Of the three remaining cytosolic proteins, we chose the small cytoplasmic protein H-NS (16kDa), which was expressed in cells treated with all of the tested macrolides (arrowheads in Figure 11A), for the subsequent *in vitro* experiments. As a control, we used an ERY-sensitive cytoplasmic protein of comparable size, OsmC (15 kDa). While the synthesis of OsmC in the *E. coli* S30 cell-free system was readily inhibited by ERY (IC_{50} = 0.8 ± 0.3 μM), translation of H-NS was only marginally affected even at higher concentrations of antibiotic, thereby recapitulating the *in vivo* results (Figures 14 A and B). The N-terminus of H-NS is the first to encounter the antibiotic in the NPET and therefore, may account for the ability of the protein to evade the macrolide inhibitory action. We tested this idea by fusing the first 18 codons of *hns* to the 5' end of the *osm*C gene and analyzing the translation of the chimeric protein in the

S30 cell-free system in the presence of ERY. In agreement with our hypothesis, the H-NS N-terminus rendered OsmC highly resistant to the drug (Figures 14 A and B).

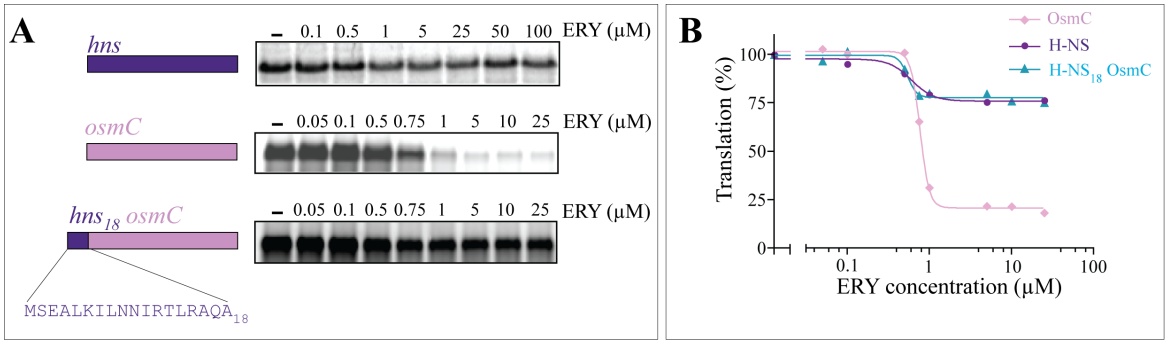

Figure 14. The N-terminal amino acid sequence of H-NS renders proteins resistant to ERY. (A) The effect of increasing concentrations of ERY on cell-free translation of H-NS (purple), OsmC (pink) and the H-NS$_{18}$OsmC hybrid. Shown gel bands represent the full-size [^{35}S]-labeled proteins resolved by SDS gel electrophoresis. (B) Quantification of the bands from gels in panel A.

The resistance of H-NS_{18}OsmC to ERY was retained when multiple synonymous codon replacements were introduced in the *hns* segment of the hybrid mRNA (Figure 15A). This result indicates that the ability to elude drug action is associated with the nascent peptide rather than with the mRNA structure. In order to better define the amino acid sequence sufficient for drug evasion, we appended a varying number of H-NS N-terminal residues to OsmC (Figure 15B). Resistance to the antibiotic started to increase when 7 or more amino acids were added and saturated upon the addition of 12-15 H-NS residues. Thus, the resistance determinant resides primarily within the M_1SEALKILNNIR_{12} N-terminal amino acid segment of H-NS.

In order to understand the importance of the N-terminal amino acid sequence in escaping macrolide inhibition *in vivo*, we appended the MSEALKILNNIR sequence to the OsmC N-terminus and monitored its production inside cells in the presence of ERY. *E. coli* strain BWDK cells expressing C-terminally his_6-tagged OsmC and H-NS_{12}OsmC were exposed to ERY (or no drug) prior to the addition of [^{35}S]-methionine. Our results show that in the absence of any antibiotic, both OsmC and H-NS_{12}OsmC were expressed *in vivo*, while treatment with ERY only permitted the synthesis of H-NS_{12}OsmC. This result underscores the importance of the nature of N-terminal amino acids of a polypeptide in bypassing ERY inhibition not only *in vitro*, but also *in vivo* (Figure 16).

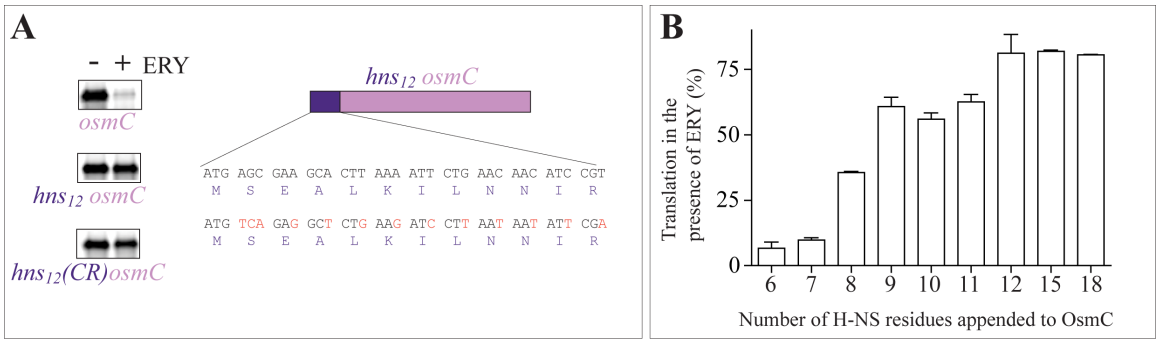

Figure 15. Characterization of the N-terminal bypass by H-NS amino acids. (A) Influence of mRNA structure on N-terminal bypass of ERY-resistance by H-NS. Synonymous codon substitutions within the twelve 5'-terminal *hns* codons of *hns*$_{12}$*osm*C do not diminish ERY resistance of the hybrid protein in the cell-free translation system. The nucleotide substitutions in the codon-replacement construct, *hns*$_{12}$*(CR)osm*C, are shown in red. (B) Effects of the number of N-terminal H-NS amino acid residues appended to OsmC in ERY-bypass. Hybrid proteins were translated in the *E. coli* S30 cell-free translation system in the absence or the presence of 50 μM ERY. The bars represent the mean value of residual translation in two independent experiments with the error bars representing absolute deviation. H-NS and OsmC are represented by purple and pink bars, respectively.

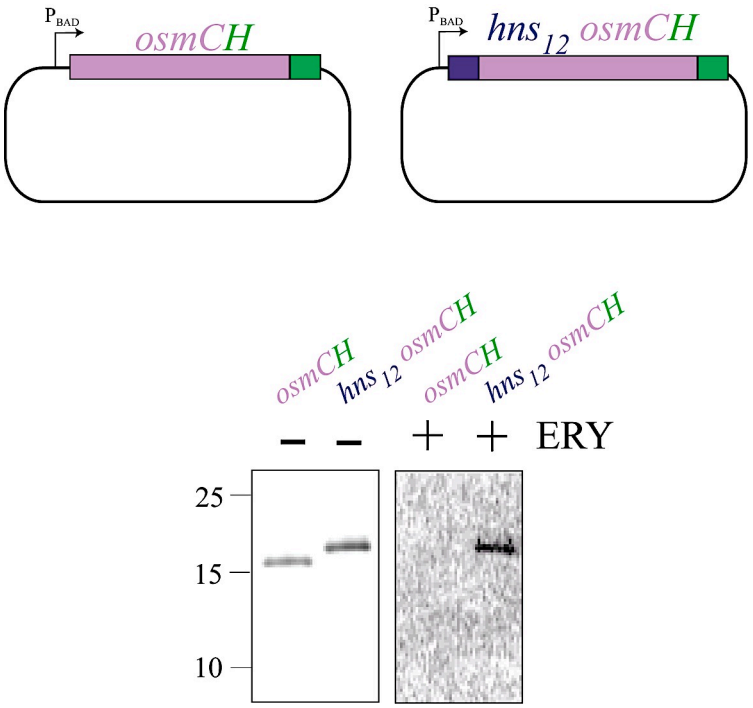

Figure 16. H-NS N-terminal sequence increases ERY-resistance of OsmC *in vivo*. *E. coli* strain BWDK cells expressing C-terminally His_6-tagged OsmC (OsmCH) or H-NS_{12}OsmCH were grown in the presence of 1 mM L-arabinose in M9AA-M medium. After 15 min incubation with 100 μg/mL of ERY or without the drug, proteins were pulse labeled with [^{35}S] methionine. Cells were lysed; the His_6-tagged proteins were purified on the Ni-NTA resin and analyzed by gel electrophoresis. Contrast of the gel image with the samples from ERY-treated cells was increased compared to the no drug control to better reveal the radioactive band.

The N-terminal 12 amino acids of H-NS are important for rendering OsmC ERY-resistant. In order to understand the importance of amino acids within this motif for the escape of antibiotic action, we replaced amino acids from this segment with unrelated sequence and tested ERY-evasion. Substituting amino acid residues 1-6 of H-NS with different amino acids had little effect on the N-terminal bypass conferred on OsmC by H-NS_{1-12} (Figure 17). However, replacing the I_7LNNIR_{12} segment of H-NS with the sequence from susceptible proteins such as LacZ (S_7SSVPG_{12}) or OsmC (G_7QAHWE_{12}) abolished resistance to ERY (Figure 17). Our previous results showed that the N-terminal amino acids I_7LNNIR_{12} of H-NS are critical for macrolide resistance (Figures 15B and 17). In order to understand the importance of the chemical properties of the amino acids constituting this motif, we searched the *E. coli* proteome for polypeptides whose N-terminal amino acids had a similar amino acid sequence compared to that of H-NS (Kanehisa et al., 2002). The [**I**LAVGM]-[I**L**AVGM]-[**N**QST]-[**N**QST]-[**I**LAVGM]-[K**R**H] 'regular-expression' was used as a query in the GenomeNet MOTIF search tool and approximately 15 hits were manually selected for the presence of an 'I_7LNNIR_{12}'-like motif within their N-terminal 15 amino acids. Within this list, we chose the protein HspQ to study evasion of ERY-action further. HspQ carries the sequence I_8GQQVR_{13} at its N-terminus whose physicochemical properties are analogous to the critical sequence I_7LNNIR_{12} of H-NS. Similar to H-NS, the *in vitro* translation of HspQ persisted at a high ERY concentration (data not shown). Furthermore, the 18 amino acid N-terminal segment of HspQ appended to OsmC rendered the hybrid protein resistant to the drug (Figure 18). This result reiterated the notion that idiosyncratic properties of the H-NS N-

terminus (specifically, I_7LNNIR_{12}) and other similar or even possibly dissimilar N-termini (Figure 14) can render a protein resistant to macrolide antibiotics.

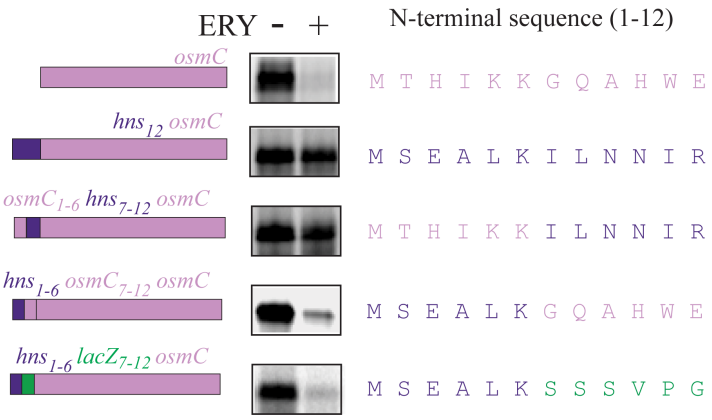

Figure 17. Importance of the 'I_7LNNIR_{12}' motif in escaping antibiotic inhibition. ERY sensitivity of the *hns*$_{12}$*osm*C hybrid constructs with different replacements within the N-terminal sequence appended to OsmC. The sequences of 12 N-terminal amino acids are shown at the right. The gels show the full-size hybrid proteins translated *in vitro* in the absence or the presence of 50 μM ERY. H-NS, OsmC and LacZ sequences are represented by purple, pink and green bars, respectively.

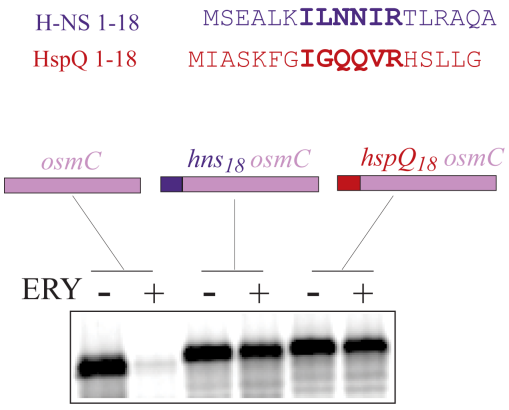

Figure 18. Idiosyncratic properties of 'I_7LNNIR_{12}' motif determine ERY-resistance. N-terminal segment of the *E. coli* protein HspQ (red), that exhibits similarity to H-NS (purple) renders OsmC (pink) resistant to ERY. The sequences of H-NS residues 7-12 and HspQ residues 8-13 are shown in bold. The gel shows the [^{35}S]-labeled translation products corresponding to the full-size proteins accumulated in cell-free translation system in the absence (-) or presence (+) of 50 μM ERY.

3.2.3 Nascent peptides can bypass the antibiotic in the ribosomal tunnel

Different scenarios may account for the ability of a protein to escape the inhibitory action of macrolides. The N-termini of some nascent peptides could displace the drug from the NPET like the short 'resistant' peptides (Lovmar et al., 2006; Tenson et al., 1997). If the drug were displaced from the NPET by the N-terminus of a resistant protein (such as H-NS_{1-12}), the nascent peptide elongated by a few more amino acids would then prevent the rebinding of the antibiotic until the complete polypeptide is released from the ribosome. An alternative scenario is that the nascent peptide could slither past the drug-obstructed NPET without displacing the antibiotic. In order to assess which of these mechanisms accounts for the resistance of H-NS to macrolides, we exploited the phenomenon of ERY-dependent ribosome stalling. The 19-codon ORF *erm*CL regulates the expression of the macrolide resistance gene *erm*C via programmed translation arrest (Figure 19) (Weisblum, 1995a). When ERY is bound in the NPET, the ribosome stalls after polymerizing the ErmCL nascent peptide MGIFSIFVI; translation arrest does not take place in the absence of the drug (Figure 19A) (Figure 20, lanes 1 and 2) (Horinouchi et al., 1980; Mayford et al., 1989; Vazquez-Laslop et al., 2008). We fused codons 2-19 of *erm*CL at the 3' end of the *hns* gene and tested whether the ribosome would stall after reaching the *erm*CL segment of the hybrid *hns-erm*CL construct (Figure 20). Primer extension inhibition analysis ('toe-printing') (Hartz et al., 1988) yielded the characteristic band on the gel indicative of the antibiotic-dependent translation arrest within the *erm*CL gene (Figure 20, lane 4). Little to no ribosome stalling was observed in the absence of the drug or when the start codon of the *hns-erm*CL fusion was mutated (Figure 20, lanes 3, 5 and 6). This result demonstrated that ribosomes that have translated

the entire H-NS protein retain ERY in the NPET, which is able to induce ribosome stalling after translating the ErmCL segment GIFSIFVI. Since the ribosome carrying a long nascent peptide is presumed to be refractory to ERY re-binding (Pestka, 1974a; Tai et al., 1974), the most likely explanation of our results is that the N-terminus of the H-NS nascent peptide threads through the NPET obstructed by the antibiotic without causing drug-dissociation.

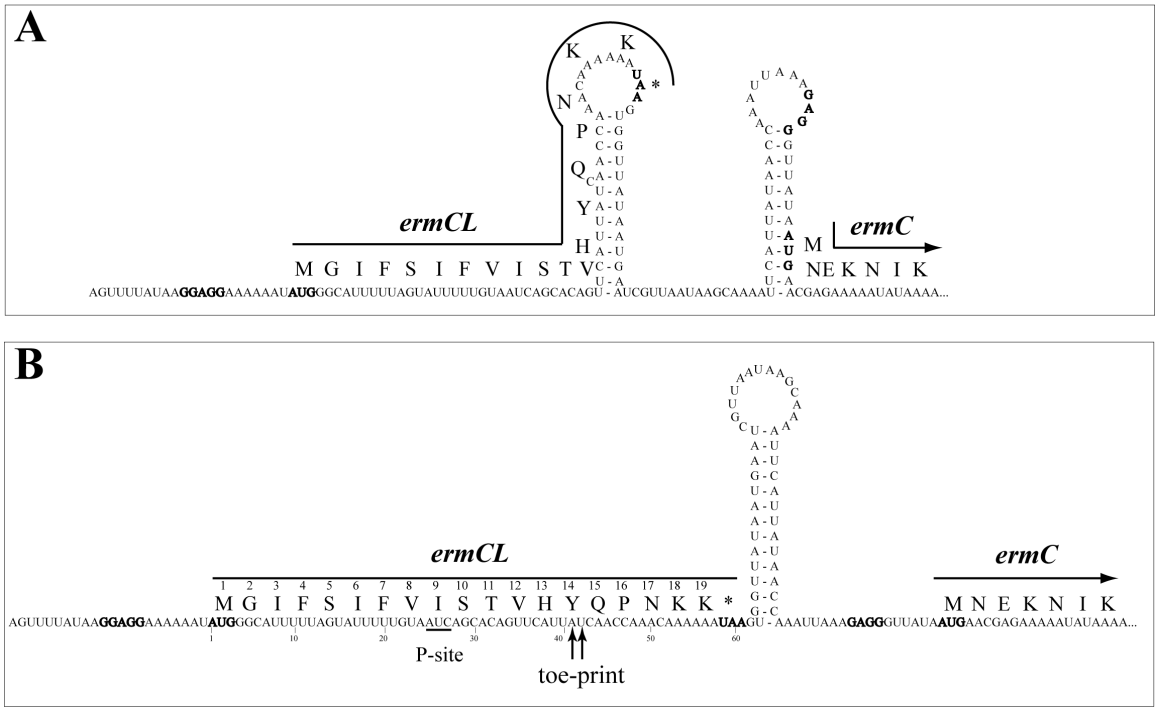

Figure 19. Induction of *erm*C expression by ERY. (A) In the absence of ERY, *erm*CL is translated from the bicistronic operon while *erm*C is not because the Shine-Dalgarno sequence and the start codon of the latter is sequestered in the secondary structure of the mRNA. (B) In the presence of ERY, ribosomes stall after polymerizing MGIFSIFVI of ErmCL, allowing the mRNA to restructure. The initiation site of *erm*C is then accessible for the ribosomes and is hence translated by a drug-free ribosome. Figure adapted from Vazquez-Laslop et al., 2008.

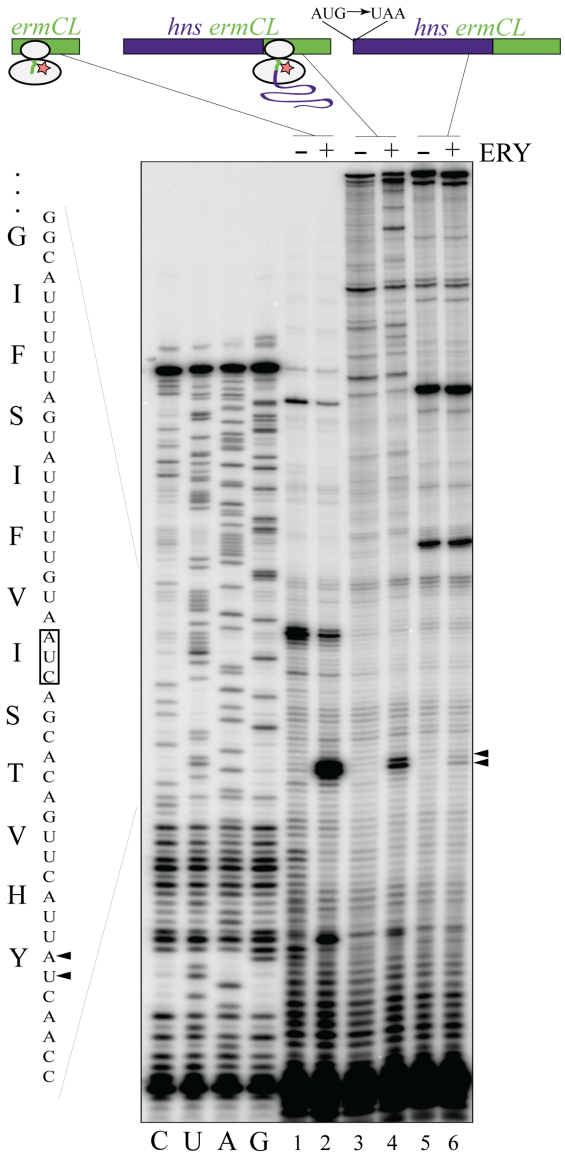

Figure 20. ERY is retained in the NPET of the ribosome synthesizing the H-NS protein. Toe-printing analysis of ERY-dependent ribosome stalling within the ErmCL coding sequence. The 19-codon *erm*CL gene (lanes 1-2) or the hybrid *hns-erm*CL constructs (lanes 3-4: hybrid with a wild type *hns* start codon, lanes 5-6: hybrid with the mutated *hns* start codon) were translated in the cell-free translation system in the absence (-) (lanes 1,3,5) or presence (+) (lanes 2,4,6) of ERY (50 μM). Ribosome stalling within the *erm*CL sequence was detected by toe-printing using the primer NV1 (Table II). Bands representing ribosome stalled within the *erm*CL sequence are indicated by triangles and the *erm*CL codon in the P-site of the stalled ribosome is boxed. The very weak toe-print bands in the start codon mutant sample (lane 6) are likely explained by low-frequency translation initiation at one of the internal AUG codons of *hns*. Cartoons above the gel represent the *erm*CL (green bar) and *hns* (purple bar) ORFs with ERY shown as a salmon star.

3.3 Discussion

For a long time, macrolide antibiotics have been considered to be general inhibitors of translation that prevent the synthesis of all cellular proteins by plugging the ribosomal tunnel. In contrast to this prevailing view, we demonstrate herein that the mode of action of these drugs is protein-specific in nature.

With the macrolide antibiotic bound in the NPET, the structure of the nascent peptide N-terminus determines whether protein synthesis is aborted, stalled or continued at the early stages of translation. When the nascent polypeptide chain grows to 5-10 amino acids and reaches the site of antibiotic binding in the NPET, translation of many polypeptides is aborted because the peptidyl-tRNA dissociates from the ribosome (Menninger, 1995; Tenson et al., 2003). In an alternative scenario involving regulatory open reading frame of macrolide resistance genes, the ribosome is stalled with the oligo-peptidyl tRNA (Vazquez-Laslop et al., 2008; reviewed in Ramu et al., 2009). Through our study, we discovered a third alternative situation (N-terminal bypass) where some peptides, by virtue of their N-terminal amino acids, bypass the antibiotic bound in the ribosome tunnel and continue to be translated on a drug-bound ribosome (Figure 21).

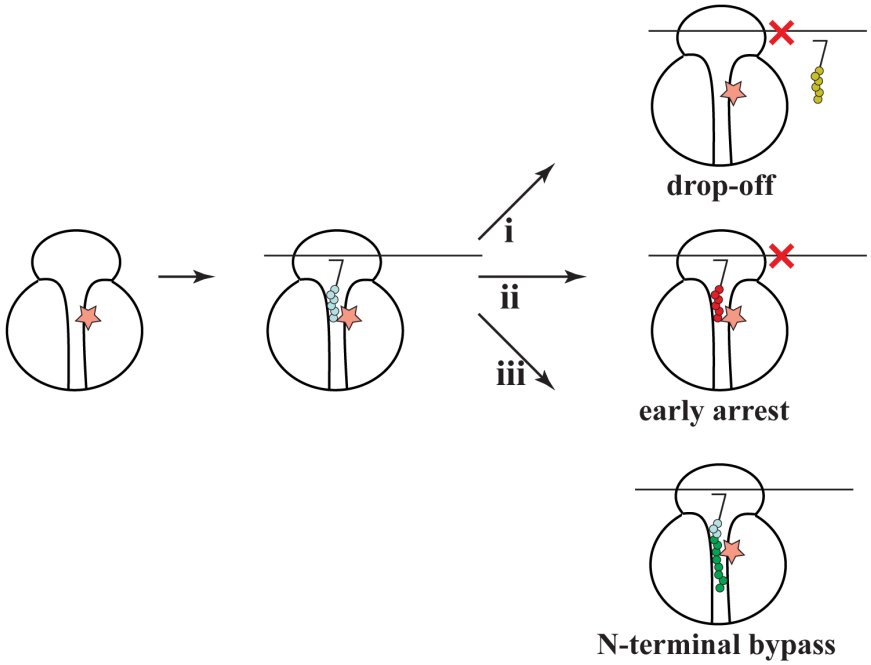

Figure 21. Previously known and new modes of action of macrolide antibiotics. Macrolides bound in the NPET can lead to i) drop-off of peptidyl-tRNA at the early rounds of translation. ii) early ribosome stalling (e.g. during the translation of *erm*CL). iii) N-terminal bypass and continued translation. The nascent peptide N-terminal sequence prone to drop-off is shown in yellow, the N-terminal bypass-promoting sequence is green

Crystallographic structures of ribosome-macrolide complexes show that macrolides do not completely block the tunnel, but leave an opening that may provide a passage for the nascent peptide (Figure 22) (Bulkley et al., 2010; Dunkle et al., 2010; Schlunzen et al., 2001; Tu et al., 2005). With limited conformational adjustments, even the bulkiest amino acid residues could pass through the constriction of the drug-obstructed NPET. However, the structure of the tunnel-bound antibiotic plays an important role in determining the spectrum of proteins that are synthesized. Our results show that ketolide antibiotics allow up to five times more protein synthesis as compared to macrolides. We speculate that this is because of the absence of the bulky C3 cladinose in ketolides that the conventional macrolides contain which occludes a significant portion of the NPET lumen when the latter is bound (Figures 2C, 11A and B).

The broad functional spectrum of macrolide resistant proteins (Figure 13) argue that it is the local structure of the N-terminal sequence rather than protein function that defines the propensity for the bypass. As few as 12 N-terminal amino acids of H-NS (MSEALKILNNIR) are sufficient for rendering a macrolide-sensitive protein (OsmC) highly resistant to the drug. Within the H-NS N-terminal structure, the first six N-terminal amino acids appear to be fairly inconsequential whereas the segment I_7LNNIR_{12} plays an important role in antibiotic evasion because its replacement with an unrelated sequence dramatically reduced the N-terminal threading capacity (Figure 17). In contrast, alanine substitutions of individual amino acids had little effect on bypass (data not shown). Either a particular folding of this segment (Bloch et al., 2003) or the cumulative effects of specific contacts of several amino acid residues with the ribosome and/or the

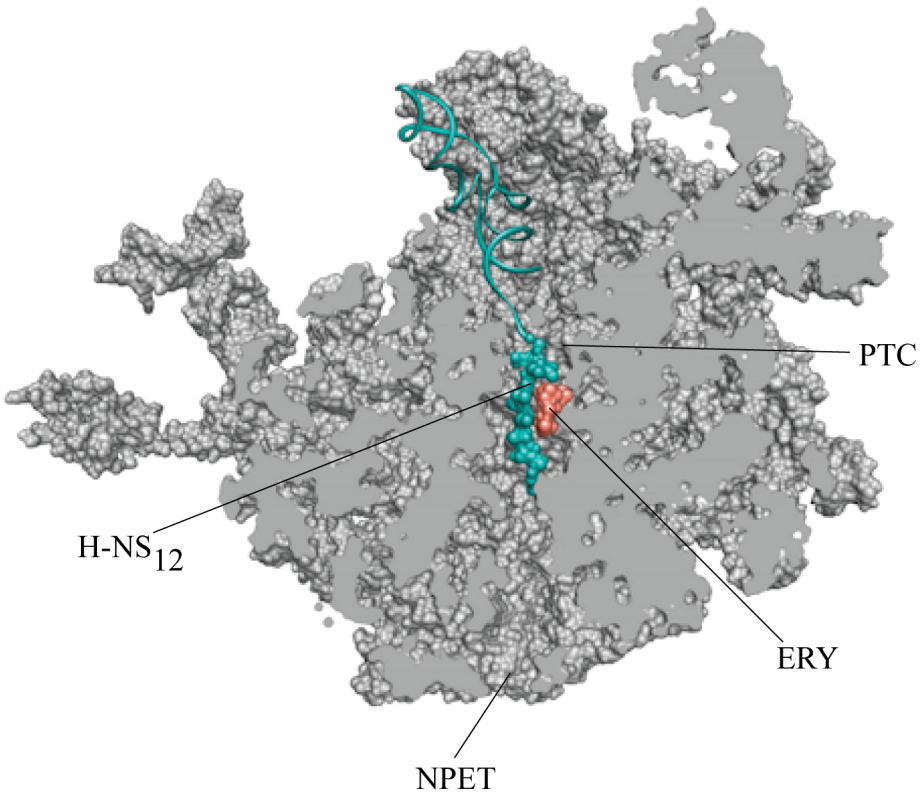

Figure 22. Possible simultaneous placement of a macrolide and nascent peptide in the NPET. A cross-cut of the large ribosomal subunit (PDB accession number 3OFR) (Dunkle et al., 2010) complexed with ERY (salmon) and the modeled 12 amino-acid long nascent peptide of H-NS esterified to the P-site tRNA (cyan).

antibiotic appear to be required for efficient threading of the peptide through the drug-obstructed tunnel. Any of these mechanisms may either orient the peptide's N-terminus for slithering through the narrow gap of the antibiotic-occupied NPET, or modify the shape of the tunnel and/or the pose of the antibiotic, thereby facilitating the bypass (Figure 22).

We show that the idiosyncratic properties of the H-NS motif I_7LNNIR_{12} are important for the bypass of antibiotic inhibition since a chemically similar I_8GQQVR_{13} motif from HspQ also confers ERY-resistance to OsmC. Nevertheless, none of the N-terminal sequences of the other ERY- or TEL-resistant proteins that we identified in the 2D gel spots (Figure 13) closely match that of H-NS. Therefore, it is obvious that the sequence constraints for the N-terminal bypass are fairly relaxed, especially in the case of ketolides, which allow for the escape of many more polypeptides. We noted, however, that N-terminal segments of several of the resistant proteins contain a stretch of 2-3 hydrophobic residues followed by a positively charged amino acid (underlined in Figure 13). It remains to be investigated whether this feature is one of the drug-evasion determinants.

The mechanism of selective N-terminal bypass can account for several previously puzzling results. The long-known resistance of polyU translation to ERY (Hardesty et al., 1990; Vazquez, 1966c) and the more recently reported poor inhibition of *in vitro* synthesis of green fluorescent protein (GFP) by macrolides (Starosta et al., 2010) can be easily rationalized if one assumes that poly(Phe) and GFP could thread through the macrolide-occupied NPET. A number of other results, from the accumulation of long peptidyl-tRNA (Menninger et al., 1994; Yao et al., 2008), the persistence of polysomes in

ERY-treated cells (Ennis, 1972), ERY resistance caused by ribosomal protein L22 mutations (Apirion, 1967; Chittum et al., 1994; Gregory et al., 1999; Lovmar et al., 2009; Moore et al., 2008), which were hard to explain within the confines of the conventional model of macrolide action, could now be rationalized in view of our findings. Although we have demonstrated that the synthesis of a protein can stem from the ability of the nascent chain to bypass the antibiotic in the NPET, we cannot rule out the possibility that some proteins might be synthesized owing to the accelerated drug-dissociation rate induced by the N-terminal nascent peptide sequence.

The understanding that macrolides do not block the synthesis of all proteins, but rather convert the universal translation machine into a selective producer of certain polypeptides, has important clinical implications. Ketolides are much more potent antibacterial compounds than the drugs of previous generations. Furthermore, ketolides exhibit increased bactericidal activity against some Gram-positive bacteria (Hamilton-Miller et al., 1998; Woosley et al., 2010; Zhanel et al., 2003). Indeed, under our experiemental conditions, TEL killed 90% of the bacteria after a four hour exposure at 100-fold MIC while ERY behaved like a typical bacteriostatic drug (Figure 23).

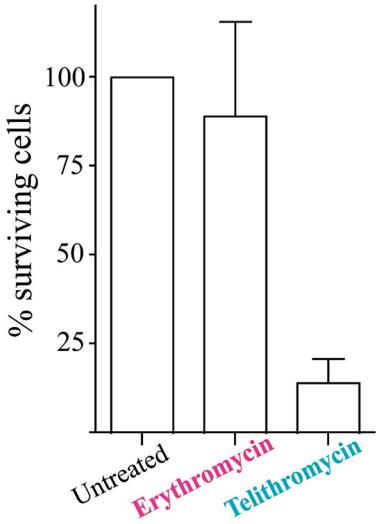

Figure 23. TEL exhibits modest bactericidal activity against *E. coli* strain BWDK cells. Exponentially growing cells were exposed to 100-fold MIC of ERY or TEL for four hours, serially diluted and plated on LB-agar without antibiotics. The number of colonies was counted after overnight incubation at 37°C and the colony forming units at the time of addition of the drugs (no-drug control) was considered as 100%.

Strikingly, ketolides license continued synthesis of far more proteins than ERY or AZM (Figures 11). It appears that blocking the expression of only a part of the cellular proteome could be more fatal to the cell than complete or near-complete inhibition of translation. Preventing translation of only a subset of proteins will presumably interrupt biochemical pathways at random steps leading to the accumulation of potentially toxic metabolic intermediates or depletion of essential cofactors, which may trigger a lethal cellular response (Kohanski et al., 2007). In contrast, inhibiting the synthesis of all proteins would eventually deprive the cell from its biosynthetic and metabolic capacity, leading to bacteriostasis. Noteworthy, whereas most of the 'global' protein synthesis inhibitors are bacteriostatic, aminoglycosides that permit some protein synthesis but render the ribosome error-prone are strongly bactericidal (Kohanski et al., 2007). We propose that future optimization of macrolide antibiotics should take into account or even be entirely based on the protein-specific action of these drugs rather than global inhibition of translation.

IV. Late-translation arrest by macrolide antibiotics

4.1 Introduction and rationale

The NPET of the ribosome is not an impartial conduit for nascent polypeptide chains. Some nascent peptides can specifically interact with the NPET, altering the rate of translation elongation and, in extreme cases, leading to translation arrest. The peptide monitoring and discriminating properties of the NPET are used by the cell for optimizing the regulation of gene expression, protein targeting and folding (reviewed in Ito et al., 2010). The recognition of individual nascent peptides in the NPET and the subsequent ribosomal response can be sensitive to cellular cues, such as the concentration of specific small metabolites. For example, nascent peptide-mediated translation arrest at the *tna*C gene is stimulated by tryptophan (Gong et al., 2002), the concentration of arginine regulates elongation of the arginine attenuator peptides in fungi (Fang et al., 2004) and ribosome progression along the cystathionine γ-synthase gene in *Arabidopsis* is sensitive to the concentration of S-adenosyl-methionine (Onouchi et al., 2005). In none of these cases is it understood how the small molecules modulate progression of the nascent peptide through the NPET, because their binding sites within the ribosome remain a mystery (Tenson et al., 2002).

Macrolide antibiotics that bind to the NPET induce the formation of stalled ribosomal complexes during the translation of short ORFs encoding a defined amino acid sequence (Horinouchi et al., 1980; Mayford et al., 1989; Vazquez-Laslop et al., 2008, reviewed in Ramu et al., 2009, Ramu et al., 2011). Such ORFs (leader ORFs) are generally found to precede the *erm* resistance genes that modify the macrolide-binding site and prevent drug binding (Weisblum, 1995a). Similar ORFs are also found upstream

of other macrolide resistance genes that encode efflux pumps or the drug-modifying enzymes (reviewed in Ramu et al., 2009). Macrolides regulate expression of most of these genes by inducing programmed ribosome stalling at the upstream regulatory ORF (Figure 19, chapter 3). During the translation of the leader ORF, the drug molecule bound to the NPET stalls the ribosome at a specific codon (Figure 19B, chapter 3). This ribosome stalling leads to isomerization of the mRNA structure and activation of downstream resistance gene expression (Figure 19B, chapter 3). The ribosome stalling orchestrated by the antibiotic involves intricate and not yet fully understood interactions between the drug, nascent peptide, and ribosome tunnel. The Erm leader peptides are classified based on the amino acid sequence motif that is strictly required for ribosome stalling (reviewed in Ramu et al., 2009). Similarly, the structure of the antibiotic is critical in determining the ability of a ribosome to stall in response to specific nascent peptides (Vazquez-Laslop et al., 2011a). Furthermore, the ribosome tunnel nucleotides are involved in sensing the nascent peptide and the drug and are critical for relaying the stalling signal to the PTC (Vazquez-Laslop et al., 2011b).

Although the length and the sequence of codons of the leader peptide ORFs differ significantly, the drug-bound ribosome invariably stalls near the 5'-end after polymerizing no more than 8-10 amino acids (reviewed in Ramu et al., 2009). This could be because placement of the stalling signal farther away from the 5' end of the ORF will prevent the ribosome from reaching it due to the premature peptidyl-tRNA drop-off induced by macrolides. In our previous study, we showed that macrolides and ketolides allow the translation of specific polypeptides and that translation of long proteins is possible on the drug-bound ribosomes. However, since the opening of the NPET is

severely occluded by the macrolide molecule, negotiating the narrowed tunnel could be problematic for some natural nascent peptide sequences even after the initial N-terminal bypass. Hypothetically, the presence of a macrolide molecule in the tunnel during the synthesis of a long polypeptide might induce the following: ribosome stalling; premature termination of translation; or peptidyl tRNA drop-off. To gain insight into these previously uninvestigated modes of macrolide action, we asked whether the tunnel-bound antibiotic could affect later rounds of translation after the N-terminus of the nascent chain has bypassed the antibiotic.

4.2 Experimental results

4.2.1 Discriminating effects of macrolide antibiotics at the late stages of protein synthesis

From our previous study, we concluded that N-terminal bypass is required for the synthesis of long polypeptides in the drug-bound ribosomes. We wanted to test whether the tunnel-bound drug can render the ribosome to discriminate against certain amino acid sequences even at the later stages of elongation. To this end, we analyzed the synthesis of several polypeptides in the S30 cell-free translation system in the presence of saturating concentrations (50 μM) of TEL. We initially used TEL instead of ERY because this ketolide allows the synthesis of a larger number of proteins compared to ERY (Figure 11, chapter 3), suggesting that more polypeptides would be able to avoid inhibition at the early rounds of their synthesis. We used several 'long' polypeptides of *E. coli* for this exercise so as to increase the variety of nascent chains encountering the drug molecule in the NPET after N-terminal bypass.

From a limited set of examined proteins, the synthesis of the *E. coli* 78 kDa translation elongation factor EF-G (encoded by the *fus*A gene) exhibited an unusual trait. When *fus*A was translated in the presence of the antibiotic, synthesis of the full-size EF-G was abolished and instead, a polypeptide with an apparent molecular weight of 40 kDa was generated (Figure 24A). The same product appeared in the presence of TEL when the 3'-truncated versions of the *fus*A gene were used as a template indicating that the drug-induced 40 kDa product corresponds to the N-terminal segment of EF-G (Figure 24B). We further verified that this fragment indeed corresponds to the N-terminus of EF-G by using a start codon mutant version of the *fus*A template. This mutant was unable to drive the synthesis of the 40 kDa fragment in the presence of TEL, confirming that the TEL-induced translation product is indeed translated from the canonical start codon (data not shown). This result showed that the ribosome with the antibiotic molecule bound in the NPET retains its discriminating properties long after the initial encounter of the nascent peptide with the drug.

The precise site of TEL-dependent translation arrest in the *fus*A gene was determined by toe-printing. A unique, strong band was observed on the gel in the TEL-containing sample, indicative of drug-dependent translation arrest at the Glu_{358} codon of *fus*A (Figure 25, lane 2). Ribosome stalling was not observed when the start codon of *fus*A was disabled by a mutation (Figure 25, lane 4). Therefore, the TEL-bound ribosomes stalled after polymerizing the N-terminal 358 amino acid-long EF-G nascent peptide.

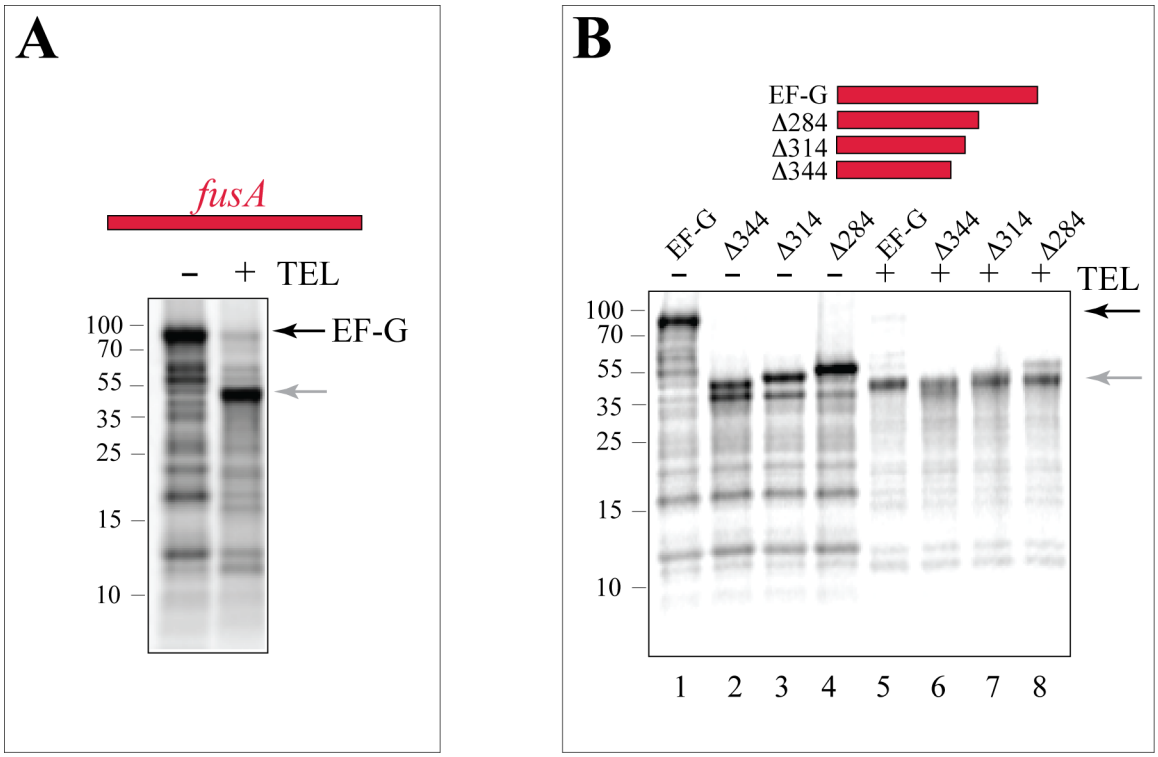

Figure 24. Selective late translation arrest: TEL-dependent arrest of EF-G translation in the cell-free system. (A) *fus*A gene was translated in the S30 cell-free transcription/translation system in the absence (-) or presence (+) of 50 μM TEL and the reaction products were resolved by SDS gel electrophoresis. (B) Translation of *fus*A and its C-terminally truncated mutants in the absence (-) or presence (+) of TEL. The number of deleted C-terminal residues is indicated. In (A) and (B), the full-length EF-G and the truncated translation product are indicated by black and grey arrows, respectively.

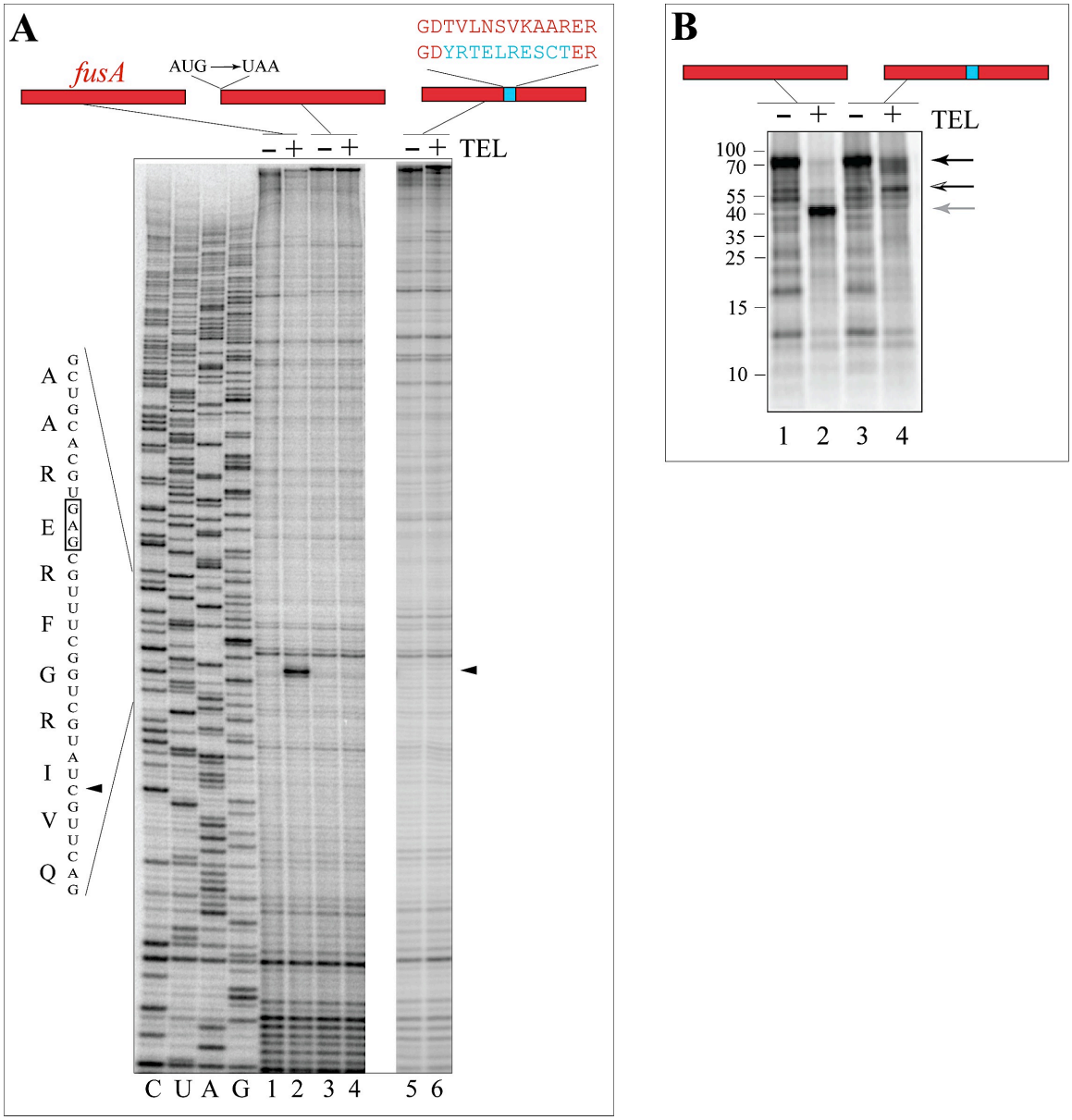

Figure 25. Characterization of TEL-induced late arrest during *fus*A translation. (A) Detection of the site of TEL-dependent ribosome stalling in the *fus*A gene by toe-printing. The wild type *fus*A gene (lanes 1 and 2), the start codon mutant (lanes 3 and 4) and the frame-shift mutant in which the amino acid residues 348-357 were changed (lanes 5 and 6) were used as templates in a cell-free translation reaction in the absence (-) or presence (+) of 50 μM TEL. Ribosome stalling was detected by toe-printing using the primer EF-G_{390} rev (Table II). The toe-printing band is indicated by a triangle and the *fus*A codon (Glu_{358}) located in the P-site of the stalled ribosome is boxed. (B) SDS gel electrophoresis analysis of the products of *in vitro* translation of wild type *fus*A (lanes 1, 2) or the frame-shift mutant (lanes 3, 4) in the absence (-) or presence (+) of TEL. A new TEL-dependent incomplete translation product of the frame-shift mutant is indicated by the bicolored arrow.

With *fus*A we were able to demonstrate ketolide-dependent late-arrest of translation. We next wanted to test whether cladinose-containing macrolide antibiotics can also trigger late translation arrest. To this end, we analyzed the *in vitro* translation of the 57 kDa protein firefly luciferase (Luc) in the presence of ERY. Translation of wild type Luc is highly sensitive to ERY and is completely inhibited when the drug concentration exceeds 1 μM (Figures 26A and B). Contrary to the ERY-resistant H-NS_{18}OsmC (Figure 15A, chapter 3), appending the 18 N-terminal amino acids of H-NS to luciferase failed to rescue the hybrid protein from antibiotic inhibition (Figures 26A and B). Instead, translation of the *$hns_{18}luc$* led to drug-dependent accumulation of a polypeptide with an apparent molecular weight of 20 kDa (Figure 26A). This result shows that the H-NS_{18}Luc N-terminus was able to bypass ERY in the NPET, but that translation of the protein was arrested after the synthesis of a ~180 amino acid-long nascent peptide. In agreement with this notion, the addition of 18 N-terminal amino acids of another ERY resistant protein, OmpX, at the beginning of luciferase also resulted in the accumulation of the same 20 kDa product in the presence of ERY (Figure 27).

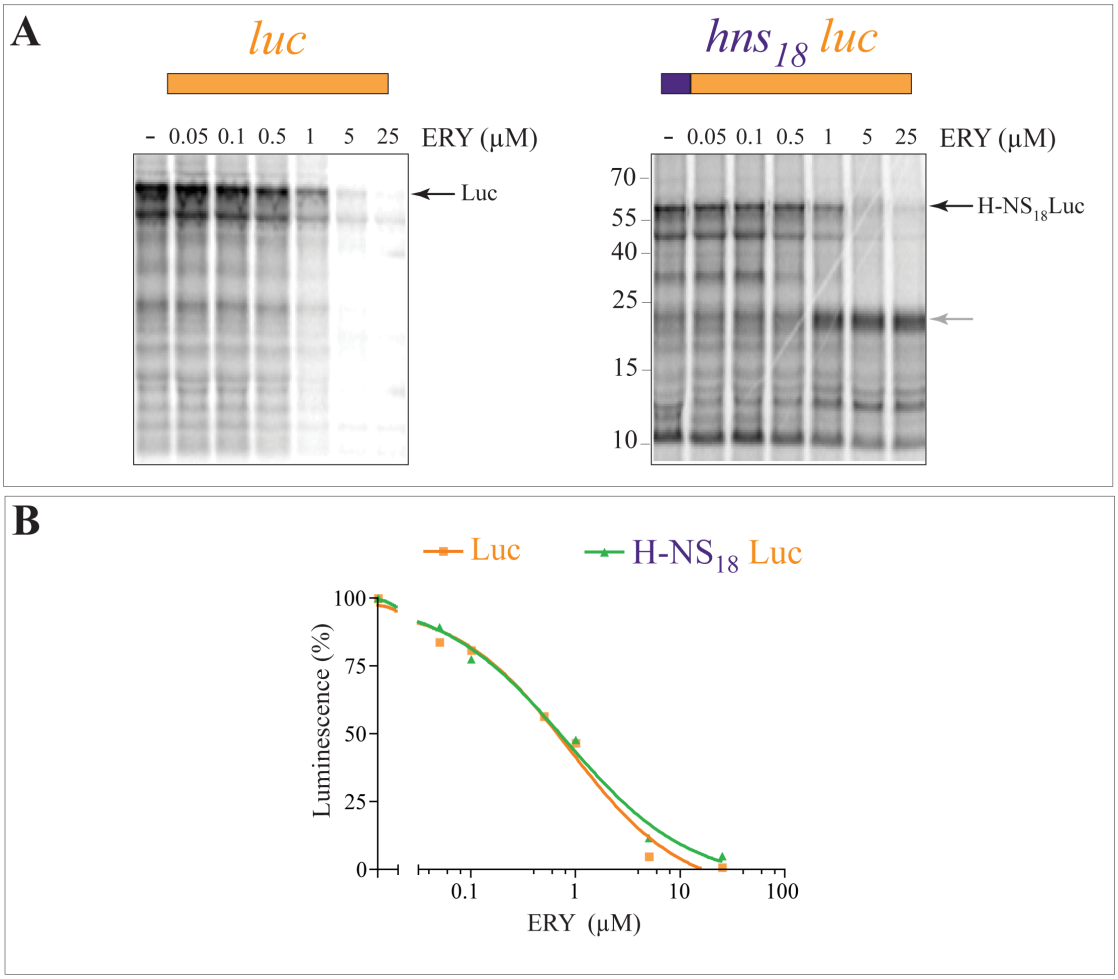

Figure 26. Late translation arrest induced by ERY. (A) SDS gel electrophoresis analysis of the products of *luc* (left) or *hns*$_{18}$*luc* (right) translation in the presence of increasing concentrations of ERY. The full-size protein is indicated by the black arrow; the ERY-induced truncated polypeptide is indicated by the grey arrow. (B) Enzymatic activity of luciferase accumulated in a cell-free system after the translation of wild type *luc* template or *hns*$_{18}$*luc* construct in the presence of increasing concentrations of ERY.

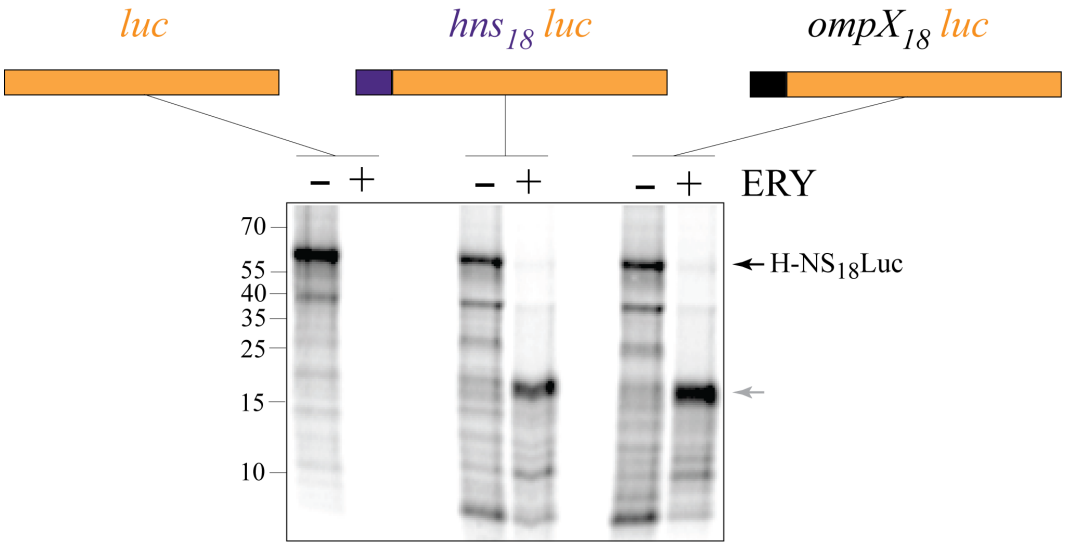

Figure 27. Role of N-terminal amino acids of OmpX during macrolide inhibition. SDS gel electrophoresis analysis of the products of *luc* or *hns*$_{18}$*luc* or *ompX*$_{18}$*luc* translation in the presence of ERY (50 µM). The full-length protein and the truncated translation product are indicated by black and grey arrows, respectively.

Toe-printing analysis revealed the formation of ERY-dependent stalled ribosome complexes at codons Pro_{189}, Pro_{199} and Asp_{205} of the *hns*$_{18}$*luc* hybrid gene (Figure 28, lane 2). The start codon mutation (Figure 28, lane 4) and the fusion of the hybrid template with the *erm*CL reporter (Figure 29B, lane 4) demonstrated that ERY remains bound in the NPET of the ribosome that comes to a stall after polymerizing a large, N-terminal-fragment of the H-NS_{18}Luc protein. These results confirmed that similar to ketolides, cladinose-containing macrolides can arrest translation long after the initial threading of the nascent peptide's N-terminus past the antibiotic.

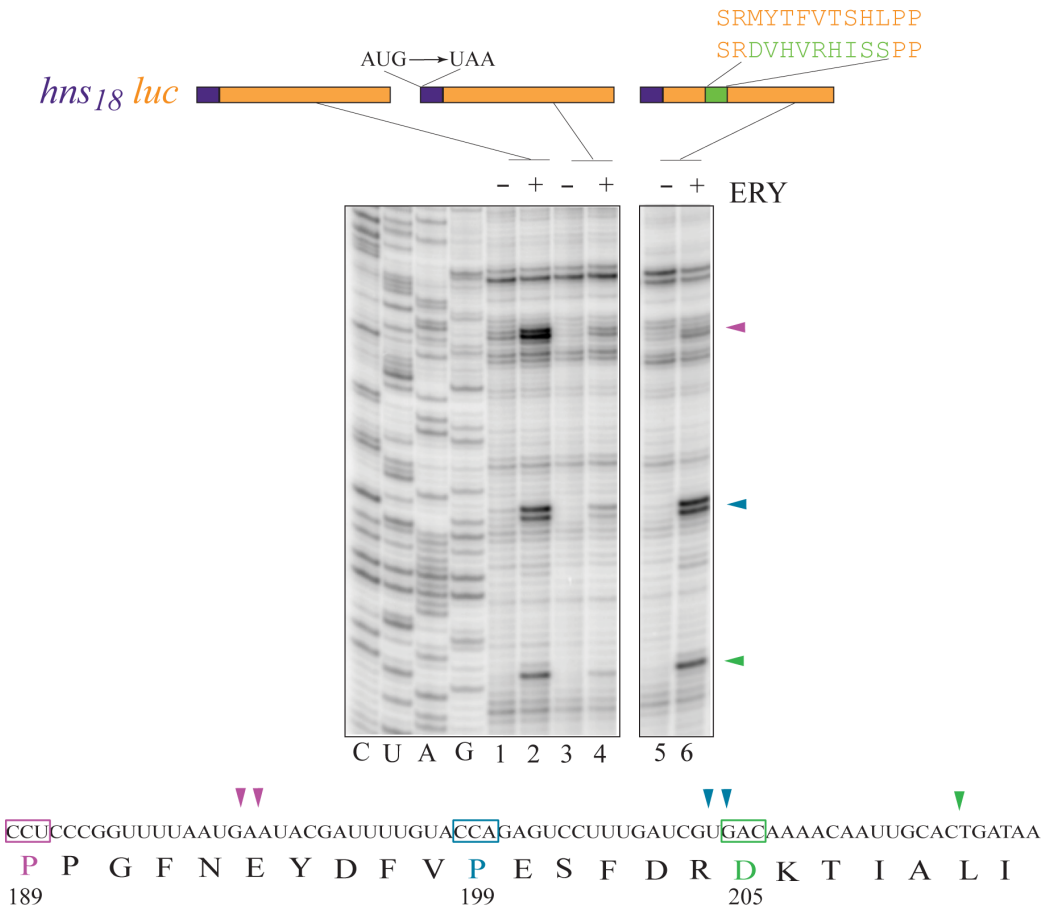

Figure 28. Mapping the sites of ERY-dependent late translation arrest in the *hns$_{18}$luc* gene. The *hns$_{18}$luc* template (lanes 1-2), the start codon mutant (lanes 3-4) and the frame-shift mutant in which the amino acid residues 180-188 were changed (lanes 5-6) were translated in a cell-free system in the absence (-) (lanes 1, 3, 5) or the presence of ERY (+) (lanes 2, 4, 6), and the site of ribosome stalling was identified by toe-printing using the primer hns$_{18}$luc TP-3 (Table II). Three prominent stalling sites are indicated by purple, blue and green triangles; the codons in the P-site of the corresponding stalled ribosomal complexes are boxed with the same color in the *luc* sequence shown below.

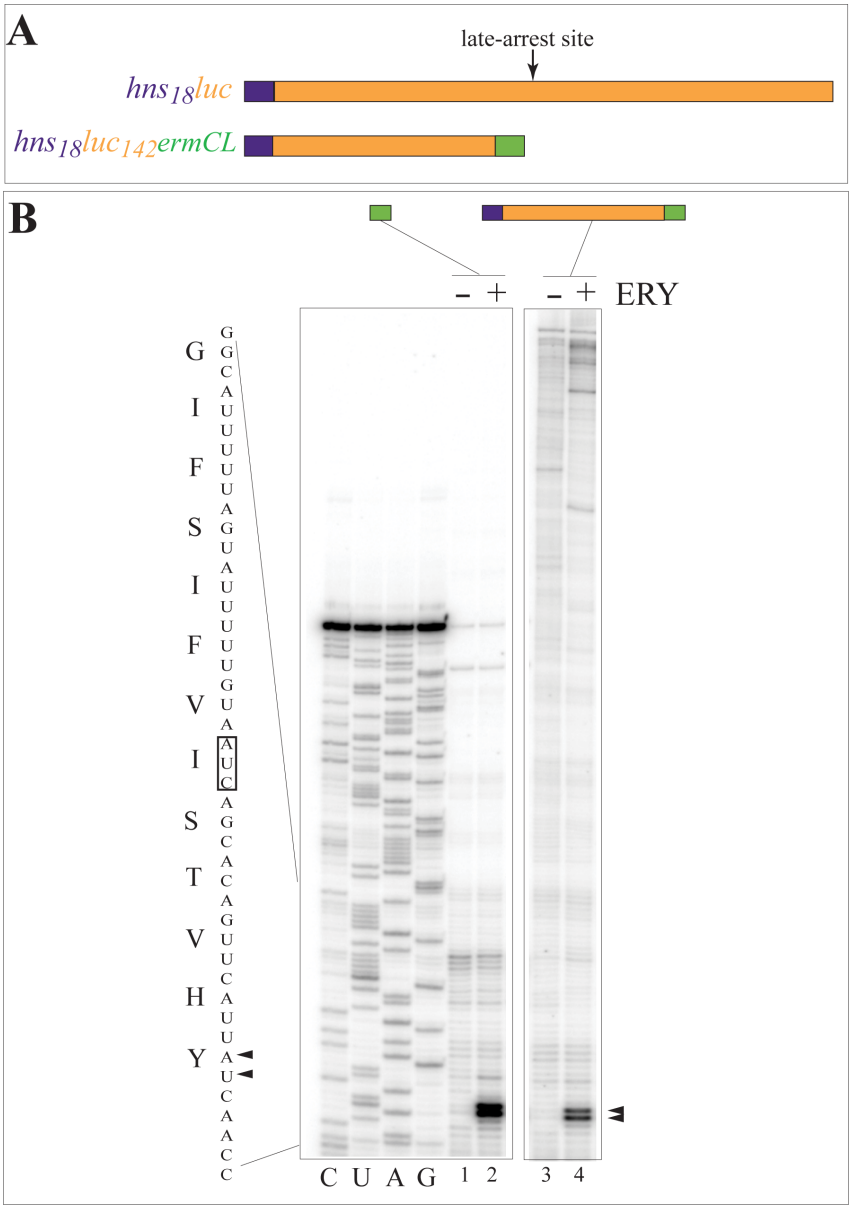

Figure 29. ERY remains bound to the ribosome translating *hns$_{18}$luc*. (A) The hybrid constructs used in this toe-printing experiment: H-NS$_{18}$Luc (H-NS–purple, Luc–yellow) and H-NS$_{18}$Luc$_{142}$ErmCL (ErmCL–green). The *erm*CL sequence was fused to the *luc* codon 160 prior to the late arrest sites (codons 189, 199 and 205). (B) Toe-printing analysis (using the primer NV1 (Table II)) of ERY-dependent ribosome stalling within the wild type *erm*CL (lanes 1, 2) and within the *erm*CL segment of the *hns$_{18}$luc$_{142}$erm*CL construct (lanes 3, 4) in the presence (+) (lanes 2, 4) or absence (-) (lanes 1, 3) of 50 μM ERY. The bands representing ribosome stalling are indicated by triangles and the *erm*CL codon positioned in the P-site of the stalled ribosome is boxed.

4.2.2 Antibiotic-induced ribosome stalling depends on the structure of the nascent peptide

In a stalled ribosome complex, four to five C-terminal amino acid residues of the nascent peptide are able to directly interact with the macrolide antibiotic (Tu et al., 2005; Vazquez-Laslop et al., 2008) and may play an important role in late translation arrest. To test whether the peptide structure defines the site of late arrest, we modified the sequence of ten EF-G amino acids (residues 348-357) at the site of TEL-dependent arrest. The alteration in the nascent peptide structure was introduced by compensatory frame-shift mutations in the *fus*A gene, which changed the sequence of this segment of EF-G with a minimal effect upon the structure of the mRNA. This change in the structure of the nascent peptide prevented TEL-dependent ribosome stalling at the Glu_{358} codon of *fus*A as indicated from the disappearance of the toe-printing band on the gel (Figure 25A, lane 6). However, in the S30 cell-free translation system, the synthesis of the full-size EF-G was not completely restored by this mutation (Figure 25B). The alleviation of stalling at the Glu_{358} codon unmasked downstream late-arrest sites leading to the production of longer, yet still incomplete proteins.

ERY-dependent late translation arrest within the *hns18-luc* open reading frame occurs at three sites: Pro_{189}, Pro_{199} and Asp_{205} (Figure 28, lane 2). When a compensatory frame-shift mutation altered the residues 180-188 of the H-NS_{18}Luc nascent peptide, ribosome stalling at the Pro_{189} codon was dramatically reduced (Figure 28, lane 6). In contrast, translation arrest at the two downstream sites, Pro_{199} and Asp_{205}, was not affected and even became more prominent, presumably because more ribosomes could reach these sites in the mutant. These results demonstrate that late translation arrest

depends on the nascent peptide structure and occurs when a ‘problematic’ amino acid sequence advances from the PTC into the NPET.

After the N-terminal bypass, the likelihood that the drug-bound ribosome will encounter a problematic nascent peptide sequence should increase with the length of a polypeptide. Indeed, the size distribution of the proteins synthesized in the presence of macrolides is shifted towards lower molecular weights compared to the no drug control (Figures 11 and 30A). The spectra and abundance of the truncated proteins generated via N-terminal bypass and late arrest are yet to be determined. However, the appearance of a number of new protein spots upon exposure of cells to TEL (Figure 30B) argues that a considerable fraction of truncated polypeptides can be generated in the bacterial cell, especially during treatment with ketolide antibiotics that are more prone to allow the N-terminal bypass.

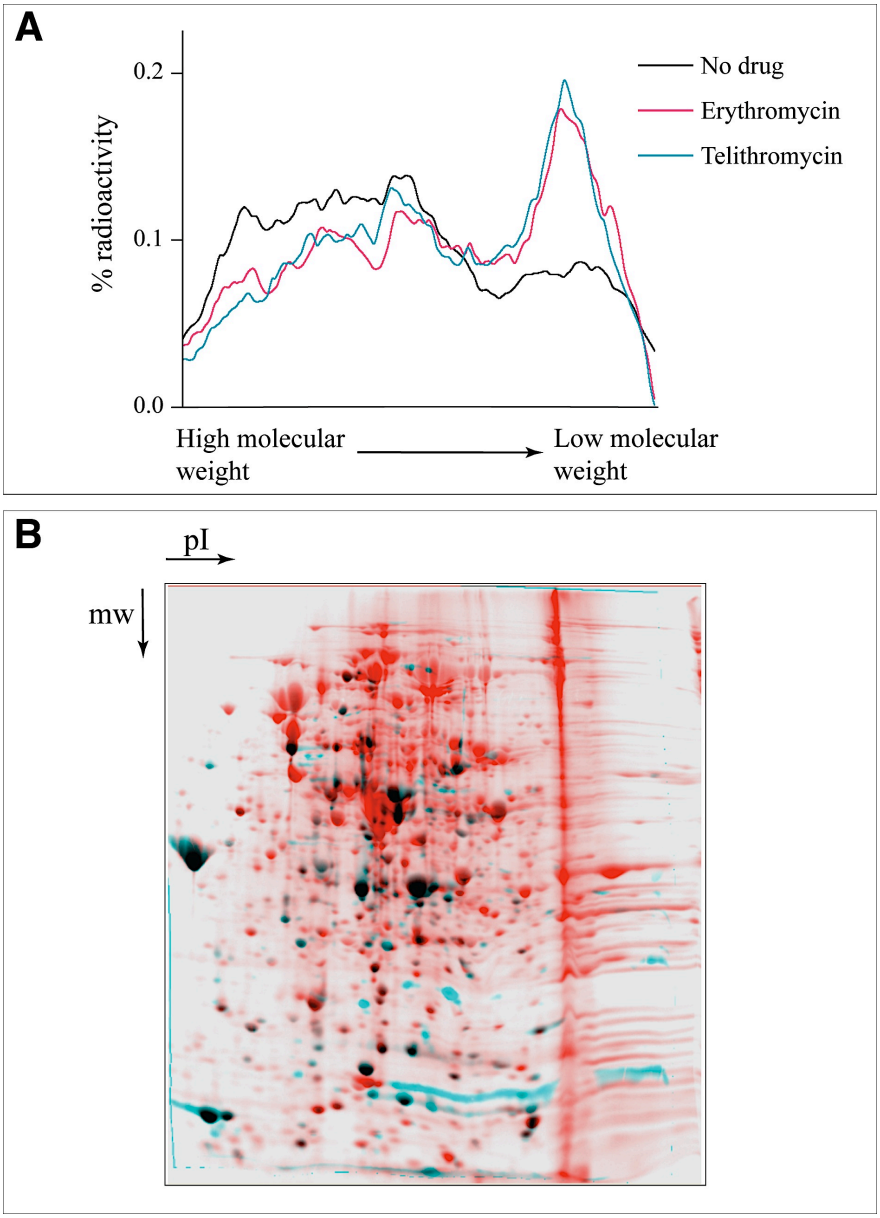

Figure 30. *In vivo* results insinuate late translation arrest events in the presence of macrolides. (A) Low molecular weight proteins escape more efficiently from macrolide inhibition. Integrated radioactivity of ~1000 sections of the 2D gels shown in Figure 11A along the electrophoretic coordinate in which proteins were separated by size. Integrated density values were calculated using ImageJ and the resulting data was fitted with a spline curve using Prism software (GraphPad). (B). New proteins that appear in the cells treated with TEL may correspond to truncated polypeptides generated via late translation arrest *in vivo*. Overlay of the radiographs of the gels with proteins from control and TEL-treated cells. The 'no drug' sample spots are shown in red, the TEL-specific protein spots are blue and the matched spots are black.

4.2.3 The structure of the NPET-bound antibiotic influences late translation arrest

The structure of the macrolide molecule can impact the efficiency and selectivity of ribosomal arrest at the regulatory ORFs of the macrolide resistance genes (Vazquez-Laslop et al., 2010). Therefore, we tested whether drug structure could also affect late translation arrest. Specifically, we compared the ability of five different macrolides to trigger late ribosomal stalling at the *hns*$_{18}$*luc* mRNA. Although all these antibiotics readily inhibited *in vitro* translation of the wild type luciferase (Figure 31A), only four of the five tested macrolides (ERY, clarithromycin, TEL and CEM-112) promoted the accumulation of a 20 kDa late arrest translation product (Figure 31B). No truncated polypeptide products were observed in the presence of troleandomycin (TAO) (Figures 31B and 32A) and, as a result, this drug had little effect on the expression of the functionally active enzyme from the *hns*$_{18}$*luc* template (Figure 32B). Toe-printing confirmed that the efficiency of TAO-dependent ribosome stalling was dramatically reduced compared to ERY (Figure 33, lanes 2 and 3). The use of the C-terminal ErmCL reporter showed that TAO remains bound to at least a fraction of the translating ribosomes (Figure 34, lane 4). We concluded that changes in the structure of the NPET-bound antibiotic might affect the sequence specificity of late translation arrest.

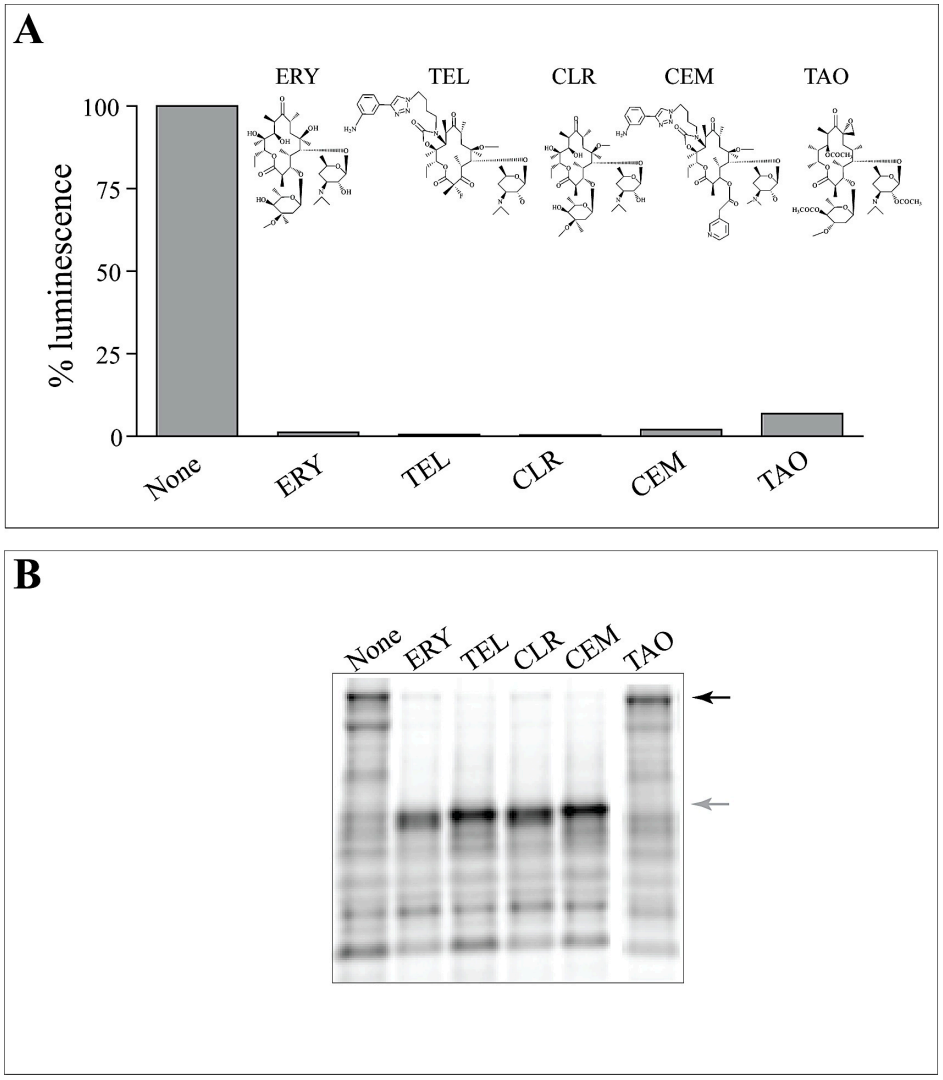

Figure 31. Chemical structure of the antibiotic affects late translation arrest events. (A) Inhibition of cell-free translation of wild type luciferase by 50 μM of different macrolides: ERY, TEL, clarithromycin (CLR), CEM-112 (CEM), and TAO. (B) SDS gel electrophoretic analysis of the products of *hns*$_{18}$*luc* translation in the presence of 50 μM macrolide antibiotics. The full-size H-NS$_{18}$Luc and the late arrest translation products are indicated by black and grey arrows, respectively.

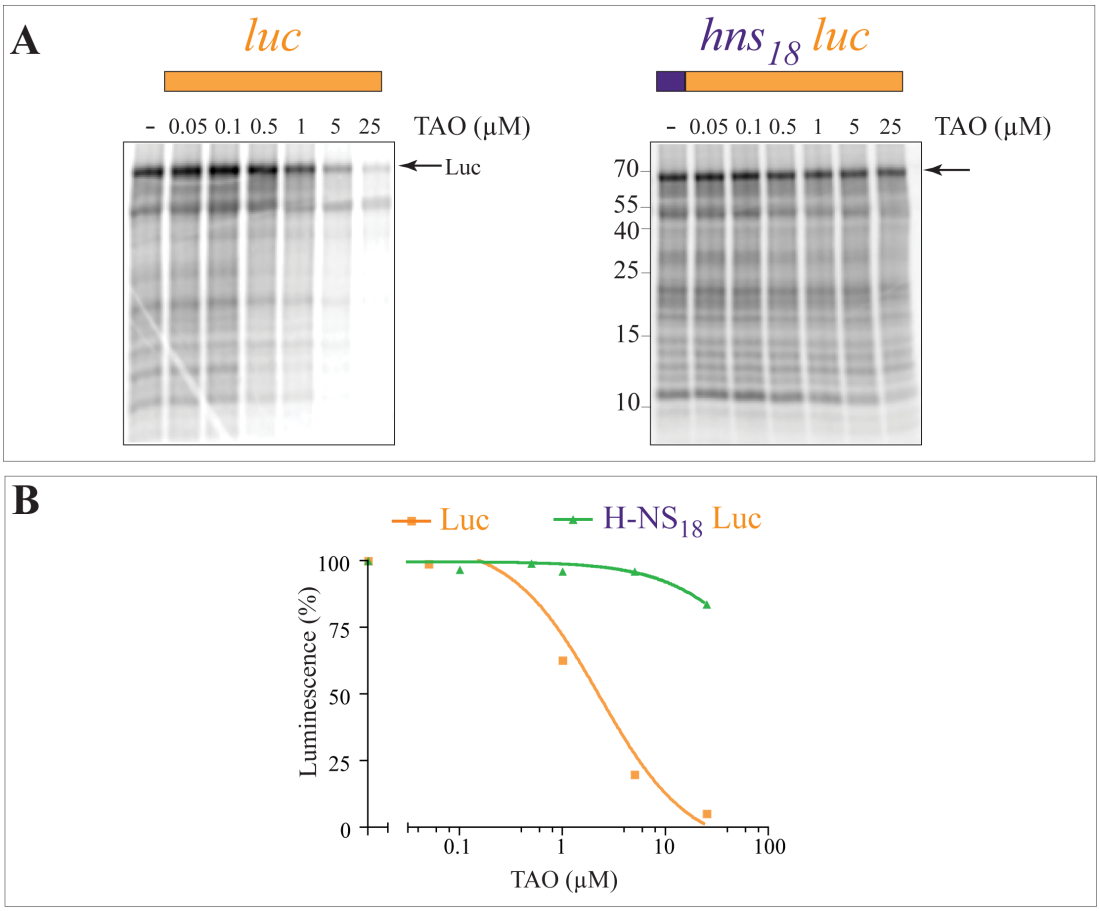

Figure 32. TAO allows the synthesis of full-length H-NS$_{18}$Luc. (A) SDS gel electrophoresis analysis of the products of *luc* (left) or *hns$_{18}$luc* (right) translation in the presence of increasing concentrations of TAO. The black arrow indicates the full-size protein. (B) Enzymatic activity of luciferase accumulated in a cell-free system after the translation of wild type *luc* template or *hns$_{18}$luc* construct in the presence of increasing concentrations of TAO.

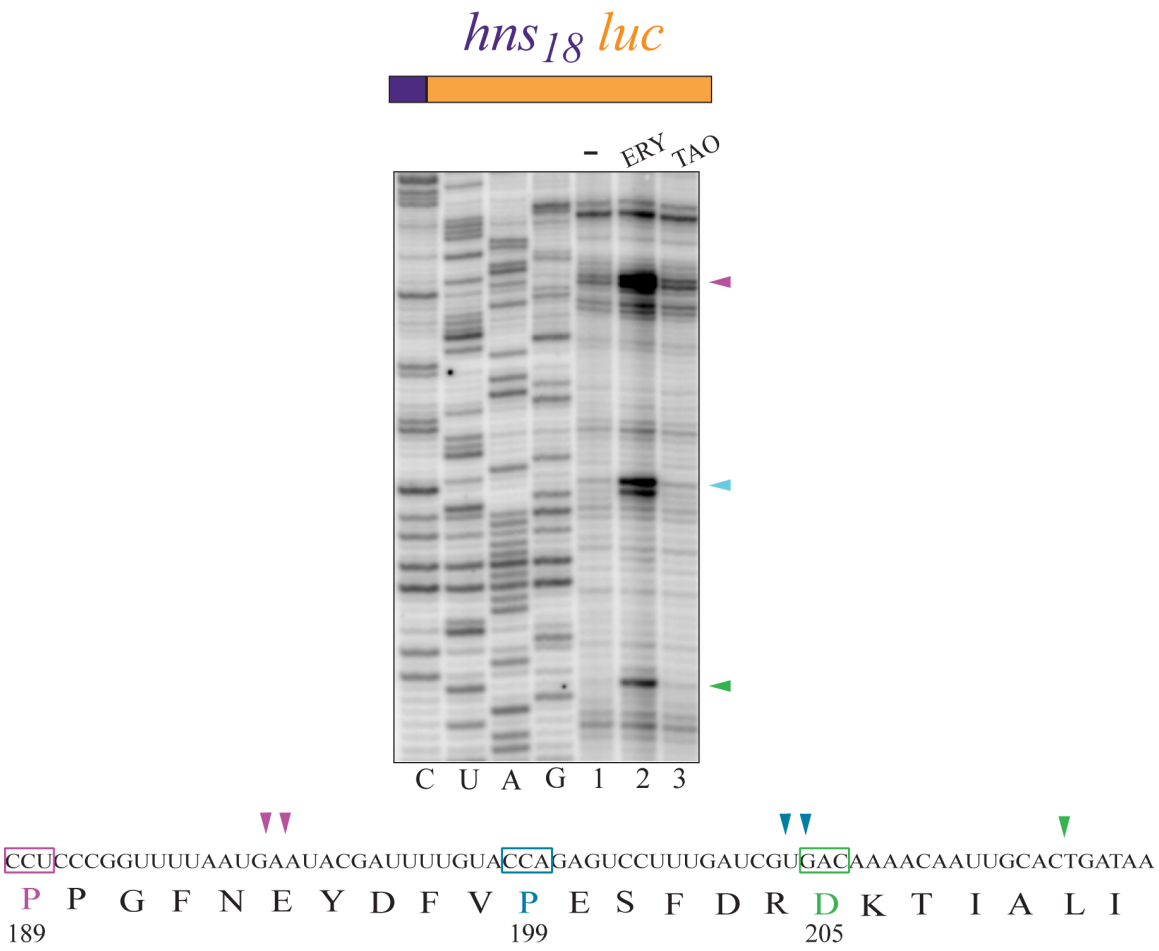

Figure 33. TAO does not stall ribosomes during the translation of *hns$_{18}$luc*. The *hns$_{18}$luc* template was translated in a cell-free system in the absence (-) (lane 1) or the presence of ERY (lane 2) or TAO (lane 3). Ribosome stalling was probed using the primer hns$_{18}$luc TP-3 (Table II). Three ERY-dependent stalling sites are indicated by purple, blue and green triangles; the codons in the P-site of the corresponding stalled ribosomal complexes are boxed with the same color in the *luc* sequence shown below.

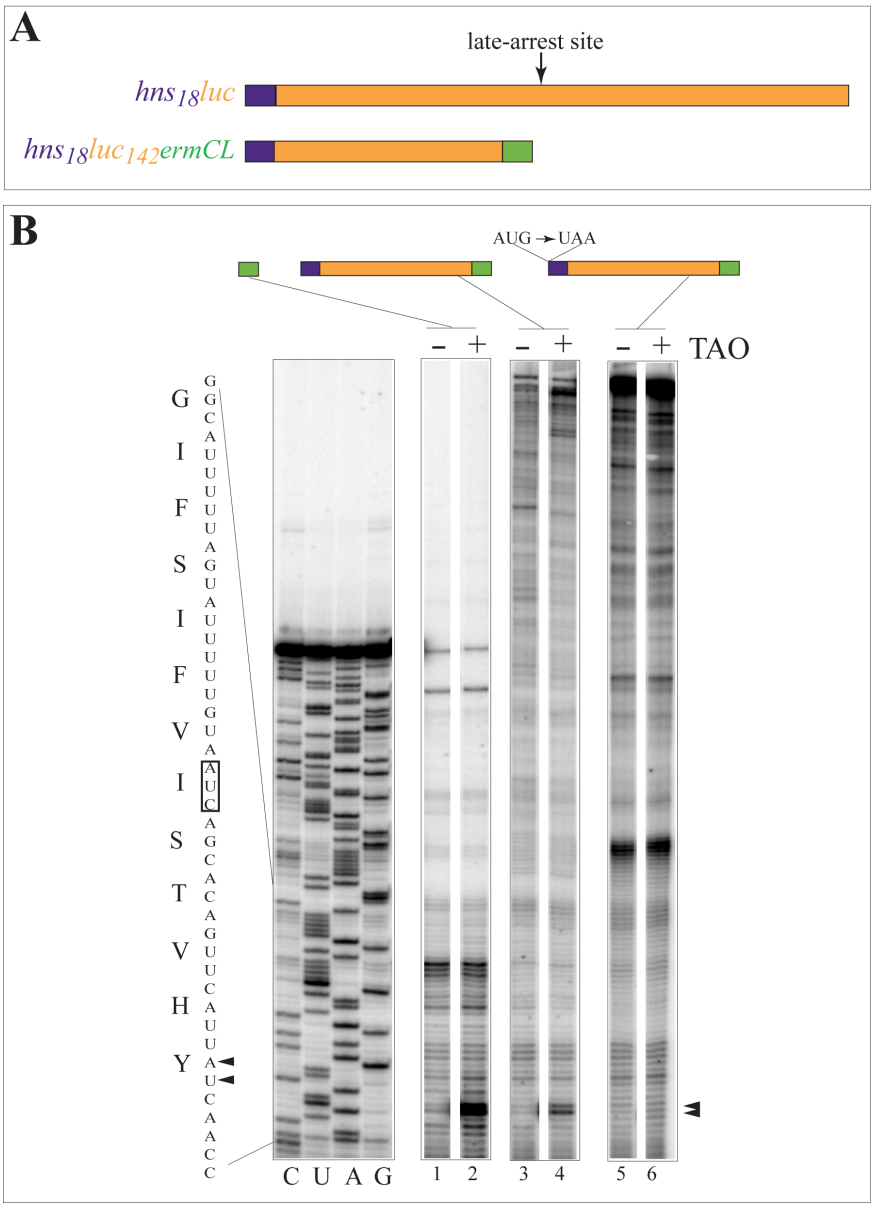

Figure 34. TAO remains bound to the ribosome translating *hns$_{18}$luc*. (A) Diagrams of the hybrid constructs used in this toe-printing experiment: H-NS$_{18}$Luc (H-NS–purple, Luc–yellow) and H-NS$_{18}$Luc$_{142}$ErmCL (ErmCL–green). The *erm*CL sequence was fused to the *luc* codon 160 prior to the late arrest sites (codons 189, 199 and 205). (B) Toe-printing analysis (using the primer NV1 (Table II)) of TAO-dependent ribosome stalling within the wild type *erm*CL (lanes 1, 2), the *erm*CL segment of the *hns$_{18}$luc$_{142}$erm*CL construct (lanes 3, 4) and the *erm*CL segment of the start codon mutant of the *hns$_{18}$luc$_{142}$erm*CL construct (5, 6). The bands representing ribosome stalling in the presence of 50 μM TAO (+) (lanes 2, 4, 6) are indicated by triangles and the *erm*CL codon.

4.2.4 Ribosome stalling depends on the structure of the exit tunnel

The shape of the NPET opening is likely critical for the progression of the newly synthesized protein. Therefore, we tested whether alterations in the NPET structure would affect the nascent peptide-discriminating properties of the drug-bound ribosome. For that, the *fus*A gene was translated in a PURE cell-free system by either wild type ribosomes or ribosomes carrying the 23S rRNA mutation A2062U (Figures 35C and D). Although this mutation did not confer TEL resistance (Table IV) or prevent antibiotic binding (Figure 35D), it significantly reduced the accumulation of the TEL-dependent 40 kDa truncated product, consequently increasing the amount of full-size EF-G (Figure 35C). Furthermore, the spectra of ERY resistant proteins synthesized in wild type cells and in mutants with tunnel mutations A2062G or U2609C showed considerable variation (Figure 35B). Strikingly, almost the entire proteome was inhibited by ERY in the NPET mutant Ψ746G compared to the wild type cells (Figure 36). Altogether, these results demonstrate that the NPET structure directly influences the selective translation properties of the antibiotic-bound ribosomes.

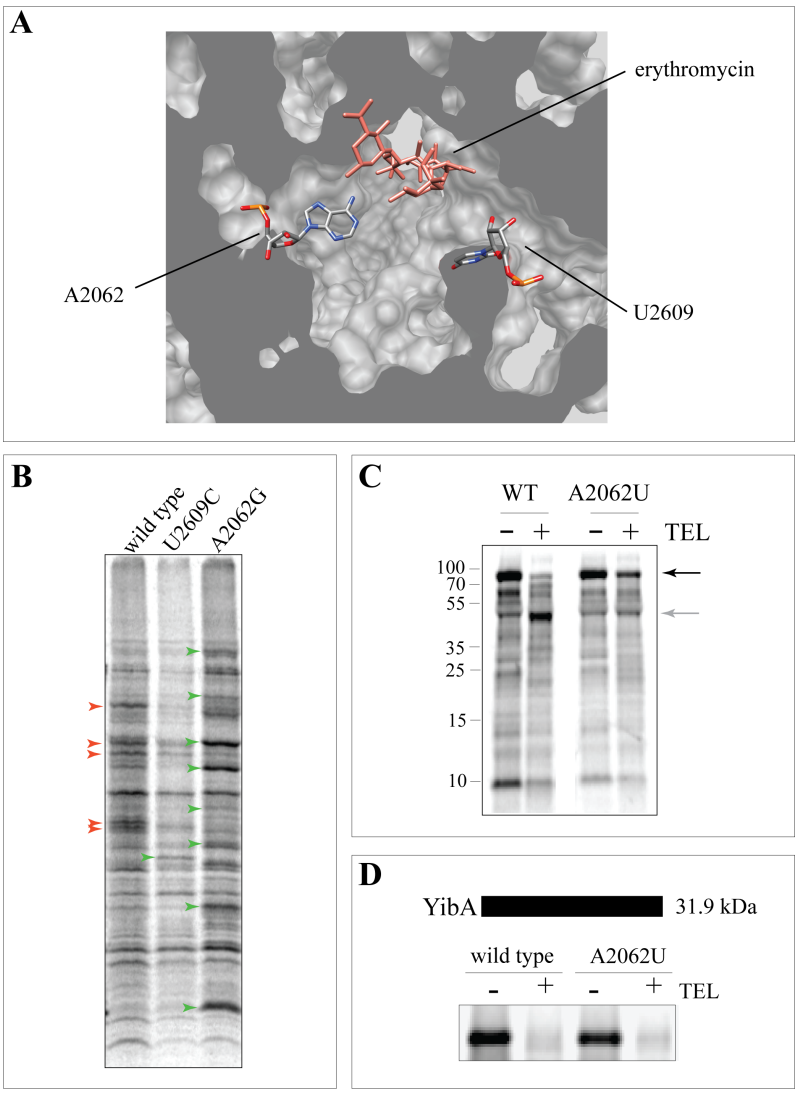

Figure 35. The NPET structure can influence the spectrum of proteins that escape ERY. (A) Relative location of ERY and the 23S rRNA residues A2062 and U2609 in the *E. coli* NPET (PDB accession number 3OFR). Cross-section of the large ribosomal subunit perpendicular to the axes of the NPET; view from the PTC side. (B) SDS gel electrophoretic analysis of proteins synthesized in the presence of 100-fold MIC of ERY in the *E. coli* strain SQtolC cells expressing wild type or mutant ribosomes. Protein bands more prominent in the wild type are marked by red arrowheads; the bands more prominent in the mutants are indicated by green arrowheads. (C) A2062U mutation reduces efficiency of TEL-dependent late translation arrest. SDS gel electrophoresis analysis of the products of translation of *fus*A by wild type or mutant (A2062U) ribosomes in the absence (-) or presence (+) of a saturating concentration of TEL (50 μM). Full-length EF-G and truncated product are indicated by black and grey arrows respectively. (D) A2062U mutation does not prevent TEL binding. Products of *in vitro* translation of the reporter gene *yib*A by the wild type and A2062U mutant ribosomes in the absence (-) and presence (+) of 10 μM TEL.

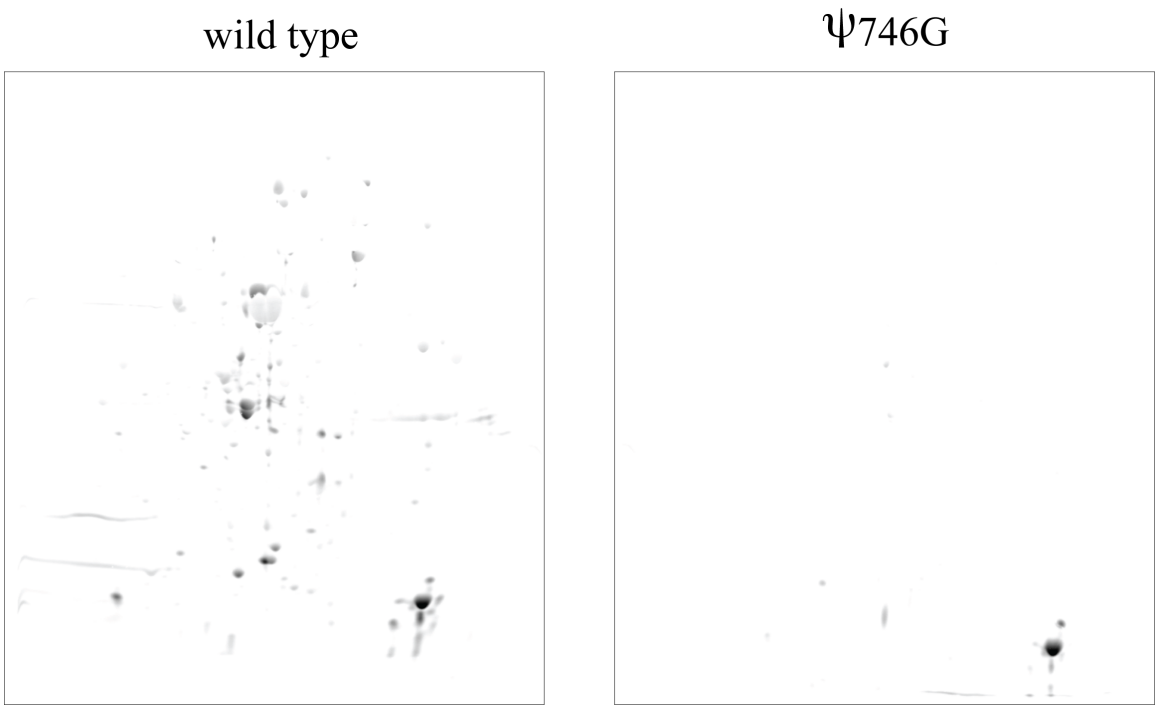

Figure 36. NPET mutation Ψ746G enables almost complete translation inhibition by ERY. SQtolC cells expressing wild type or Ψ746G mutant ribosomes were exposed to 100-fold MIC (Table IV) of ERY. Radiolabeled proteins synthesized after antibiotic exposure were analyzed using 2D-gels.

4.3 Discussion

Ribosome stalling induced by the macrolide and ketolide antibiotics during the synthesis of N-terminal amino acids of specific leader peptides has been well established. Through this study, we introduce the novel concept of late translation arrest wherein the ribosome is stalled not at the N-terminus of the peptide but during very late stages of elongation (Figure 37). Hence, the presence of an antibiotic molecule in the NPET renders the ribosome selective not only at the beginning of protein synthesis, but also during later stages of the nascent peptide polymerization. Following N-terminal bypass, translation of some polypeptides can continue unimpeded (e.g., H-NS), whereas elongation of other proteins can be arrested at a subsequent phase (e.g., EF-G), leading to the phenomenon of macrolide-dependent late translation arrest (Figure 37). Previously, we showed that the N-terminal amino acids are extremely important for the initial evasion of inhibition by macrolide bound to the NPET. However, the N-terminal amino acids play only an indirect role in late-arrest: the initial bypass of the macrolide molecule will determine whether or not the ribosomes reach the late-stalling motif. Besides this, the N-terminal amino acids do not directly control the mechanics of the late translation arrest.

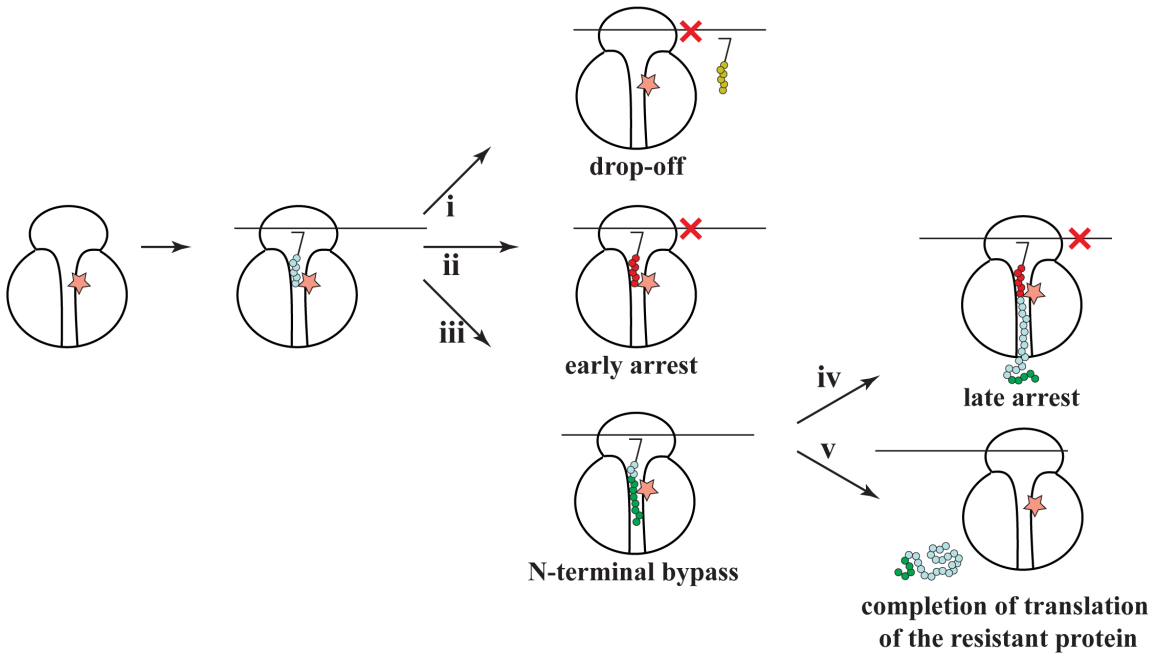

Figure 37. An additional mode of macrolide action. As described in Figure 21, macrolide antibiotics can cause i) drop-off of peptidyl-tRNA, ii) early ribosome stalling and iii) N-terminal bypass. Through this study we established an additional mode, late-arrest (iv) that can occur after the N-terminal bypass. Without late-arrest, the full-size protein can be produced by the drug-bound ribosome (v). The nascent peptide N-terminal sequence prone to drop-off is shown in yellow, the N-terminal bypass-promoting sequence is green and the peptide segments directing early or late translation arrest are red. The macrolide antibiotic is shown as a salmon star.

Similar to the N-terminal bypass, the structure of the nascent peptide, and more specifically of its PTC-proximal segment, is a key factor in defining the site of the late arrest since altering a short C-terminal nascent peptide sequence at the arrest site (Figures 25, lane 6 and 28, lane 6) can alleviate ribosome stalling. Although the molecular mechanism of the late arrest remains to be investigated, we noted that the site of TEL-dependent arrest within the *fus*A gene (Arg_{357}-Glu_{358}-Arg_{359}, with the Glu codon positioned in the P-site of the stalled ribosome) resembles the conserved motif (Arg-Leu-Arg) of the 'RLR' class of short stalling peptides of the inducible macrolide resistance genes (reviewed in Ramu et al., 2009). Moreover, just like several other N-terminal stalling peptides, the identity of the P-site amino acid (Glu_{358}) is extremely important for the late arrest (data not shown). This suggests that the basic principles of late translation arrest and early drug-dependent ribosome stalling could generally be similar, although additional studies are necessary to corroborate this idea.

The aperture of the ribosome tunnel opening is controlled by the placement of a highly flexible rRNA residue A2062 (Fulle et al., 2009; Seidelt et al., 2009; Vazquez-Laslop et al., 2008). In the absence of a nascent peptide, A2062 comes into close contact with the macrolide molecule, occluding the tunnel lumen (Figures 38A and B) (Tu et al., 2005). Some nascent peptides might force the A2062 base to reposition closer to the NPET wall which would open a larger space in the tunnel, facilitating the passage of the polypeptide chain (Schmeing et al., 2005) (Figure 38B). The important role of A2062 in nascent peptide surveillance is further emphasized by the fact that its mutation alleviates both early ERY-dependent ribosome stalling at the regulatory ORFs of macrolide resistance genes (Vazquez-Laslop et al., 2008), as well as TEL-dependent late translation

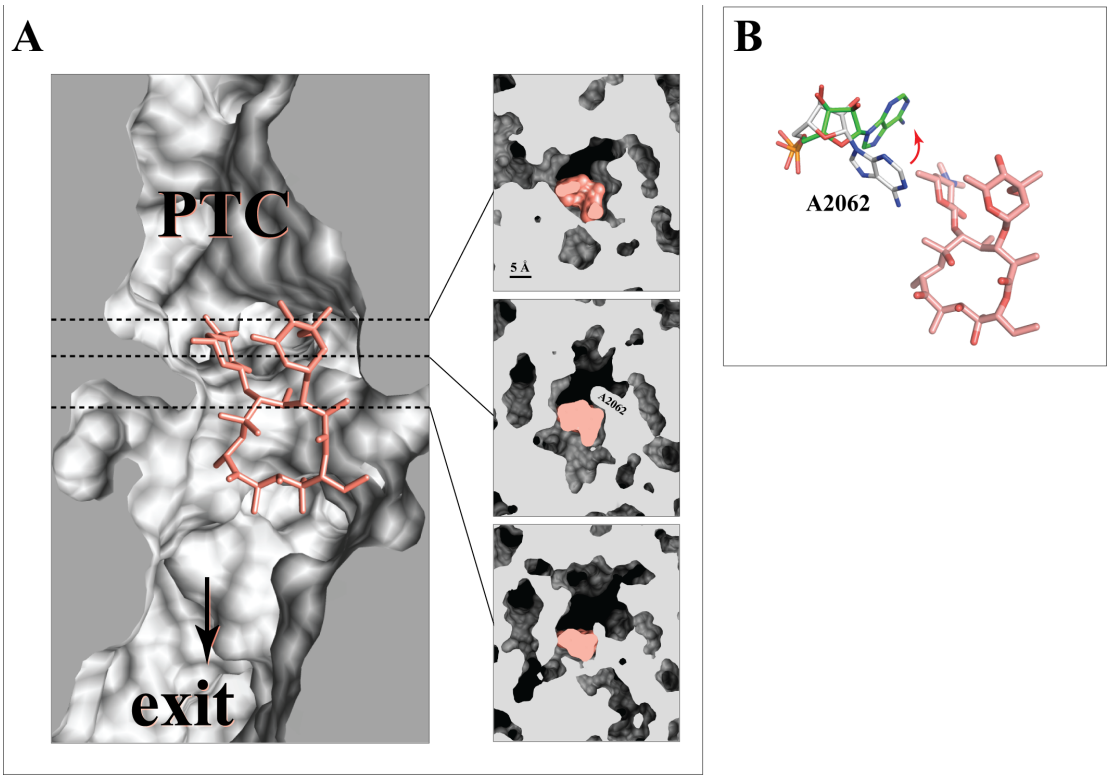

Figure 38. Role of A2062 in the mode of action of macrolides. (A) The space left by the macrolide molecule in the NPET is influenced by A2062. The cross-cut of the NPET along the tunnel axes (left) and perpendicular to the tunnel axes (right) of the *E. coli* ribosome complexed with ERY (PDB accession number 3OFR) (Dunkle et al., 2010). ERY is colored in salmon and the position of the perpendicular cross-cut planes relative to the drug are shown by dotted lines and the location of A2062 is marked. (B) Different putative conformations of A2062 in the NPET. In the absence of the nascent peptide, A2062 comes into a close contact with the macrolide narrowing the opening of the NPET (grey carbon atoms – PDB accession number 3OFR (Dunkle et al., 2010)). In the presence of the nascent peptide, the residue can potentially re-orient to open up the tunnel space. The orientation shown for A2062 (green carbon atoms) corresponds to the placement of the residue in the *H. marismortui* large ribosomal subunit complexed with the transition state analog (PDB accession number 1VQ7(Schmeing et al., 2005)).

arrest within the *fus*A gene (Figure 28C).

Extraribosomal cues may be involved in avoiding late arrest *in vivo*. Several secreted proteins, including OmpX, were actively synthesized in *E. coli* exposed to ERY (Figure 13, chapter 3) but their translation was inhibited in the cell-free system. Although fusion of the N-terminal 18 amino acid segment of OmpX to luciferase promoted the N-terminal bypass (Figure 27), the *in vitro* translation of the full-size OmpX protein remained sensitive to ERY likely due to late translation arrest (data not shown). Interaction of the OmpX nascent peptide with the cytoplasmic components of the secretion machinery (Huber et al., 2011) and/or the pulling force of the translocon (Chiba et al., 2011; Nakatogawa et al., 2002) could facilitate the bypass of the late arrest site(s), thus ensuring the successful elongation of the membrane protein *in vivo*.

The late arrest of translation by macrolides and ketolides may have important clinical implications. As discussed in previous chapters, ketolide antibiotics are far more potent than conventional macrolides and exhibit considerable bactericidal activity in select pathogenic strains. Although, the higher toxicity of ketolides could simply arise from their ability to license synthesis of more proteins that results in an imbalance in cellular metabolites, late translation arrest could also contribute to the exaggerated bactericidal activity of ketolides. One important consequence of late arrest is the production of truncated proteins, which have been reported to cause excessive toxicity in several organisms (Machado et al., 2002; Lenhard et al., 1998). Late translation arrest could also potentially lead to the accumulation of a significant fraction of non-translating, stalled ribosomes and the exhaustion of cellular tRNA pools, which could further contribute to the improved potency of ketolides. Although both macrolides and ketolides

can cause late translation arrest *in vitro*, ketolides allow a significantly higher fraction of proteins to be synthesized *in vivo*. This increased N-terminal bypass allowed specifically by ketolides allows much more ribosomes to reach the late arrest site in the presence of a ketolide as opposed to when bound by a macrolide molecule. Thus, we predict that late translation arrest significantly contributes to the mode of action of ketolides rather than macrolides. Through this study, we uncovered an additional mode by which macrolide and ketolide antibiotics act and offer rationalizations for the better activity of the ketolide antibiotics. These attributes of the ketolide molecules can be further exploited for the development of novel, more potent compounds with an increased disposition to allow higher N-terminal bypass and late translation arrest in the cell.

V. Streptogramin B antibiotics are selective inhibitors of translation

5.1 Rationale

In the previous chapters we established that macrolide antibiotics that bind to the NPET selectively inhibit translation of cellular proteins allowing the production of specific polypeptides. Since this was the first demonstration that a small molecule binding to the NPET can serve as a translation regulator, an obvious remaining question is whether selective protein synthesis is unique to macrolide antibiotics or if any small molecule capable of binding to the NPET could exhibit this property. In this study, we test the generality of defined translation phenomenon by using a small molecule drug that is chemically distinct from macrolides (Figure 6) but that also binds to the NPET (Figure 39). To examine this, we chose a molecule from the streptogramin B group, which is also a clinically important class of protein synthesis inhibitors. Streptogramin B antibiotics (e.g., QUI), although chemically distinct from macrolides (Figure 6), bind to the NPET at a site that overlaps with the binding site of macrolides (Figure 39) (Tu et al., 2005) and like macrolides, these compounds do not affect initiation, but interfere with peptide elongation typically after the polymerization of 3-4 amino acids (Tenson et al., 2003; Vazquez, 1966b). In order to assess if the members of the streptogramin-B group also permit selective protein synthesis like macrolides, we measure inhibition of bulk translation in the presence of QUI and further visualize residual protein synthesis in the presence of the drug.

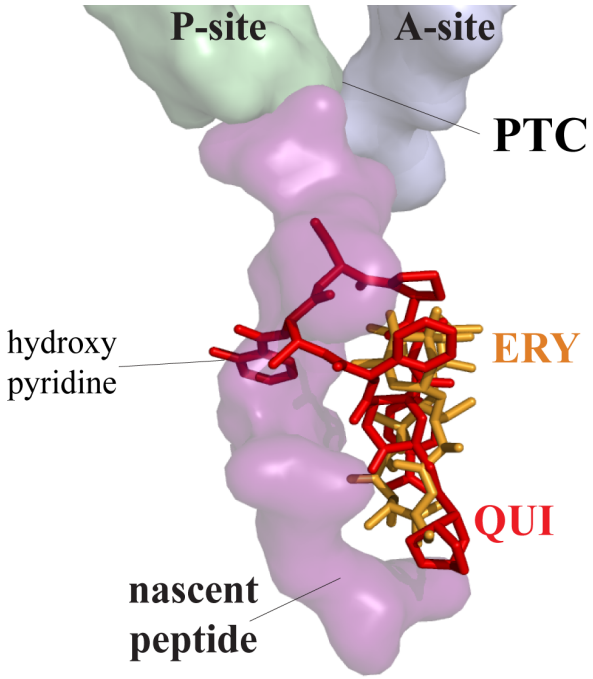

Figure 39. QUI binds to the same site as the macrolide ERY. Shown is the structural overlay of QUI (red) and ERY (orange) when they are bound in the *H. marismortui* ribosome. PDB accession numbers: 1YJW-QUI and 1YI2-ERY (Tu et al., 2005). The bulkier QUI occupies more tunnel space than ERY, with the hydroxy pyridine molecule intruding into the tunnel lumen.

5.2 Experimental results and discussion

The first step towards understanding selective protein synthesis in the presence of QUI was to test the residual protein synthesis that takes place at high concentrations of the antibiotic. The model Gram-positive organism *S. aureus* (strain RN4220) was subjected to increasing concentrations of QUI (1- to 100-fold MIC) and residual translation was monitored following incorporation of [^{35}S]-methionine into the TCA-precipitable protein fraction. At ~50-fold MIC, both QUI and ERY exhibited a maximum inhibition of 94%-95% and even at 100-fold MIC the same level of residual translation was observed (Figure 40A).

In order to test the nature of the proteins synthesized in the presence of QUI, we visualized them by 2D-gel electrophoresis. 2D-gels revealed that much like ERY, QUI allowed a selective fraction of the cellular proteome to be synthesized even at a high concentration of the drug. Several proteins synthesized in the presence of QUI were also among the ERY-resistant polypeptides. Interestingly, a number of QUI-resistant proteins were distinct from those resistant to ERY (Figure 40B, blue triangles). These results with QUI confirms the idea that small molecules bound to the NPET can regulate translation and also expands this concept by emphasizing that the structure of the NPET-bound molecule plays a critical role in defining the spectrum of the resistant polypeptides (the 'resistome').

In the crystallographic complexes of QUI bound to ribosome (Figure 39), the hydroxy pyridine moiety and a portion of the cyclic peptide ring of the drug projects into the tunnel lumen and obstructs the tunnel lumen more severely than a macrolide molecule, whose macrolactone ring lays flat against the tunnel wall. The fact that some

proteins continue to be synthesized in the presence of the drug suggests that the conformation of the drug may change when the nascent peptide reaches the site of QUI binding in the NPET. In contrast to our experiments with macrolides, we did not have any suitable reporters to verify whether QUI remains bound to the ribosomes translating long polypeptides. No QUI-dependent stalling systems have been established so far. Therefore, we cannot exclude the possibility that specific N-terminal nascent peptide sequences may displace the QUI molecule from the NPET. Such protein-specific drug eviction may also account for the observed selectivity of protein synthesis in the presence of QUI.

Regardless of the uncertainty about the exact molecular mechanism that accounts for the selectivity of action of the streptogramin B antibiotics, our results demonstrate that compounds dramatically different in their chemical structures but with the same binding site in the NPET can serve as context-specific modulators of cellular translation. This demonstrates the generality of the phenomenon that binding of small molecules in the NPET can render the ribosome highly selective thereby converting a universal protein synthesis machine into a highly selective polypeptide producer.

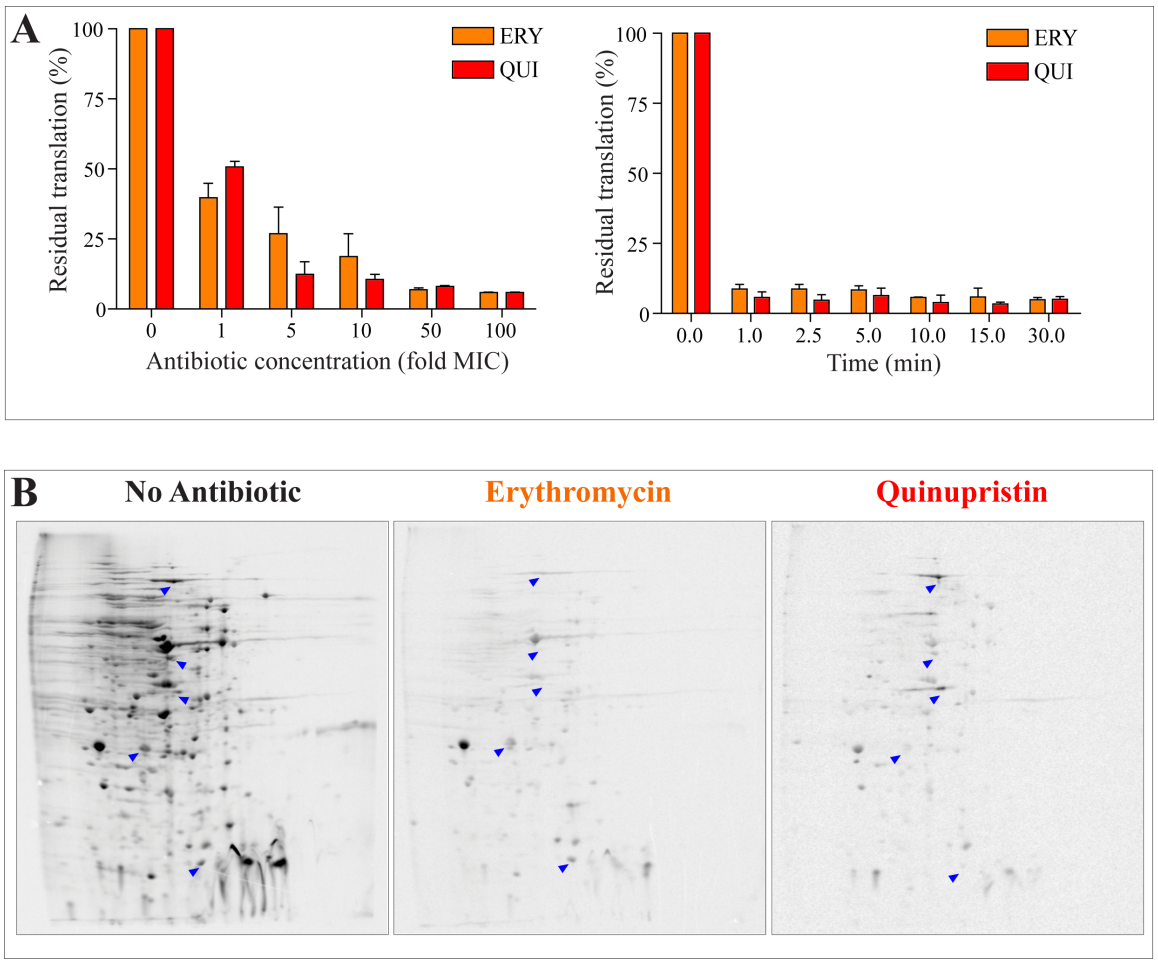

Figure 40. Residual translation profile of QUI vs. ERY. (A) Residual translation in the presence of increasing concentrations of QUI or ERY (left) or in the presence of 100-fold MIC of the drugs incubated for varying time periods (right). Pulse-incorporation of [^{35}S]-methionine in the proteins was determined after exposure of *S. aureus* RN4220 cells to varying concentrations (left) or 100-fold MIC of the drugs (right) for 15 minutes (left) or different time periods (right). Minimal drug inhibitory concentrations are indicated in Table IV. (B) 2D-gel analysis of proteins synthesized *in vivo* in the presence of different ribosomal antibiotics. Radiolabeled proteins, isolated from *S. aureus* strain RN4220 exposed for 15 minutes to 100-fold MIC of QUI or ERY, were resolved by 2D gel-electrophoresis. Blue triangles mark proteins differentially synthesized between ERY and QUI samples.

VI. Context-specific inhibition of translation by PTC-targeting ribosomal antibiotics

6.1 Introduction and rationale

Several natural, semi-synthetic and entirely synthetic antibiotics target the PTC of the ribosome (reviewed in Vazquez, 1979; Yonath, 2005; Wilson, 2009). Several classes of these drugs, such as phenicols (CHL), oxazolidinones (LZD) or lincosamides (CLI) occupy the A-site (Figure 7C). As a result of their binding, these antibiotics sterically prevent the placement of the acceptor end of the aminoacyl-tRNA in the active site, thus blocking peptide bond formation (reviewed in Vazquez, 1979; Wilson, 2009).

Similar to macrolides, which were considered to be indiscriminatory inhibitors of protein translation, PTC-targeting antibiotics are thought to lack any specificity with respect to the context of the inhibited protein. This view has prevailed due to the nature of experimental systems commonly used for the investigation of the mechanisms of antibiotic action. Most studies involving the antibiotic mode of action either analyzed the general effects of protein synthesis inhibitors on the production of bulk cellular proteins *in vivo* or employed cell-free translation systems to test the interference of antibiotics with the synthesis of very few model reporter polypeptides. Such results were extrapolated to all the cellular proteins. Furthermore, much of what we know about the molecular modes of action of the PTC-binding antibiotics came from the studies that reported drug interference with ribosome-catalyzed reactions employing artificially simplified substrates of translation. CLI and CHL are considered to be classic inhibitors of peptide bond formation because they interfere with the 'fragment reaction', which measures transfer of formyl-methionine from a short fragment derived from the fMet-tRNA to an aminoacyl-tRNA analog, puromycin (Monro et al., 1967; Celma et al., 1971).

Experiments of this kind, while illuminating the basics of the inhibition mechanism, could not reveal any context specificity of drug action, and hence the concept of substrate specificity was considered non-existent.

Recent crystallographic structures of ribosome-antibiotic complexes were largely in line with the older biochemical data. X-ray structures confirmed the binding of CHL, CLI and LZD in the PTC A-site thereby providing a structural rationale for interference with aminoacyl-tRNA binding and peptide bond formation (Dunkle et al., 2010; Wilson et al., 2008). The binding of CLI in the PTC is somewhat shifted down towards the NPET compared to binding of CHL (Figure 8B). Such placement of CLI might clash with the nascent peptide, explaining why CLI does not bind to elongating polysomes and only inhibits the formation of the very first peptide bond (Pestka, 1972). In contrast, CHL, which binds specifically in the PTC A-site, can inhibit translation elongation. It can readily bind to polysomes and can 'freeze' them at their functional state by preventing subsequent rounds of aminoacyl-tRNA binding and peptide bond formation (Ennis, 1972). Such an understanding about the action of CHL even justified the use of CHL in the recently developed ribosome profiling technology where the antibiotic is used to stabilize polysomes during cell lysis and polysome isolation (Oh et al., 2011) with the assumption that CHL should inhibit peptide bond formation at all mRNA codons.

The general mode of action of CHL can be simplified as follows: as long as the A-site of the ribosome is available for binding, the drug should bind and prevent the association of the aminoacyl-tRNA and addition of the subsequent amino acid to the growing polypeptide chain (Vazquez, 1975). Binding of the drug to the non-translating or initiating ribosomes should interfere with the first peptide bond formation thereby

preventing such ribosomes from entering the elongation phase. By extrapolation, the mode of action of one of the newest antibiotics, LZD, whose binding site directly overlaps with that of CHL, is expected to follow a similar pattern. Importantly, this view does not include the concept of context-specificity and assumes that the ribosome can be arrested equally and efficiently at any mRNA codon.

However, the generally accepted model for CHL action fails to explain some previously published experimental results. For example, CHL is known to induce the expression of resistance genes encoding a drug-modifying enzyme, chloramphenicol acetyl transferase enzyme (e.g., Cat86), and an efflux pump (e.g., CmlA). The induction mechanism involves programmed translation arrest that takes place at the upstream regulatory ORFs preceding these resistance genes. CHL stalls the ribosome at a specific site in the regulatory ORFs (Figure 41) (Alexieva et al., 1988; Dorman et al., 1985). This induction mechanism implies that the ribosome should be fairly resistant to the action of the drug until it reaches a precise codon of the regulatory ORF; in other words, the translating ribosome should become hypersusceptible to the binding and inhibition by CHL only at a critical mRNA codon. In a few other experimental cases, CHL has shown differential ability to inhibit the transpeptidation reaction depending on the nature of the mRNA template (Tanaka et al., 1971; Kucan et al., 1964; Rheinberger et al., 1990). Specifically, CHL only modestly interferes with the polymerization of Phe or Tyr/Ile when poly(U) or poly(UA) are used as templates respectively, whereas poly(A)-directed poly(Lys) synthesis or poly(C)-directed poly(Pro) formation are more efficiently inhibited (Kucan et al., 1964).

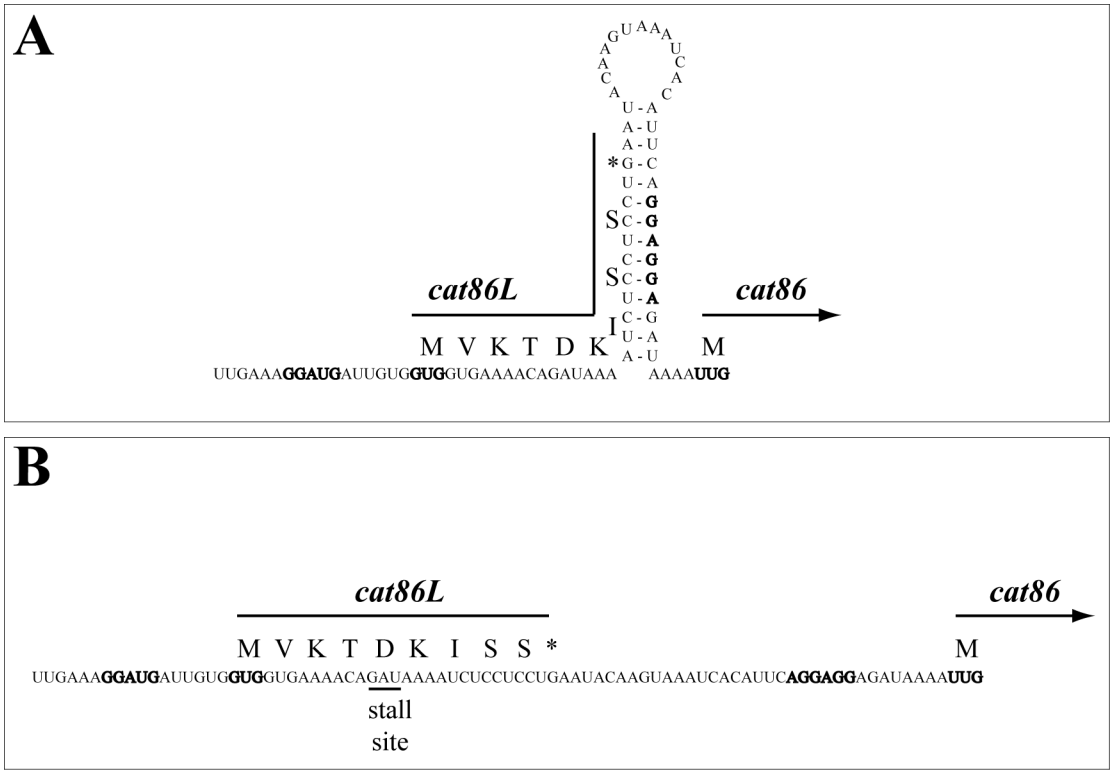

Figure 41. CHL induction of *cat86* translation. (A) In the absence of CHL, *cat86*L is synthesized but *cat86* is not, since the ribosome-binding site of the *cat86* gene is sequestered into the secondary structure of mRNA. (B) Upon CHL binding, ribosomes stall after synthesizing the nascent chain MVKTD of *cat86*L, since CHL inhibits the peptide bond formation between Asp (D) and Lys (K). Ribosome stalling leads to the rearrangement of the mRNA secondary structure resulting in *cat86* translation.

Although the binding mode of LZD is very similar to that of CHL (Wilson et al., 2008; Ippolito et al., 2008), the biochemical knowledge in regards to the workings of this drug is even more controversial. In spite of binding at the PTC A-site, LZD fails to inhibit poly(U)-directed poly(Phe) synthesis, but is able to abolish phage MS2 mRNA-driven translation (IC_{50} = 1.8 μM) (Shinabarger et al., 1997). Unlike CHL or CLI, LZD does not interfere with formation of the peptide bond between the formyl-methionyl-tRNA donor and the puromycin acceptor (Kloss, 1999; Fernandez-Munos et al., 1973; Kouvela et al., 2006). While oxazolidinones efficiently inhibit *in vitro* translation of specific mRNAs (IC_{90} = 10 μM for LZD) (Shinabarger et al., 1997), their affinity for the empty 70S ribosome is very low (K_d = 200 μM) (Zhou et al., 2002) implying that LZD may preferentially bind to translating ribosomes (Wilson, 2011). Even more perplexing was the observation that *in vivo* LZD could be cross-linked to the ribosomal back-translocase LepA (Colca et al., 2003), further implying that a specific state of the translating ribosome (also recognized by LepA) may promote a high-affinity LZD binding.

All these discrepancies with regards to the mechanism of action of PTC-targeting antibiotics, along with our previous work that revealed context specificity of macrolide antibiotics, prompted us to re-examine the mechanisms of action of CHL and LZD and test if translation inhibition by these drugs could be influenced by the nature of ligands present in the ribosome.

6.2 Experimental results

Since LZD is one of the newest and clinically important antibiotics used for the treatment of Gram-positive infections, we decided to use an appropriate experimental

model organism that is more clinically relevant than *E. coli*, which we used in our experiments with macrolide compounds. Therefore, all the experiments described in this section have been carried out using a laboratory strain of *S. aureus* (RN4220). As a first step towards understanding the mode of action of LZD and CHL, we evaluated the general inhibition of bulk protein synthesis by these drugs. This was achieved by monitoring the incorporation of radioactive [^{35}S]-methionine into polypeptides after pre-incubating the exponentially growing *S. aureus* strain RN4220 cells with different concentrations of antibiotics. We included CLI as a control antibiotic since it is expected to be a non-specific A-site inhibitor that interferes with the placement of aminoacyl-tRNA and inhibits the first peptide bond formation. As expected, the incorporation of [^{35}S]-methionine in the protein fraction progressively decreased with increasing concentration of all drugs tested. At about 50-fold MIC, CHL and LZD, as well as the control A-site antibiotic, CLI, almost completely abolished translation, allowing less than 1% of protein synthesis to continue (Figure 42A). The same amount of residual translation (less than 1%) was retained even after 30 minutes of incubation with the drug (Figure 42B).

The minimal residual translation in the presence of very high concentrations of these drugs was generally compatible with the presumed context-independent effects of these antibiotics on translation. However, it did not completely exclude a possibility that the remaining basal translation could still exhibit a certain level of protein-specificity. Therefore, we visualized the proteins synthesized in *S. aureus* strain RN4220 in the presence of 100-fold MIC of CHL and LZD (and CLI) by 2D-gel electrophoresis (Figure 43).

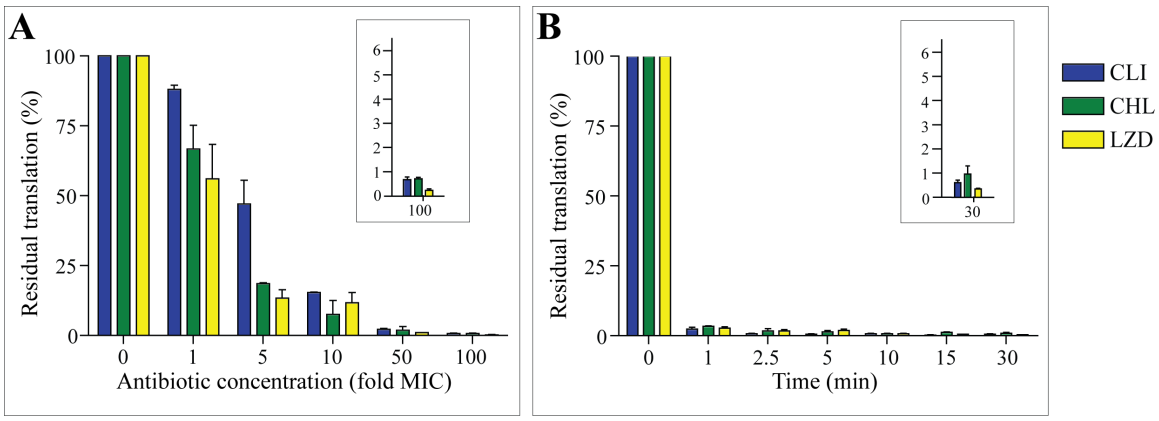

Figure 42. Protein synthesis in cells exposed to A-site binding antibiotics. (A) Residual translation in the presence of increasing concentrations of CLI, CHL or LZD. Pulse-incorporation of [^{35}S]-methionine in the proteins was determined after 15 min exposure of *S. aureus* RN4220 cells to varying concentrations of drug. MICs are indicated in Table IV. (B) Residual protein synthesis after exposure of *S. aureus* strain RN4220 cells to the 100-fold MIC of CLI, CHL or LZD after preincubation with drug for different time periods. The insets in both (A) and (B) show the final data point from each graph with a smaller range of the Y-axis scale.

The 2D-gels corroborated our observation that protein synthesis was efficiently inhibited by treatment with the A-site targeting antibiotics: very few weak protein spots were observed in the gel (Figure 43). Importantly, similar spots were observed with different antibiotics suggesting that these spots simply represent the most actively translated proteins in the cell. The residual translation of the highly expressed proteins is not surprising. Drug-bound and drug-free ribosomes exist in a dynamic equilibrium. Even at a high concentration of drug, there is a possibility of aminoacyl-tRNA binding after a spontaneous dissociation of the drug molecule from the ribosome. Therefore, in strict terms, the antibiotics that interfere with aminoacyl-tRNA binding do not 'block' translation elongation, but rather dramatically slow this process. The more actively a protein is translated, and shorter its length, the higher is the chance that some amount of full-size protein will be produced from the corresponding mRNA even in the presence of the drug. However, this consideration cannot account for a puzzling observation that the intensity of protein spots observed in 2D gels varied for different antibiotics (Figure 43, red triangles). While CHL and LZD exhibited very similar profiles of residual translation, in agreement with the same mode of their binding to the A-site, their profiles differed from those seen with CLI (Figure 43, red arrows, spots 1-3). This result suggested the idiosyncratic nature of inhibition of translation by LZD/CHL vs CLI, which could be potentially dictated by the nature of the nascent chain, mRNA and/or the tRNA substrates.

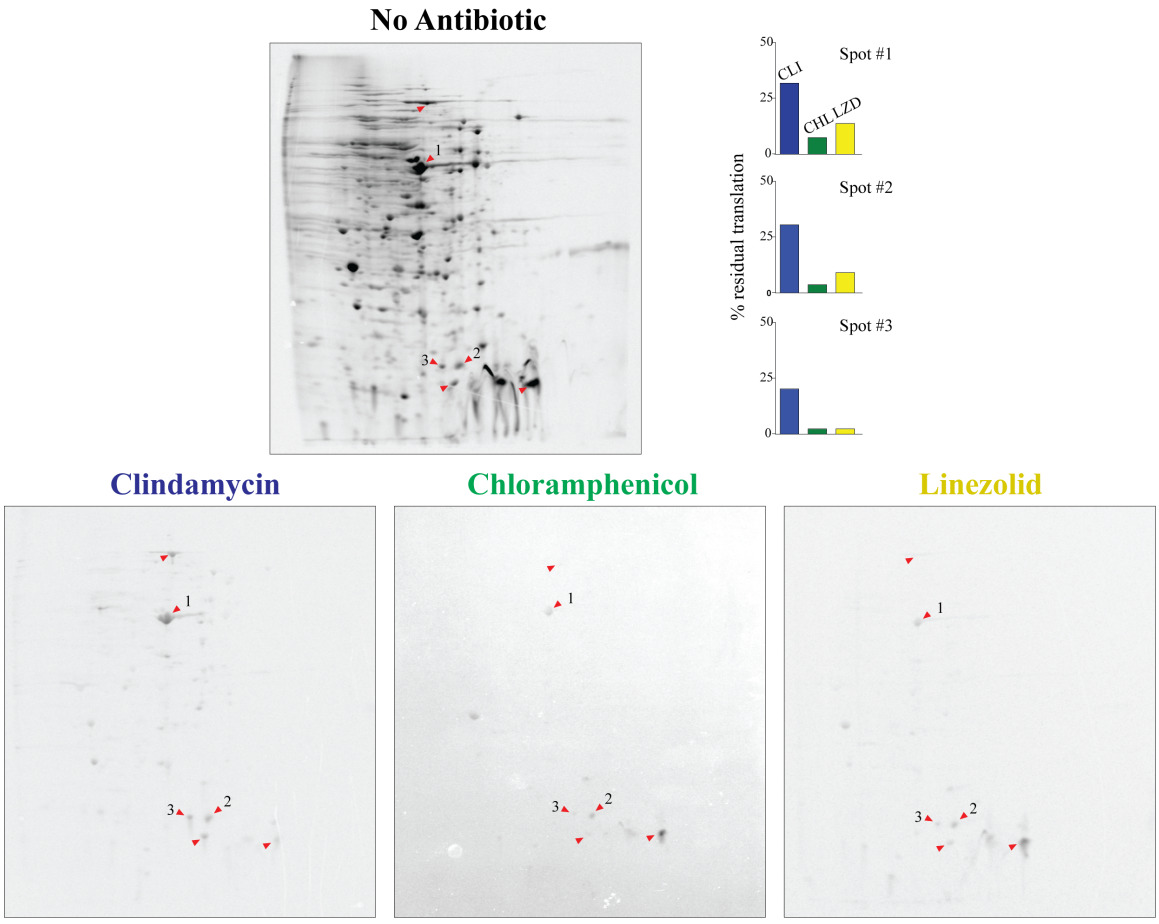

Figure 43. 2D-gel analysis of proteins synthesized *in vivo* in the presence of different ribosomal antibiotics. Radiolabeled proteins, isolated from *S. aureus* strain RN4220 exposed for 15 min to 100-fold MIC of CLI, CHL or LZD, were resolved by 2D gel-electrophoresis. Spots containing proteins that are differentially synthesized in the presence of each antibiotic are indicated by red triangles. Integrated density of some spots (1-3) were measured and expressed as a fractional percentage of the corresponding spots in the no antibiotic control.

This observation prompted us to further probe the mode of action of CHL and LZD. For this, we followed the ability of these drugs to inhibit translation of several natural and synthetic genes *in vitro*. According to the current model, the presence of the drug at a high concentration at the onset of the translation reaction should inhibit the first peptide bond formation regardless of the type of mRNA template and the ribosome should be arrested at the initiator codon. Such translation arrest can be readily detected by toe-printing.

We used different naturally occurring mRNA templates, such as *hns*, *osm*C, *mip*A, *csp*A, and *erm*BL genes, and a synthetic 20-codon ORF, *rst1*. These templates were chosen simply because of their availability in our collection of templates that are suitable for cell-free translation in the PURE system. We included TET in the toe-printing experiments as a control drug along with CLI because TET is also a non-specific A-site initiation inhibitor, but unlike CLI, it can inhibit elongation as well (like CHL and LZD). The results of *in vitro* translation and toe-printing analysis showed that both CLI and TET acted like typical A-site inhibitors: they efficiently inhibited the first peptide bond formation and consequently arrested the ribosomes at the start codon (Figures 44 A-D, lanes 2 and 5). Noteworthy, TET-dependent arrest was not complete; in addition to stalling the ribosome at the initiator codon, a series of toe-printing bands corresponding to random arrest of translation at subsequent mRNA codons was also observed. This result is in line with the above-discussed kinetic nature of antibiotic binding and action (Figures 44 A-D, lane 5).

In contrast, we observed that CHL and LZD neither inhibited the formation of the first peptide bond (like CLI), nor caused random arrest of translation elongation (like

TET). Instead, these antibiotics stalled the ribosome at specific mRNA codons after the polymerization of several amino acids (Figures 44 A-D, lanes 3-4; 45A, lane 2; 45B lanes 3-4). Several of the CHL- and LZD- arrest sites were similar; however, some sites exhibited antibiotic specificity. By utilizing several templates, we were able to generate a small collection of ribosome stalling sites induced by CHL and LZD (Figure 46). When the nascent peptide sequences were aligned with respect to the C-terminal amino acid (at the P-site) some weak trends could be detected, such as a prevalence of charged or polar residues at the C-terminus of the nascent peptide. However, so far, we have been unable to identify a clear nascent peptide motif or a specific combination of donor and acceptor substrates that define the sites of translation inhibition by CHL and LZD. Nevertheless, the observation that the A-site-binding antibiotics CHL and LZD can arrest translation at specific mRNA codons unequivocally shows that the drugs binding to the PTC can also exhibit context specific activity.

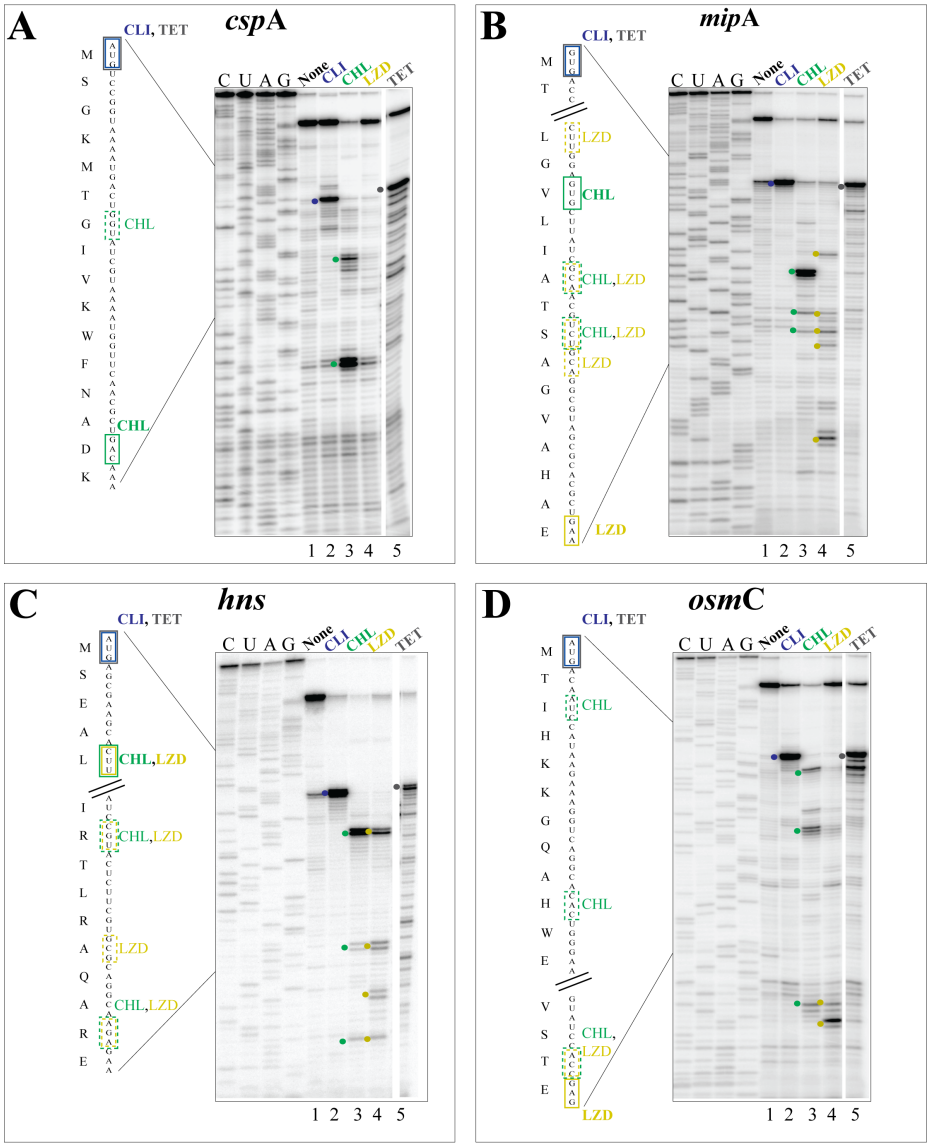

Figure 44. Context-specific inhibition of translation by ribosomal antibiotics. Detection of the site of ribosome stalling near the N-terminus of (A) *csp*A, (B) *mip*A, (C) *hns* and (D) *osm*C mRNA by toe-printing. Antibiotic concentrations used in the reaction are 200 μM for CHL and CLI, and 1 mM for TET and LZD. Toe-printing primers (osmC100 rev, hns toeprinting-4, mipA100 rev, cspA110 rev (Table II)) were annealed ~100 nucleotides from the start codon of each template. P-site codon of the stalled ribosomes is marked by full or dashed boxes corresponding to a strong or weak toe-printing signal respectively. Toe-prints on the gel are marked by color-coded dots for each antibiotic: CLI-blue, CHL-green, LZD-dirty yellow and TET-grey.

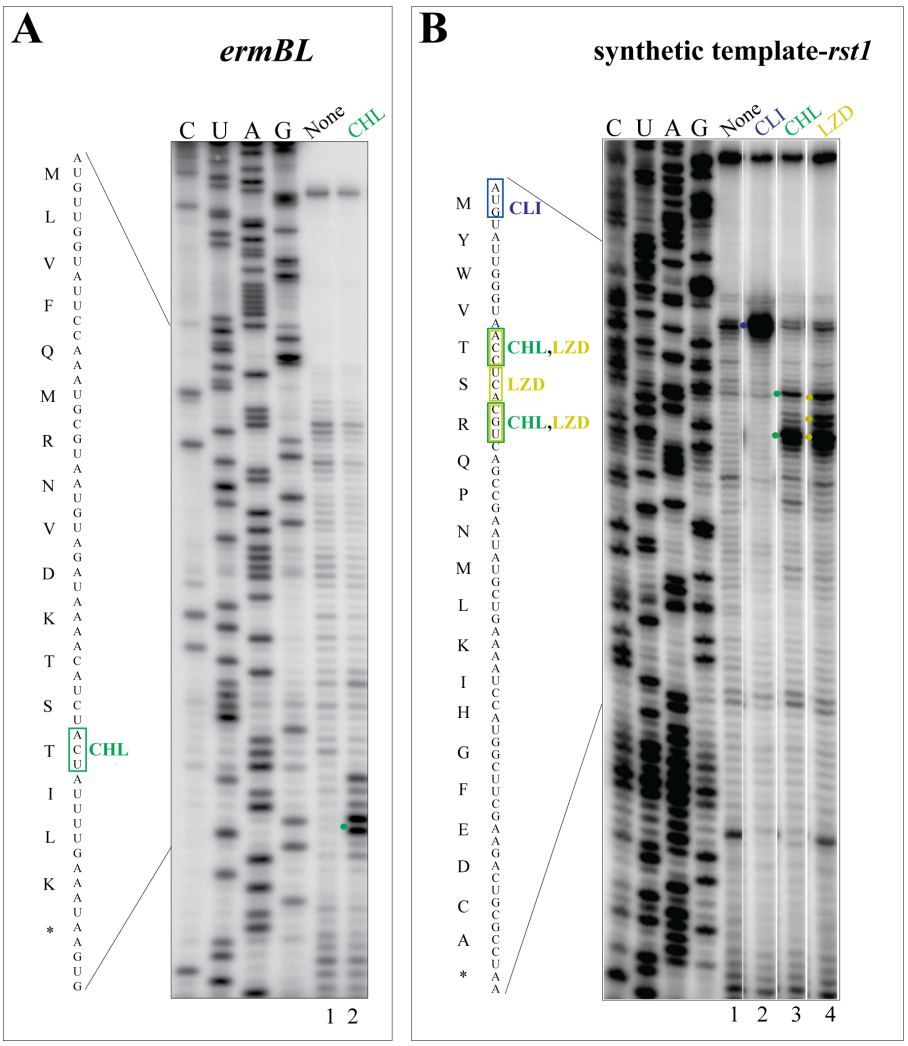

Figure 45. Drug-dependent ribosome stalling at *erm*BL and the synthetic template *rst1*. CHL-dependent stalling at *erm*BL and CHL-, CLI- and LZD- dependent stalling at *rst1* were mapped using toe-printing. 50 μM of each antibiotic was used in this assay. Toe-printing primer NV1 (Table II) was annealed to the mRNA to detect stalled ribosome complexes. The rest of the procedures and labeling of the gel-image are similar to that described in Figure 33. This experiment was performed by Anna Ochabowicz.

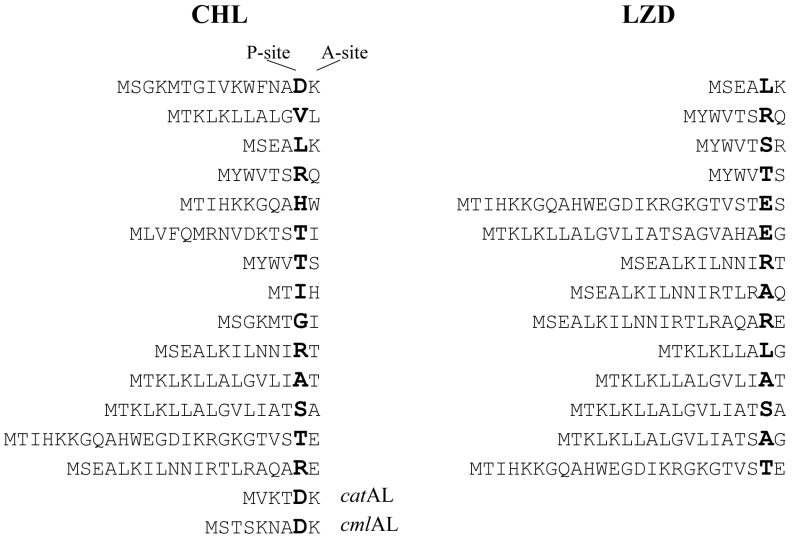

Figure 46. Nascent peptides inducing drug-dependent ribosome stalling. Amino acid sequences of nascent peptides from Figures 44 and 45 are aligned with respect to the P-site (C-terminus) of the stalled ribosome. P-site amino acid is marked in bold and the incoming A-site amino acid is indicated. Peptides are ordered with respect to the strength of stalling with the first peptide in each list being the strongest staller. Known drug-dependent, ribosome-stalling peptides are also included.

6.3 Discussion

We observed that not only tunnel-binding inhibitors of translation such as ERY or TEL but also PTC-binding drugs such as CHL and LZD can exhibit context specificity in their mode of action. The A-site binding antibiotics inhibit peptide bond formation at specific mRNA codons while permitting the catalysis of transpeptidation at the other codons (Figures 47).

In contrast to CLI and TET that efficiently interfere with the first peptide bond formation, CHL and LZD allow the ribosome to catalyze the first peptide bond and even incorporate several subsequent amino acids into the nascent peptide prior to arresting translation at specific downstream codons (Figures 47). As often observed, even at the 'inhibitory' codons, the arrest of translation was not always complete: a fraction of ribosomes could still continue polymerization and reach several downstream 'arrest' sites. As a result, if antibiotic is present during the onset of translation, the ribosomes stall at several locations close to the 5' end of the mRNA.

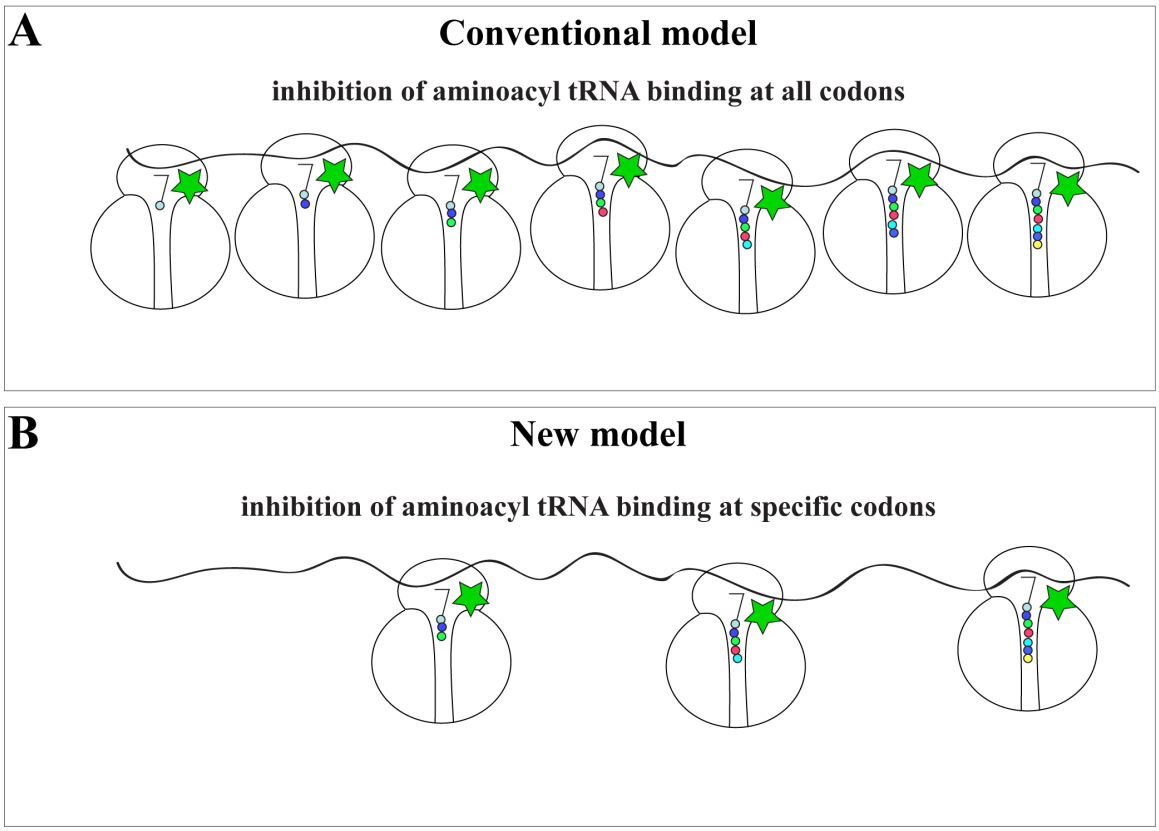

Figure 47. Mode of action of CHL and LZD. (A) The commonly accepted model is that CHL and LZD (green star) inhibit the association of any incoming aminoacyl tRNA and stop the formation of the first and every subsequent peptide bond. (B) In the new model, these drugs inhibit not all, but rather specific peptide bond formation in a ribosomal-ligand context-dependent manner.

Although the rules that underlie the mechanism of arrest are yet unclear, its context-specific nature is obvious. This finding dramatically changes our view of how CHL and LZD antibiotics act. Our results demonstrate that the stage at which translation is inhibited is non-stochastic and could be influenced either by the nature of tRNAs, the nascent peptide and/or the mRNA. In this regard, it is noteworthy that in the crystalline state, the conformation of LZD is slightly different in the archaeal (*H. marismortui*) ribosome, which also contains the CCA-Phe substrate in the P-site, compared to the eubacterial (*D. radiodurans*) ribosome where LZD was bound in the absence of a P-site ligand (Ippolito et al., 2008, Wilson et al., 2008). Although this difference can stem from a variation in the structure of PTC between these ribosomes, it most likely reflects the influence of ribosomal cofactors on drug binding.

In our experiments, CHL inhibited translation shortly after initiation and never the first peptide bond formation. These *in vitro* results are in line with the previously reported *in vivo* data that showed the accumulation of short oligopeptides upon CHL treatment of *E. coli* cells (Cremer et al., 1974). Taken together, these results suggest that the affinity of the ribosome for CHL could be influenced by the specific peptidyl-tRNAs substrates or that some aminoacyl-tRNAs more efficiently compete with CHL for binding to the A-site. In fact, CHL has been shown to more efficiently inhibit the association of the model A-site substrate CCA-Lys than the binding of CCA-Phe (Lessard et al., 1972). However, putative A-site (also P-site) substrate specificity alone is clearly not sufficient to explain all the observed effects. For instance, while CHL inhibits the peptide bond formation between Asp (D) and Lys (K) during the translation of *csp*A (Figure 44A, lane 3), it does not do so during ErmBL synthesis (Figure 45A, lane 2). A similar trend was observed in

the presence of LZD; the peptide bond formation between Leu (L) and Lys (K) was inhibited during the synthesis of H-NS (Figure 44C, lane 4) but the bond between the same substrates was allowed to form during production of MipA (Figure 44B, lane 4). This result implies that the context of the nascent peptide (or potentially, the mRNA) plays a significant role in defining the sites of CHL and LZD inhibition rather than the donor and acceptor substrates themselves.

Several arguments make us favor a model wherein the nascent peptide in the NPET influences the action of CHL and LZD. Binding of CHL to the PTC alters the structure of the NPET. Specifically, CHL influences the accessibility of several tunnel nucleotides (2058, 2059 and 2062) to modification with dimethyl sulfate (Moazed et al., 1987a) even though these nucleotide residues are not in direct contact with the drug. Conversely, binding of macrolides in the tunnel allosterically affects the modification of some PTC nucleotides (e.g. U2585) by 1-methyl-7-nitroisatoic anhydride (Vazquez-Laslop and Klepacki, unpublished). Furthermore, ERY, which binds to the NPET, can compete with CHL binding to the PTC (Vazquez, 1966a; Pestka et al., 1974b) even though the binding sites of these antibiotics do not overlap. Our lab has previously demonstrated that the nature of the nascent peptide in the macrolide-bound NPET might directly influence properties of the PTC A-site (Ramu et al., 2011). All of these results suggest the existence of an allosteric association between the NPET and the PTC. Therefore, at least in theory, specific nascent peptides in the NPET could allosterically and specifically alter the PTC A-site and thus, facilitate drug binding only at precise mRNA codons. The rules that govern the context specificity of action of LZD and CHL will likely emerge when a much larger dataset of the ‘specific’ sites of action of these

drugs becomes available. We are currently investigating the specificity of action of these antibiotics at the whole genome level using ribosome-profiling technology (Ingolia et al., 2009).

Regardless of the underpinnings of the mechanism, our findings dramatically change the view of how CHL and LZD act. In contrast to the prevailing view of stochastic binding of these antibiotics to the unoccupied PTC A-site, we think that a high affinity binding site for LZD and/or CHL is created during translation and that the properties of this state are dictated by the nature of the ribosomal ligands (tRNA substrates, nascent peptide and possibly, mRNA).

Our findings not only reconcile several biochemical observations that could not be explained by the conventional model but also provide a molecular explanation for the site-specific translation arrest required for the inducible CHL-resistance where CHL directs ribosome stalling at specific codons of the regulatory ORF (Figure 41). We propose that during the translation of the upstream ORFs of *cat* or *cml* operons, a high affinity site for CHL is generated in the translating ribosome only when it reaches the stalling site following which, drug binding ensues and the catalysis of the peptide bond formation specifically between the peptidyl-tRNA at the Asp codon and the acceptor Lys-tRNA in both leader peptides (Figure 44) is inhibited. Interestingly, in one of the templates used in this study, CspA, CHL inhibits the formation of the peptide bond between the same donor and acceptor substrates (Figure 44).

Antibiotics were always assumed to interact with ribosomes and inhibit translation regardless of the type of the protein being synthesized. Our study challenges this view by establishing a new paradigm for translation inhibition by CHL and LZD that

could potentially depend on the specific functional state and the nature of the substrates of the translating ribosome. Detailed examination of such functional states could not only improve our understanding about the dynamics of the ribosome during translation but also lead to discovery of new antibiotics targeting such states.

VII. CONCLUSIONS

Through this study, we established several new important aspects of the mode of action of several classes of ribosomal antibiotics that are currently used to combat bacterial infections.

We discovered that macrolides and their more potent derivatives, ketolides, do not inhibit translation completely even at saturating concentrations. Instead, these drugs render the ribosome highly selective compelling it to synthesize a limited fraction of the cellular proteome. It is the N-terminal amino acid sequence of the protein that defines its propensity for initially bypassing the macrolide molecule in the tunnel of the ribosome. The concept that long polypeptides can be synthesized by the drug-bound ribosome deviates significantly from the popular belief that a macrolide molecule and the nascent chain cannot co-exist in the NPET.

The spectrum of the proteins that escape from QUI inhibition is mostly similar to those that escape from ERY with some exceptions indicating that the structure of the antibiotics can influence the 'resistome'. On the other hand, TEL allows for many more proteins to be synthesized compared to ERY or QUI. There appears to be a surprisingly inverse correlation between the amount of proteins that escape inhibition and the bactericidal activity of these drugs. Our results with ERY and TEL suggest that inhibition of production of specific polypeptides that can lead to a metabolic imbalance may be more detrimental for the cell than a complete inhibition of translation. This view suggests a new direction for drug development focusing on selective, rather than global inhibition of translation.

Even after the N-terminal bypass, the synthesis of a polypeptide can be still arrested by macrolides at later stages of elongation depending on the local nascent peptide sequence. Inhibition of translation by macrolides and ketolides at late stages of elongation leads to the production of truncated proteins, which can cause cellular toxicity. Genome-wide ribosome profiling experiments that are currently underway are expected to help us generate a complete catalog of late-stalling sites in the presence of TEL and specifically identify the late-arrest events causing the increased bactericidal activity of this drug. With this information, one can potentially optimize the drug structure for promoting late arrest at specific sites, thus increasing the toxic effects of the drug associated with the production of truncated proteins in the cells.

Context-specificity of drug action is not limited to tunnel-bound antibiotics that can directly interact with the nascent peptide. CHL, one of the oldest ribosomal antibiotics and LZD, one of the newest drugs, both act upon the PTC and thus do not come in direct contact with the nascent peptide. Nevertheless, these drugs arrest translation at specific mRNA codons, implying that the nature of the ribosomal substrates plays a key role in the mechanism of action of these antibiotics. Further studies are necessary to better define what these functional states of the ribosome are and what role the nascent peptide or the mRNA context may play. Nonetheless, we believe that our study will open a new avenue for studying the dynamics of the ribosome during translation and understanding the mechanism of action of PTC-targeting drugs. We can also envision the search for new translation inhibitors targeting those sites on the ribosome that are created or become accessible at specific functional states of the ribosome, possibly in response to the cues from the mRNA or nascent peptide.

CITED LITERATURE

Ackermann, G., and Rodloff, A.C. (2003). Drugs of the 21st century: telithromycin (HMR 3647)--the first ketolide. J. Antimicrob. Chemother.3 *51*, 497-511.

Alexieva, Z., Duvall, E.J., Ambulos, N.P., Jr., Kim, U.J., and Lovett, P.S. (1988). Chloramphenicol induction of *cat-86* requires ribosome stalling at a specific site in the leader. Proc. Natl. Acad. Sci. USA *85*, 3057-3061.

Andersson, S., and Kurland, C.G. (1987). Elongating ribosomes *in vivo* are refractory to erythromycin. Biochimie *69*, 901-904.

Apirion, D. (1967). Three genes that affect *Escherichia coli* ribosomes. J. Mol. Biol. *30*, 255-275.

Baba, T., Ara, T., Hasegawa, M., Takai, Y., Okumura, Y., Baba, M., Datsenko, K.A., Tomita, M., Wanner, B.L., and Mori, H. (2006). Construction of *Escherichia coli* K-12 in-frame, single-gene knockout mutants: the Keio collection. Mol. Syst. Biol. *2*, 2006 0008.

Ban, N., Nissen, P., Hansen, J., Moore, P.B., and Steitz, T.A. (2000). The complete atomic structure of the large ribosomal subunit at 2.4 Å resolution. Science *289*, 905-920.

Bloch, V., Yang, Y., Margeat, E., Chavanieu, A., Auge, M.T., Robert, B., Arold, S., Rimsky, S., and Kochoyan, M. (2003). The H-NS dimerization domain defines a new fold contributing to DNA recognition. Nat. Struct. Biol. *10*, 212-218.

Brock, T.D., and Brock, M.L. (1959). Similarity in mode of action of chloramphenicol and erythromycin. Biochim. Biophys. Acta *33*, 274-275.

Brodersen, D.E., Clemons, W.M., Jr., Carter, A.P., Morgan-Warren, R.J., Wimberly, B.T., and Ramakrishnan, V. (2000). The structural basis for the action of the antibiotics tetracycline, pactamycin, and hygromycin B on the 30S ribosomal subunit. Cell *103*, 1143-1154.

Bulkley, D., Innis, C.A., Blaha, G., and Steitz, T.A. (2010). Revisiting the structures of several antibiotics bound to the bacterial ribosome. Proc. Natl. Acad. Sci. USA *107*, 17158-17163.

Celma, M.L., Monro, R.E., and Vazquez, D. (1971). Substrate and antibiotic binding sites at the peptidyl transferase centre of *E. coli* ribosomes: Binding of UACCA-Leu to 50 S subunits. FEBS Lett. *13*, 247-251.

Champney, W.S., and Miller, M. (2002a). Inhibition of 50S ribosomal subunit assembly in *Haemophilus influenzae* cells by azithromycin and erythromycin. Curr. Microbiol. *44*, 418-424.

Champney, W.S., and Pelt, J. (2002b). Telithromycin inhibition of protein synthesis and 50S ribosomal subunit formation in *Streptococcus pneumoniae* cells. Curr. Microbiol. *45*, 328-333.

Champney, W.S., and Pelt, J. (2002c). The ketolide antibiotic ABT-773 is a specific inhibitor of translation and 50S ribosomal subunit formation in *Streptococcus pneumoniae* cells. Curr. Microbiol. *45*, 155-160.

Chiba, S., Kanamori, T., Ueda, T., Akiyama, Y., Pogliano, K., and Ito, K. (2011). Recruitment of a species-specific translational arrest module to monitor different cellular processes. Proc. Natl. Acad. Sci. USA *108*, 6073-6078.

Chittum, H.S., and Champney, W.S. (1994). Ribosomal protein gene sequence changes in erythromycin-resistant mutants of *Escherichia coli*. J. Bacteriol. *176*, 6192-6198.

Colca, J.R., McDonald, W.G., Waldon, D.J., Thomasco, L.M., Gadwood, R.C., Lund, E.T., Cavey, G.S., Mathews, W.R., Adams, L.D., Cecil, E.T.*, et al.* (2003). Cross-linking in the living cell locates the site of action of oxazolidinone antibiotics. J. Biol. Chem. *278*, 21972-21979.

Contreras, A., and Vazquez, D. (1977). Synergistic interaction of the streptogramins with the ribosome. Eur. J. Biochem. *74*, 549-551.

Contreras, A., and Vazquez, D. (1977). Co-operative and antagonistic interactions of peptidyl-tRNA and antibiotics with bacterial ribosomes. Eur. J. Biochem. *74*, 539-547.

Cremer, K., Silengo, L., and Schlessinger, D. (1974). Polypeptide formation and polyribosomes in *Escherichia coli* treated with chloramphenicol. J. Bacteriol. *118*, 582-589.

Datsenko, K.A., and Wanner, B.L. (2000). One-step inactivation of chromosomal genes in *Escherichia coli* K-12 using PCR products. Proc. Natl. Acad. Sci. USA *97*, 6640-6645.

Demeshkina, N., Jenner, L., Yusupova, G., and Yusupov, M. (2010). Interactions of the ribosome with mRNA and tRNA. Curr. Opin. Struct. Biol. *20*, 325-332.

Dorman, C.J., and Foster, T.J. (1985). Posttranscriptional regulation of the inducible nonenzymatic chloramphenicol resistance determinant of IncP plasmid R26. J. Bacteriol. *161*, 147-152.

Douthwaite, S., Powers, T., Lee, J.Y., and Noller, H.F. (1989). Defining the structural requirements for a helix in 23S ribosomal RNA that confers erythromycin resistance. J. Mol. Biol. *209*, 655-665.

Dunkle, J.A., Xiong, L., Mankin, A.S., and Cate, J.H. (2010). Structures of the *Escherichia coli* ribosome with antibiotics bound near the peptidyl transferase center explain spectra of drug action. Proc. Natl. Acad. Sci. USA *107*, 17152-17157.

Duthie, E.S., and Lorenz, L.L. (1952). Staphylococcal coagulase; mode of action and antigenicity. J. Gen. Microbiol. *6*, 95-107.

Ennis, H.L. (1972). Polysome metabolism in *Escherichia coli*: effect of antibiotics on polysome stability. Antimicrob. Agents Chemother. *1*, 197-203.

Ettayebi, M., Prasad, S.M., and Morgan, E.A. (1985). Chloramphenicol-erythromycin resistance mutations in a 23S rRNA gene of *Escherichia coli*. J. Bacteriol. *162*, 551-557.

Fang, P., Spevak, C.C., Wu, C., and Sachs, M.S. (2004). A nascent polypeptide domain that can regulate translation elongation. Proc. Natl. Acad. Sci. USA *101*, 4059-4064.

Fernández-Muñoz, R. and Vazquez, D. (1973). Quantitative binding of [^{14}C]-erythromycin a to *E. coli* ribosomes. J. Antibiot. (Tokyo) *26*, 107-108.

Frank, J., Zhu, J., Penczek, P., Li, Y., Srivastava, S., Verschoor, A., Radermacher, M., Grassucci, R., Lata, R.K., and Agrawal, R.K. (1995). A model of protein synthesis based on cryo-electron microscopy of the *E. coli* ribosome. Nature *376*, 441-444.

Fulle, S., and Gohlke, H. (2009). Statics of the ribosomal exit tunnel: implications for cotranslational peptide folding, elongation regulation, and antibiotics binding. J. Mol. Biol. *387*, 502-517.

Gerrits, M.M., de Zoete, M.R., Arents, N.L., Kuipers, E.J., and Kusters, J.G. (2002). 16S rRNA mutation-mediated tetracycline resistance in *Helicobacter pylori*. Antimicrob. Agents Chemother. *46*, 2996-3000.

Giachino, P., Engelmann, S., and Bischoff, M. (2001). Sigma(B) activity depends on RsbU in *Staphylococcus aureus*. J. Bacteriol. *183*, 1843-1852.

Goldman, R.A., Hasan, T., Hall, C.C., Strycharz, W.A., and Cooperman, B.S. (1983). Photoincorporation of tetracycline into *Escherichia coli* ribosomes. Identification of the major proteins photolabeled by native tetracycline and tetracycline photoproducts and implications for the inhibitory action of tetracycline on protein synthesis. Biochemistry *22*, 359-368.

Gong, F., and Yanofsky, C. (2002). Instruction of translating ribosome by nascent peptide. Science *297*, 1864-1867.

Graham, M.Y., and Weisblum, B. (1979). 23S ribosomal ribonucleic acid of macrolide-producing streptomycetes contains methylated adenine. J. Bacteriol. *137*, 1464-1467.

Gregory, S.T., and Dahlberg, A.E. (1999). Erythromycin resistance mutations in ribosomal proteins L22 and L4 perturb the higher order structure of 23S ribosomal RNA. J. Mol. Biol. *289*, 827-834.

Guzman, L.M., Belin, D., Carson, M.J., and Beckwith, J. (1995). Tight regulation, modulation, and high-level expression by vectors containing the arabinose P_{BAD} promoter. J. Bacteriol. *177*, 4121-4130.

Hamilton-Miller, J.M., and Shah, S. (1998). Comparative in-vitro activity of ketolide HMR 3647 and four macrolides against gram-positive cocci of known erythromycin susceptibility status. J. Antimicrob. Chemother. *41*, 649-653.

Hansen, J.L., Ippolito, J.A., Ban, N., Nissen, P., Moore, P.B., and Steitz, T.A. (2002). The structures of four macrolide antibiotics bound to the large ribosomal subunit. Mol. Cell *10*, 117-128.

Hardesty, B., Picking, W.D., and Odom, O.W. (1990). The extension of polyphenylalanine and polylysine peptides on *Escherichia coli* ribosomes. Biochim. Biophys. Acta *1050*, 197-202.

Hartz, D., McPheeters, D.S., Traut, R., and Gold, L. (1988). Extension inhibition analysis of translation initiation complexes. Methods Enzymol. *164*, 419-425.

Hillebrecht, J.R., and Chong, S. (2008). A comparative study of protein synthesis in *in vitro* systems: from the prokaryotic reconstituted to the eukaryotic extract-based. BMC Biotechnol. *8*, 58.

Hilliard, J.J., Goldschmidt, R.M., Licata, L., Baum, E.Z., and Bush, K. (1999). Multiple mechanisms of action for inhibitors of histidine protein kinases from bacterial two-component systems. Antimicrob. Agents Chemother. *43*, 1693-1699.

Horinouchi, S., and Weisblum, B. (1980). Posttranscriptional modification of mRNA conformation: mechanism that regulates erythromycin-induced resistance. Proc. Natl. Acad. Sci. USA *77*, 7079-7083.

Huber, D., Rajagopalan, N., Preissler, S., Rocco, M.A., Merz, F., Kramer, G., and Bukau, B. (2011). SecA interacts with ribosomes in order to facilitate posttranslational translocation in bacteria. Mol. Cell *41*, 343-353.

Hughes, J., and Mellows, G. (1978). Inhibition of isoleucyl-transfer ribonucleic acid synthetase in *Escherichia coli* by pseudomonic acid. Biochem. J. *176*, 305-318.

Ingolia, N.T., Ghaemmaghami, S., Newman, J.R., and Weissman, J.S. (2009). Genome-wide analysis *in vivo* of translation with nucleotide resolution using ribosome profiling. Science *324*, 218-223.

Ippolito, J.A., Kanyo, Z.F., Wang, D., Franceschi, F.J., Moore, P.B., Steitz, T.A., and Duffy, E.M. (2008). Crystal structure of the oxazolidinone antibiotic linezolid bound to the 50S ribosomal subunit. J. Med. Chem. *51*, 3353-3356.

Ito, K., Chiba, S., and Pogliano, K. (2010). Divergent stalling sequences sense and control cellular physiology. Biochem Biophys. Res. Commun. *393*, 1-5.

Kanehisa, M., Goto, S., Kawashima, S., and Nakaya, A. (2002). The KEGG databases at GenomeNet. Nucleic Acids Res. *30*, 42-46.

Kannan, K., and Mankin, A.S. (2011). Macrolide antibiotics in the ribosome exit tunnel: species-specific binding and action. Ann. N Y Acad. Sci. *1241*, 33-47.

Kloss, P., Xiong, L., Shinabarger, D.L., and Mankin, A.S. (1999). Resistance mutations in 23 S rRNA identify the site of action of the protein synthesis inhibitor linezolid in the ribosomal peptidyl transferase center. J. Mol. Biol. *294*, 93-101.

Kohanski, M.A., Dwyer, D.J., Hayete, B., Lawrence, C.A., and Collins, J.J. (2007). A common mechanism of cellular death induced by bactericidal antibiotics. Cell *130*, 797-810.

Kouvela, E.C., Petropoulos, A.D., and Kalpaxis, D.L. (2006). Unraveling new features of clindamycin interaction with functional ribosomes and dependence of the drug potency on polyamines. J. Biol. Chem. *281*, 23103-23110.

Kucan, Z., and Lipmann, F. (1964). Differences in chloramphenicol sensitivity of cell-free amino acid polymerization systems. J. Biol. Chem. *239*, 516-520.

Lenhard, B., Praetorius-Ibba, M., Filipic, S., Soll, D., and Weygand-Durasevic, I. (1998). C-terminal truncation of yeast SerRS is toxic for *Saccharomyces cerevisiae* due to altered mechanism of substrate recognition. FEBS Lett. *439*, 235-240.

Lessard, J.L., and Pestka, S. (1972). Studies on the formation of transfer ribonucleic acid-ribosome complexes. 23. Chloramphenicol, aminoacyl-oligonucleotides, and *Escherichia coli* ribosomes. J. Biol. Chem. *247*, 6909-6912.

Lovmar, M., Nilsson, K., Lukk, E., Vimberg, V., Tenson, T., and Ehrenberg, M. (2009). Erythromycin resistance by L4/L22 mutations and resistance masking by drug efflux pump deficiency. EMBO J. *28*, 736-744.

Lovmar, M., Nilsson, K., Vimberg, V., Tenson, T., Nervall, M., and Ehrenberg, M. (2006). The molecular mechanism of peptide-mediated erythromycin resistance. J. Biol. Chem. *281*, 6742-6750.

Machado, R.C., Pereira, R.N., Costa, M.S., and Ramos, R.G. (2002). "*In vivo*" toxicity of a truncated version of the Drosophila Rst-IrreC protein is dependent on the presence of a glutamine-rich region in its intracellular domain. An. Acad. Bras. Cienc. *74*, 285-295.

Mankin, A.S. (2008). Macrolide myths. Curr. Opin. Microbiol. *11*, 414-421.

Mayford, M., and Weisblum, B. (1989). *erm*C leader peptide. Amino acid sequence critical for induction by translational attenuation. J. Mol. Biol. *206*, 69-79.

McGuire, J.M., Bunch, R.L., Anderson, R.C., Boaz, H.E., Flynn, E.H., Powell, H.M., and Smith, J.W. (1952). Ilotycin, a new antibiotic. Schweiz Med. Wochenschr *82*, 1064-1065.

Menninger, J.R. (1979). Accumulation of peptidyl tRNA is lethal to *Escherichia coli*. J. Bacteriol. *137*, 694-696.

Menninger, J.R. (1995). Mechanism of inhibition of protein synthesis by macrolide and lincosamide antibiotics. J. Basic Clin. Physiol. Pharmacol. *6*, 229-250.

Menninger, J.R., Coleman, R.A., and Tsai, L.N. (1994). Erythromycin, lincosamides, peptidyl-tRNA dissociation, and ribosome editing. Mol. Gen. Genet. *243*, 225-233.

Menninger, J.R., and Otto, D.P. (1982). Erythromycin, carbomycin, and spiramycin inhibit protein synthesis by stimulating the dissociation of peptidyl-tRNA from ribosomes. Antimicrob. Agents Chemother. *21*, 811-818.

Miller, H.J. (1992). A Short Course in Bacterial Genetics – A Laboratory Manual and Handbook for *Escherichia coli* and Related Bacteria. Cold Spring Harbor Laboratory Press.

Moazed, D., and Noller, H.F. (1987a). Chloramphenicol, erythromycin, carbomycin and vernamycin B protect overlapping sites in the peptidyl transferase region of 23S ribosomal RNA. Biochimie *69*, 879-884.

Moazed, D., and Noller, H.F. (1987b). Interaction of antibiotics with functional sites in 16S ribosomal RNA. Nature *327*, 389-394.

Monro, R.E., and Vazquez, D. (1967). Ribosome-catalysed peptidyl transfer: effects of some inhibitors of protein synthesis. J. Mol. Biol. *28*, 161-165.

Moore, S.D., and Sauer, R.T. (2008). Revisiting the mechanism of macrolide-antibiotic resistance mediated by ribosomal protein L22. Proc. Natl. Acad. Sci. USA *105*, 18261-18266.

Nakatogawa, H., and Ito, K. (2002). The ribosomal exit tunnel functions as a discriminating gate. Cell *108*, 629-636.

Nissen, P., Hansen, J., Ban, N., Moore, P.B., and Steitz, T.A. (2000). The structural basis of ribosome activity in peptide bond synthesis. Science *289*, 920-930.

O'Farrell, P.H. (1975). High-resolution two-dimensional electrophoresis of proteins. J. Biol. Chem. *250*, 4007-4021.

Odom, O.W., Picking, W.D., Tsalkova, T., and Hardesty, B. (1991). The synthesis of polyphenylalanine on ribosomes to which erythromycin is bound. Eur. J. Biochem. *198*, 713-722.

Oh, E., Becker, A.H., Sandikci, A., Huber, D., Chaba, R., Gloge, F., Nichols, R.J., Typas, A., Gross, C.A., Kramer, G.*, et al.* (2011). Selective ribosome profiling reveals the cotranslational chaperone action of trigger factor in vivo. Cell *147*, 1295-1308.

Oleinick, N.L. (1975). The Erythromycins. In Antibiotics, Mechanism of action of antimicrobial and tumor agents, Corcoran, J.W. and Hahn, F.E., eds. (New York: Springer-Verlag), *3*, pp. 397-419.

Onouchi, H., Nagami, Y., Haraguchi, Y., Nakamoto, M., Nishimura, Y., Sakurai, R., Nagao, N., Kawasaki, D., Kadokura, Y., and Naito, S. (2005). Nascent peptide-mediated translation elongation arrest coupled with mRNA degradation in the *CGS1* gene of *Arabidopsis*. Genes Dev. *19*, 1799-1810.

Otaka, T., and Kaji, A. (1975). Release of (oligo) peptidyl-tRNA from ribosomes by erythromycin A. Proc. Natl. Acad. Sci. USA *72*, 2649-2652.

Pestka, S. (1972). Studies on transfer ribonucleic acid-ribosome complexes. Effect of antibiotics on peptidyl puromycin synthesis on polyribosoms from *Escherichia coli*. J. Biol. Chem. *247*, 4669-4678.

Pestka, S. (1974a). Antibiotics as probes of ribosome structure: binding of chloramphenicol and erythromycin to polyribosomes; effect of other antibiotics. Antimicrob. Agents Chemother. *5*, 255-267.

Pestka, S., and LeMahieu, R.A. (1974b). Inhibition of [^{14}C]chloramphenicol binding to *Escherichia coli* ribosomes by erythromycin derivatives. Antimicrob. Agents Chemother. *6*, 39-45.

Pioletti, M., Schlunzen, F., Harms, J., Zarivach, R., Gluhmann, M., Avila, H., Bashan, A., Bartels, H., Auerbach, T., Jacobi, C.*, et al.* (2001). Crystal structures of complexes of the small ribosomal subunit with tetracycline, edeine and IF3. EMBO J. *20*, 1829-1839.

Poehlsgaard, J., Pfister, P., Bottger, E.C., and Douthwaite, S. (2005). Molecular mechanisms by which rRNA mutations confer resistance to clindamycin. Antimicrob. Agents Chemother. *49*, 1553-1555.

Poulsen, S.M., Kofoed, C., and Vester, B. (2000). Inhibition of the ribosomal peptidyl transferase reaction by the mycarose moiety of the antibiotics carbomycin, spiramycin and tylosin. J. Mol. Biol. *304*, 471-481.

Putnam, S.D., Castanheira, M., Moet, G.J., Farrell, D.J., and Jones, R.N. (2010). CEM-101, a novel fluoroketolide: antimicrobial activity against a diverse collection of Gram-positive and Gram-negative bacteria. Diagn. Microbiol. Infect. Dis. *66*, 393-401.

Ramu, H., Mankin, A., and Vazquez-Laslop, N. (2009). Programmed drug-dependent ribosome stalling. Mol. Microbiol. *71*, 811-824.

Ramu, H., Vazquez-Laslop, N., Klepacki, D., Dai, Q., Piccirilli, J., Micura, R., and Mankin, A.S. (2011). Nascent peptide in the ribosome exit tunnel affects functional properties of the A-site of the peptidyl transferase center. Mol. Cell *41*, 321-330.

Rheinberger, H.J., and Nierhaus, K.H. (1990). Partial release of AcPhe-Phe-tRNA from ribosomes during poly(U)-dependent poly(Phe) synthesis and the effects of chloramphenicol. Eur J Biochem *193*, 643-650.

Ross, J.I., Eady, E.A., Cove, J.H., and Cunliffe, W.J. (1998). 16S rRNA mutation associated with tetracycline resistance in a gram-positive bacterium. Antimicrob. Agents Chemother. *42*, 1702-1705.

Schagger, H., and von Jagow, G. (1987). Tricine-sodium dodecyl sulfate-polyacrylamide gel electrophoresis for the separation of proteins in the range from 1 to 100 kDa. Anal. Biochem. *166*, 368-379.

Schlunzen, F., Harms, J.M., Franceschi, F., Hansen, H.A., Bartels, H., Zarivach, R., and Yonath, A. (2003). Structural basis for the antibiotic activity of ketolides and azalides. Structure *11*, 329-338.

Schlunzen, F., Zarivach, R., Harms, J., Bashan, A., Tocilj, A., Albrecht, R., Yonath, A., and Franceschi, F. (2001). Structural basis for the interaction of antibiotics with the peptidyl transferase centre in eubacteria. Nature *413*, 814-821.

Schmeing, T.M., Huang, K.S., Strobel, S.A., and Steitz, T.A. (2005). An induced-fit mechanism to promote peptide bond formation and exclude hydrolysis of peptidyl-tRNA. Nature *438*, 520-524.

Schmeing, T.M., and Ramakrishnan, V. (2009). What recent ribosome structures have revealed about the mechanism of translation. Nature *461*, 1234-1242.

Seidelt, B., Innis, C.A., Wilson, D.N., Gartmann, M., Armache, J.P., Villa, E., Trabuco, L.G., Becker, T., Mielke, T., Schulten, K.*, et al.* (2009). Structural insight into nascent polypeptide chain-mediated translational stalling. Science *326*, 1412-1415.

Shimizu, Y., Inoue, A., Tomari, Y., Suzuki, T., Yokogawa, T., Nishikawa, K., and Ueda, T. (2001). Cell-free translation reconstituted with purified components. Nat. Biotechnol. *19*, 751-755.

Shimizu, Y., Kanamori, T., and Ueda, T. (2005). Protein synthesis by pure translation systems. Methods *36*, 299-304.

Shinabarger, D.L., Marotti, K.R., Murray, R.W., Lin, A.H., Melchior, E.P., Swaney, S.M., Dunyak, D.S., Demyan, W.F., and Buysse, J.M. (1997). Mechanism of action of oxazolidinones: effects of linezolid and eperezolid on translation reactions. Antimicrob. Agents Chemother. *41*, 2132-2136.

Siibak, T., Peil, L., Xiong, L., Mankin, A., Remme, J., and Tenson, T. (2009). Erythromycin- and chloramphenicol-induced ribosomal assembly defects are secondary effects of protein synthesis inhibition. Antimicrob. Agents Chemother. *53*, 563-571.

Skripkin, E., McConnell, T.S., DeVito, J., Lawrence, L., Ippolito, J.A., Duffy, E.M., Sutcliffe, J., and Franceschi, F. (2008). Rχ-01, a new family of oxazolidinones that overcome ribosome-based linezolid resistance. Antimicrob. Agents Chemother. *52*, 3550-3557.

Spizek, J., and Rezanka, T. (2004). Lincomycin, clindamycin and their applications. Appl. Microbiol. Biotechnol. *64*, 455-464.

Starosta, A.L., Karpenko, V.V., Shishkina, A.V., Mikolajka, A., Sumbatyan, N.V., Schluenzen, F., Korshunova, G.A., Bogdanov, A.A., and Wilson, D.N. (2010). Interplay between the ribosomal tunnel, nascent chain, and macrolides influences drug inhibition. Chem. Biol. *17*, 504-514.

Tai, P.C., Wallace, B.J., and Davis, B.D. (1974). Selective action of erythromycin on initiating ribosomes. Biochemistry *13*, 4653-4659.

Tanaka, K., Teraoka, H., and Tamaki, M. (1971). Peptidyl puromycin synthesis; effect of several antibiotics which act on 50 S ribosomal subunits. FEBS Lett. *13*, 65-67.

Taubman, S.B., So, A.G., Young, F.E., Davie, E.W., and Corcoran, J.W. (1963). Effect of Erythromycin on Protein Biosynthesis in *Bacillus Subtilis*. Antimicrob. Agents Chemother. (Bethesda) *161*, 395-401.

Tenson, T., DeBlasio, A., and Mankin, A. (1996). A functional peptide encoded in the *Escherichia coli* 23S rRNA. Proc. Natl. Acad. Sci. USA *93*, 5641-5646.

Tenson, T., and Ehrenberg, M. (2002). Regulatory nascent peptides in the ribosomal tunnel. Cell *108*, 591-594.

Tenson, T., Lovmar, M., and Ehrenberg, M. (2003). The mechanism of action of macrolides, lincosamides and streptogramin B reveals the nascent peptide exit path in the ribosome. J. Mol. Biol. *330*, 1005-1014.

Tenson, T., and Mankin, A.S. (2001). Short peptides conferring resistance to macrolide antibiotics. Peptides *22*, 1661-1668.

Tenson, T., Xiong, L., Kloss, P., and Mankin, A.S. (1997). Erythromycin resistance peptides selected from random peptide libraries. J. Biol. Chem. *272*, 17425-17430.

Thompson, J., Pratt, C.A., and Dahlberg, A.E. (2004). Effects of a number of classes of 50S inhibitors on stop codon read through during protein synthesis. Antimicrob. Agents Chemother. *48*, 4889-4891.

Tritton, T.R. (1977). Ribosome-tetracycline interactions. Biochemistry *16*, 4133-4138.

Tu, D., Blaha, G., Moore, P.B., and Steitz, T.A. (2005). Structures of MLS_BK antibiotics bound to mutated large ribosomal subunits provide a structural explanation for resistance. Cell *121*, 257-270.

Vazquez, D. (1966a). Binding of chloramphenicol to ribosomes. The effect of a number of antibiotics. Biochim. Biophys. Acta *114*, 277-288.

Vazquez, D. (1966b). Studies on the mode of action of the streptogramin antibiotics. J. Gen. Microbiol. *42*, 93-106.

Vazquez, D. (1966c). Antibiotics affecting chloramphenicol uptake by bacteria. Their effect on amino acid incorporation in a cell-free system. Biochim. Biophys. Acta *114*, 289-295.

Vazquez, D. (1979). Inhibitors of protein biosynthesis. Mol. Biol. Biochem. Biophys. *30*, i-x, 1-312.

Vazquez-Laslop, N., Klepacki, D., Mulhearn, D.C., Ramu, H., Krasnykh, O., Franzblau, S., and Mankin, A.S. (2011a). Role of antibiotic ligand in nascent peptide-dependent ribosome stalling. Proc. Natl. Acad. Sci. USA *108*, 10496-10501.

Vázquez-Laslop, N., Ramu, H. and Mankin, A.S. (2011b). Nascent peptide-mediated ribosome stalling promoted by antibiotics. In Ribosomes, Green, R., Rodnina, R., and Wintermeyer, W., eds. Section V, pp. 377-392.

Vazquez-Laslop, N., Ramu, H., Klepacki, D., Kannan, K., and Mankin, A.S. (2010). The key function of a conserved and modified rRNA residue in the ribosomal response to the nascent peptide. EMBO J. *29*, 3108-3117.

Vazquez-Laslop, N., Thum, C., and Mankin, A.S. (2008). Molecular mechanism of drug-dependent ribosome stalling. Mol. Cell *30*, 190-202.

Vester, B., and Garrett, R.A. (1987). A plasmid-coded and site-directed mutation in *Escherichia coli* 23S RNA that confers resistance to erythromycin: implications for the mechanism of action of erythromycin. Biochimie *69*, 891-900.

Vimberg, V., Xiong, L., Bailey, M., Tenson, T., and Mankin, A. (2004). Peptide-mediated macrolide resistance reveals possible specific interactions in the nascent peptide exit tunnel. Mol. Microbiol. *54*, 376-385.

Voss, N.R., Gerstein, M., Steitz, T.A., and Moore, P.B. (2006). The geometry of the ribosomal polypeptide exit tunnel. J. Mol. Biol. *360*, 893-906.

Weisblum, B. (1995a). Erythromycin resistance by ribosome modification. Antimicrob. Agents Chemother. *39*, 577-585.

Weisblum, B. (1995b). Insights into erythromycin action from studies of its activity as inducer of resistance. Antimicrob Agents Chemother *39*, 797-805.

Wilson, D.N. (2009). The A-Z of bacterial translation inhibitors. Crit. Rev. Biochem. Mol. Biol. *44*, 393-433.

Wilson, D.N. (2011). On the specificity of antibiotics targeting the large ribosomal subunit. Ann. N Y Acad. Sci. *1241*, 1-16.

Wilson, D.N., Schluenzen, F., Harms, J.M., Starosta, A.L., Connell, S.R., and Fucini, P. (2008). The oxazolidinone antibiotics perturb the ribosomal peptidyl-transferase center and effect tRNA positioning. Proc. Natl. Acad. Sci. USA *105*, 13339-13344.

Woosley, L.N., Castanheira, M., and Jones, R.N. (2010). CEM-101 activity against Gram-positive organisms. Antimicrob. Agents Chemother. *54*, 2182-2187.

Xiong, L., Korkhin, Y., and Mankin, A.S. (2005). Binding site of the bridged macrolides in the *Escherichia coli* ribosome. Antimicrob. Agents Chemother. *49*, 281-288.

Xu, H., and Freitas, M.A. (2007). A mass accuracy sensitive probability based scoring algorithm for database searching of tandem mass spectrometry data. BMC Bioinformatics *8*, 133.

Yao, S., Blaustein, J.B., and Bechhofer, D.H. (2008). Erythromycin-induced ribosome stalling and RNase J1-mediated mRNA processing in *Bacillus subtilis*. Mol. Microbiol. *69*, 1439-1449.

Yonath, A. (2005). Antibiotics targeting ribosomes: resistance, selectivity, synergism and cellular regulation. Annu. Rev. Biochem. *74*, 649-679.

Yonath, A., Leonard, K.R., and Wittmann, H.G. (1987). A tunnel in the large ribosomal subunit revealed by three-dimensional image reconstruction. Science *236*, 813-816.

Zaporojets, D., French, S., and Squires, C.L. (2003). Products transcribed from rearranged *rrn* genes of *Escherichia coli* can assemble to form functional ribosomes. J. Bacteriol. *185*, 6921-6927.

Zhanel, G.G., Hisanaga, T., Nichol, K., Wierzbowski, A., and Hoban, D.J. (2003). Ketolides: an emerging treatment for macrolide-resistant respiratory infections, focusing on *S. pneumoniae*. Expert Opin. Emerg. Drugs *8*, 297-321.

Zhou, C.C., Swaney, S.M., Shinabarger, D.L., and Stockman, B.J. (2002). ^{1}H nuclear magnetic resonance study of oxazolidinone binding to bacterial ribosomes. Antimicrob. Agents Chemother. *46*, 625-629.

VITA

EDUCATION

B. Tech, Industrial Biotechnology, Anna University, India, 2006

Candidate for Ph.D., Pharmacognosy, University of Illinois at Chicago, Chicago, Illinois, 2012

PUBLICATIONS

Krishna Kannan, Nora Vázquez-Laslop and Alexander S Mankin. Selective escape of proteins from ribosome-bound macrolides. ***Cell*** 151 (3) 508-520. (2012)

Swaminathan Palanisami, **Krishna Kannan** and Uma Lakshmanan. Tannase activity from the marine cyanobacterium *Phormidium valderianum* BDU140441. ***J. App. Phycol.*** 24 (5) 1093-1098. (2011)

Nora Vázquez-Laslop, Haripriya Ramu, Dorota Klepacki, **Krishna Kannan**, Alexander S Mankin. The key function of a conserved and modified rRNA residue in the ribosomal response to the nascent peptide. ***EMBO J.*** 29, 3108-3117. (2010)

Mary E. Rumpho, Jared M. Worful, Jungho Lee, **Krishna Kannan**, Mary S. Tyler, Debashish Bhattacharya, Ahmed Moustafa, and James R. Manhart. Horizontal gene transfer of the algal nuclear gene *psbO* to the photosynthetic sea slug Elysia chlorotica. ***Proc. Nat. Acad. Sci. USA*** 105 (46), 17867–17871. (2008)

INVITED BOOK CHAPTERS

Krishna Kannan and Alexander S Mankin. Macrolide antibiotics in the ribosome exit tunnel: species-specific binding and action. ***Ann. NY. Acad. Sci.*** 1241, 33-47. (2011)

SELECTED TALKS

'Late' Translation Arrest: An Unconventional Mode of Inhibition of Protein Synthesis by Macrolide Antibiotics. ***RNA 2012 : The 17th Annual Meeting of the RNA Society****, Ann Arbor, Michigan, 2012.*

'Protein escape' – the unknown mechanisms of action of clinically important macrolide antibiotics. ***EMBO Conference Series*** *(Protein Synthesis and Translational Control). Heidelberg, Germany, 2011.*

POSTER PRESENTATIONS

Krishna Kannan, Nora Vázquez-Laslop and Alexander Mankin. "Late" translation arrest: an unconventional mode of inhibition of protein synthesis by macrolides. ***College of Pharmacy Research Day****, UIC, 2012*.

Pulkit Gupta, **Krishna Kannan**, Alexander Mankin, and Nora Vázquez-Laslop. Molecular mechanism of ketolide dependent induction of the antibiotic resistance gene *ermC*. ***College of Pharmacy Research Day****, UIC, 2012.*

Pulkit Gupta, **Krishna Kannan**, Alexander Mankin, and Nora Vázquez-Laslop. Molecular mechanism of ketolide dependent induction of the antibiotic resistance gene *ermC*. ***Cell Symposium*** *(Regulatory RNAs). Chicago, 2011.*

Krishna Kannan, Nora Vázquez-Laslop and Alexander Mankin. Incomplete inhibition of protein synthesis by macrolide antibiotics. ***ICAAC****. Chicago, 2011.*

Pulkit Gupta, **Krishna Kannan**, Alexander Mankin, and Nora Vázquez-Laslop. Molecular mechanism of ketolide dependent induction of the antibiotic resistance gene *ermC*. ***ICAAC****. Chicago, 2011.*

Krishna Kannan, Liisa Arike, Hua Xu, Lauri Peil, Tanel Tenson and Alexander Mankin. Translation regulation by rRNA posttranscriptional modifications in the ribosome exit tunnel. ***EMBO Conference Series*** *(Protein Synthesis and Translational Control). Heidelberg, Germany, 2011*

Pulkit Gupta, **Krishna Kannan**, Elena Guerra, Alexander Mankin and Nora Vázquez-Laslop. The frameshifting activity of ketolides is reponsible for the activation of the antibiotic resistance gene ermC. ***EMBO Conference Series*** *(Protein Synthesis and Translational Control). Heidelberg, Germany, 2011.*

Pulkit Gupta, Yijia Luo, **Krishna Kannan**, Alexander Mankin and Nora Vázquez-Laslop. Molecular mechanism of Ketolide dependent induction of the antibiotic resistance gene ermC. ***ICAAC***. *Chicago, 2011.*

Nora Vázquez-Laslop, **Krishna Kannan**, Pulkit Gupta, Haripriya Ramu, Dorota Klepacki and Alexander S. Mankin. Sensing nascent peptides and small ligands in the exit tunnel of the ribosome. ***Cell Symposium*** *(Regulatory RNAs). Chicago, 2011.*

Pulkit Gupta, Yijia Luo, **Krishna Kannan**, Alexander S. Mankin and Nora-Vázquez Laslop. An alternative mechanism for the induction of antibiotic resistance gene ermC. ***ASM conference on Regulation with RNA in bacteria***. *Puerto Rico, 2011.*

Krishna Kannan, Nora Vázquez-Laslop and Alexander Mankin. Novel mechanisms of action of clinically important macrolides**.** ***College of Pharmacy Research Day****, UIC, 2011*

Krishna Kannan, Nora Vázquez-Laslop and Alexander Mankin. New insights into the mechanism of action of old antibiotics. ***Riboclub****, Canada, 2010.*

Krishna Kannan, Nora Vázquez-Laslop and Alexander Mankin. Mechanism of action of macrolides: how true are the old paradigms? ***17th Midwest Microbial Pathogenesis Conference****, St. Louis, 2010.*

Krishna Kannan, Nora Vázquez-Laslop and Alexander Mankin. Mechanism of action of macrolides: how true are the old paradigms? ***Ribosome 2010***. *Orvieto, Italy.*

Blanca Martinez-Garriga, Hua Xu, **Krishna Kannan**, Alexander Mankin. The role of nascent peptide-ribosome interactions in gene regulation using quantitative mass spectrometry with ^{15}N-stable isotope labeling. ***American Society for Mass Spectrometry****, Philadelphia, PA, 2009.*

Mary E. Rumpho, Jared M. Worful, Jungho Lee, **Krishna Kannan**, Kara Soule, mary Tyler, James Manhart. The Search for Horizontal Gene Transfer in a Kleptoplastic Sea Slug. ***Botany and Plant Biology Joint Congress****, 2007.*

AWARDS

Provost's & Deiss Awards for Graduate Research, UIC (2012).

Travel fellowship**,** 17th Annual meeting of the RNA society (2012).

W. E van Doren Scholar, College of Pharmacy, UIC (2012).

Charles Wesley Petranek Scholarship award, College of Pharmacy, UIC (2011).

First Place for poster presentation, College of Pharmacy Research Day, UIC (2011).

Graduate Student Council Travel Award; UIC (2010).

Second place for poster presentation, Riboclub, Canada (2010).

PROFESSIONAL AFFILIATIONS

The American Society for Microbiology

The RNA Society